THE ASTROPHYSICAL JOURNAL

AN INTERNATIONAL REVIEW OF SPECTROSCOPY AND ASTRONOMICAL PHYSICS

VOLUME 80 NOVEMBER 1934 NUMBER 4

A STUDY OF STELLAR SPECTRA IN THE REGION 6562–7593 A

By F. E. ROACH

ABSTRACT

On grating spectrograms of Procyon, Arcturus, Aldebaran, and Betelgeuze, 426 stellar lines have been measured in the region between $H\alpha$ and the head of the atmospheric A band. Satisfactory identifications of a large number of the lines have been made.

In Vega and Sirius this part of the spectrum has 33 lines, most of which are not strong.

Radial velocities deduced from the measures of the first group of stars are found to agree with the values obtained for the ordinary spectral region.

Lines of the following elements are definitely present: *H*, *Al*, *Si*, *S*, *Ca*, *Ti*, *V*, *Cr*, *Fe*, *Zr*.

The unblended lines of neutral silicon are weakened appreciably in the cooler stars.

Three lines of neutral sulphur are found in Procyon, strengthening the case for this element in the sun.

Titanium is represented by 29 lines, of which 17 are probably unblended. They are prominent in the red stars. *TiO* bands of the red infra-red system are very strong in Betelgeuze and moderately so in Aldebaran.

Iron contributes to about 150 stellar lines in this region. In the cooler stars the low excitation lines are enhanced relative to those of high excitation potential. In Procyon the converse is true.

Twenty-four lines are attributed to neutral zirconium.

With the development of improved emulsions for the red and near infra-red it is possible to extend to longer wave-lengths our knowledge of stellar spectra. In three papers P. W. Merrill and O. C. Wilson, Jr.,[1] have discussed their investigations covering chiefly the region to the red of the terrestrial A band. The purpose of the present study is to fill the gap between the spectral region available with the panchromatic emulsions and that covered by Merrill.

[1] *Ap. J.*, **74**, 188, 1931; *Mt. W. Contr.*, No. 432; *Ap. J.*, **79**, 183, 1934; *Mt. W. Contr.*, No. 486; *Ap. J.*, **80**, 19, 1934; *Mt. W. Contr.*, No. 494.

OBSERVATIONAL MATERIAL

The twenty spectrograms used in this investigation were taken with the Yerkes auto-collimating grating spectrograph attached to the 69-inch reflector of the Perkins Observatory. Eastman emul-

TABLE I

LIST OF SPECTROGRAMS MEASURED

Star	Date (U.T.)	Exp. Time Minutes	Radial Velocity	No. of Lines*	Velocity†
α Ori	1933 Nov. 20.3‡	60	+18.9	7	+21.0
	Dec. 23.3	70	+18.8	9	.....
	1934 Feb. 10.1	230	+21.3	18	.....
	Mar. 7.1	210	+21.0	17	.....
α Tau	1933 Oct. 14.3	60	+50.4	8	+54.1
	1934 Jan. 22.0	196	+53.2	23	.....
	Jan. 27.2	240	+52.7	13	.....
α Boo	1933 June 6.2	140	− 3.9	53	− 5.1
	June 15.1	90	− 2.5	42	.....
	1934 Apr. 9.2	154	− 3.0	13	.....
	Apr. 10.2	30	− 7.0	35	.....
	May 31.2	150	− 2.2	36	.....
α CMi	Mar. 29.1	166	− 9.1	9	− 4.3§
	Apr. 9.1	160	− 7.5	15	.....
	Apr. 10.0	88	− 4.7	25	.....
	Apr. 10.1	62	−10.8	18	.....
α CMa	Jan. 21.1	180	.....	.....	.....
α Lyr	1933 July 17.2	201	.....	.....	.....
	July 18.2	320	.....	.....	.....
	1934 Apr. 10.4	90	.....	.....	.....

* Number of lines used in radial velocity determination.

† *Lick Obs. Pub.*, **18**, 1932.

‡ This plate is one belonging to the Perkins Observatory and loaned to the writer by Dr. Bobrovnikoff.

§ Velocity of Procyon computed from formula in *Trans. I.A.U.*, **3**, 175, 1928.

sions IV-N, III-U, and IV-U were used, chiefly IV-N. All plates were hypersensitized in a 4 per cent ammonia solution. Development was with Eastman D-11.

In Table I are the data concerning the spectrograms. The second plate of α Orionis and the first of α Tauri are strong exposures on panchromatic (Eastman III-F) emulsion, which extend somewhat to the red of $H\alpha$.

The measures were made with the small Gaertner measuring machine of the Perkins Observatory. The comparison spectrum is from a neon lamp, giving 16 lines over this region. The linear dispersion varies from about 26.6 A per millimeter at *Hα* to 26.4 A per millimeter at 7500 A. The slight departure from normality justifies the use of a parabolic interpolation formula for the reduction of the measures to wave-lengths. The probable error of a single wave-length determination from one plate is ±0.08 A.

INTENSITY SCALE OF LINES

Each line was given an estimate of intensity at the time of measurement, from 0 for a line whose reality is doubtful to 10 for a very

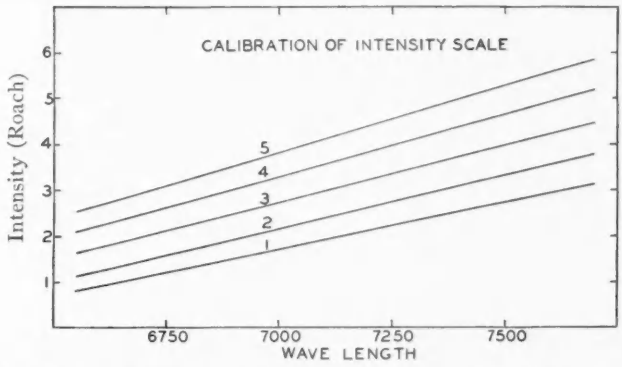

FIG. 1.—The straight lines indicate the intensities of the *Revised Rowland*

strong line. In order to evaluate my scale it has been compared with that of the *Revised Rowland*[2] for this region, using solar plates taken under the same instrumental conditions as were the stellar spectrograms. Figure 1 indicates the nature of the relationship. Near *Hα* a line of intensity 1 on the Rowland scale is just visible on my plates, while at 7500 A a line of Rowland intensity 1 is about 3 on my scale.

It is of interest to note that the same change in the *Revised Rowland* scale has been observed by G. F. W. Mulders.[3] He ascribes the variation to a change with wave-length in the gradation of the plates on which the original Rowland measures were made.

[2] St. John, Moore, Ware, Adams, and Babcock, *Revision of Rowland's Preliminary Table of Solar Spectrum Wave-Lengths*, 1928.

[3] *Zs. f. Ap.*, **8**, 62, 1934.

RADIAL VELOCITIES

The radial velocities are recorded in Table I. Attention is called to a range of 6 km/sec. in the velocity of Procyon (the probable errors are ± 0.6 and ± 1.0 km/sec. for plates 315 and 316). The material is insufficient to establish this variation. For Arcturus the range is 5 km/sec.

LINES OF TERRESTRIAL ORIGIN

The presence of a large number of telluric lines in this spectral region complicates the identification of the stellar lines. Table II

TABLE II

LINES OF TERRESTRIAL ORIGIN

Wave-Length	Int.	Source	Wave-Length	Int.	Source	Wave-Length	Int.	Source
6867.235	20	*O*	6986.592	2	wv	7236.150	1	Atm
6869.96	0	*O*	6989.001	2	wv	7240.578	7	Atm
6871.147	2	*O*	6990.391	1	wv	7243.645	3	Atm
6872.558	2	*O*	6993.731	3	wv	7245.690	3	Atm
6874.716	2	*O*	6998.981	4	wv	7247.224	2	Atm
6877.188	2	*O*	7004.766	4	wv	7250.230	0	Atm
6879.350	2	*O*	7011.342	1	wv *Fe*	7252.938	8	Atm
6883.844	3	*O*	7016.452	5	wv	7257.952	4	Atm
6886.283	5d	*O*	7019.368	0	Atm	7267.011	1	.....
6889.456	7d	*O*	7023.517	2	Atm wv	7265.324	5	Atm
6892.869	6d	*O*	7027.491	4	Atm−	7270.....	3	.....
6896.530	6d	*O*	7037.555	3	Atm	7272.987	4	Atm
6900.441	5d	*O*	7039.807	3	Atm	7275.411	2	Atm
6904.581	5d	*O*	7167.918	4	Atm	7277.405	3	Atm
6908.997	5d	*O*	7170.580	4	Atm	7287.643	4	Atm
6913.661	5d	*O*	7173.191	5	Atm	7290.426	6	Atm
6918.576	5d	*O*	7176.064	1	Atm	7292.444	1	Atm
6923.753	4d	*O*	7177.506	5	Atm	7295.047	2	Atm *Fe*
6929.179	3d	*O*	7181.614	4	Atm	7299.937	3	Atm
6933.730	3	*Fe*, *O*, wv	7184.472	3	Atm	7303.799	5	Atm
6934.867			7186.719	5	Atm	7309.279	5	Atm
6937.901	1	wv	7191.692	5	Atm	7312.632	2	Atm
6940.008	2	wv, *O*	7193.672	3	Atm	7315.530	1	Atm
6941.987	1	wv, wv	7195.052	1	Atm	7317.310	1	Atm
6943.815	1	wv	7198.001	4	Atm	7318.707	3	Atm
6947.552	3	wv	7200.775	6	Atm	7323.986	2	Atm
6949.032	2	wv	7204.185	3	Atm	7327.388	2	Atm
6950.774	2	wv	7206.433	4	Atm	7330.876	2	Atm
6953.586	3	wv	7209.513	2	*Ti* Atm	7333.683	4	Atm
6956.433	4	wv	7216.541	3	Atm	7335.334	0	Atm
6959.467	2½	wv	7223.652	4	Atm *Fe*	7349.490	3	Atm
6961.275	3	wv	7227.507	3	Atm	7369.208	2	Atm
6964.564	0	wv	7232.749	5	Atm	7383.722	3	Atm
6977.487	2	wv	7234.750	5	Atm	7593.699	.....	.....
6981.474	2	wv						

lists the atmospheric lines, which are based on the following criteria: (1) inclusion in the *Revised Rowland;* (2) absence of radial velocity shift; (3) presence in stars of all spectral classes considered in this paper, namely, Ao–M2. The wave-lengths are from the *Revised Rowland* and represent the weighted mean when two or more lines are blended on my plates. Intensities are on my scale. The letter "d" in the intensity column indicates that the line is just visibly double. The data for the source columns are from the *Revised Rowland.*

LINES IN FOUR STARS, 6562–7593 A

In Table III the results of the wave-length determinations in Betelgeuze, Aldebaran, Arcturus, and Procyon are summarized. In the first column are the observed wave-lengths. The second, third, fourth, and fifth columns record the measured wave-lengths, followed by the estimated intensities of the lines in the respective stars. Columns 6–8 give the suggested identifications. In column 7 are the wave-lengths taken from the *Revised Rowland,* wherever possible, followed by the laboratory intensities. Wherever the *Revised Rowland* wave-lengths are not employed, the recorded value is in italics. The excitation potentials in volts are given in column 8. The data for the solar intensities in disk and spot are from the *Revised Rowland,* with the exception of a few of the disk intensities of lines beyond about 7300 A, which are taken from Meggers.[4] In the last column an estimate has been made of the extent to which the laboratory line contributes to the observed stellar line. "A" denotes a principal contributor; "B," an important contributor; "C," a minor contributor; and no letter indicates a slight or doubtful contributor.

LINES IN VEGA AND SIRIUS

Because lines due to the ionized elements tend to lie in the photographic region of the spectrum, it is not surprising that only a few lines have been found in these A-type stars. Of the 33 stellar lines recorded in Table IV, only one is identified with certainty, namely, *Hα.* The line at 7389.5 A is identified provisionally with *Fe* 7389.39. Six other coincidences with high excitation iron lines are noted.

[4] *Pub. of the Allegheny Obs.,* **6,** 13, 1929.

TABLE III

Absorption Lines in Four Stars, 6562–7593 A

Wave-Length Obs.	Betel-geuze	Alde-baran	Arc-turus	Pro-cyon	Identification				Sun		Con-trib-utor
					El.	W.-L.	Int.	E.P.	Dk.	Sp.	
6562	2.64	2.74	2.89	2.80	*H*	2.82	....	10.2	40	20	A
6565	.....	5.85 2	5.92 1	.....	*V?*	5.85	2	1.2	− 3	− 1?	.....
6566	6.62 2	.....	.....	.....	.....	.....	.....	.....	.....	.....	.....
6569	9.31 2	9.31 2	9.13 2	9.24 1	*Fe*	9.23	5	4.7	4	3	A
6570	.....	.....	0.53 1	.....	*Mn*	*0.79*	...	...	.....	.....	.....
6572	2.81 3	2.76 3	2.42 2	.....	*Ca*	2.80	8	0.0	1	6	A
					Cr	*2.89*	2	1.0	.....	.....	.....
					Fe	4.24	2	1.0	1	3	B
6574	4.68 3	4.75 3	4.75 3	4.87 1	*Fe*	5.05	2	2.6	2	2	B
					Ti	5.19	3	2.6	.....	− 1	.....
					⊙	6.60	...	...	.....	− 2	.....
6576	6.7 0	6.52 1	7.07 1	.....	*Ni*	6.91	pr	5.3	− 3	.....	.....
					V	8.97	....	1.0	.....	− 2	.....
6578	8.6 0	8.84	.....	.....	⊙	9.09	...	...	.....	− 2	.....
6581	1.08 3	1.07 3	1.09 3	.....	*Cr*	*0.91*	1	1.0	.....	− 1	B
					Fe	1.23	2	1.5	0	1	A
6586	6.20 2	6.24 3	6.29 3	.....	*Ni* *Fe*	6.33	6	1.9	1	3	A
6589	.....	9.25 1	.....	.....	.....	.....	.....	.....	.....	.....	.....
6592	3.36 6	3.15 5	2.87 2	3.04 1	*Fe*	2.93	10	2.7	6	7	A
6593			3.86 2	3.92 1	*Fe*	3.89	4	2.4	4	7	A
6596	.....	.....	6.24 1	.....	*Co*	5.91	12	3.7	− 2N	.....	.....
					Cr	7.58	2	4.2	2	1	.....
6597	.....	7.42 1	.....	.....	*Fe*	7.58	....	4.8	2	1	.....
6598	8.94 4	8.98 3	8.91 3	9.14 1	*Ni*	8.62	3	4.2	0	− 1	B
					Ti	9.13	12	0.9	− 1	4	A
6600	0.76 1	.....	0.78 1	.....	.....	.....	.....	.....	.....	.....	.....
6601	.....	.....	.....	1.66 1	.....	.....	.....	.....	.....	.....	.....
6602	.....	.....	2.52 1	.....	.....	.....	.....	.....	.....	.....	.....
6603	3.11 1	.....	.....	.....	*Fe?*	3.37	pr	2.4	− 3N	.....	.....
					Zr	*3.27*	8	1.5	.....	.....	C
6604	.....	.....	4.30 1	4.19 1	*Sc+*	4.61	10	1.4	1	0	B
6605	5.56 2	5.82 2	6.09 1	.....	*Mn*	5.58	6	4.4	− 2	1	B
					V	5.93	5	1.2	− 2N	2	A
6607	7.97 1	7.87 1	.....	.....	*V?*	7.90	....	1.3	.....	− 1	B
					Fe	8.05	2	2.3	0	1	A
					Fe	9.13	4	2.5	3	5	A
6609	9.32 3	9.29 3	9.30 3	.....	*FeA*	9.59	1	1.0	− 1	− 1?	.....
					⊙	9.70	...	...	− 2	1	C
6612	.....	.....	2.25 1	.....	*Cr*	2.25	3	4.1	− 2	.....	.....
6613	3.85 2	3.77 3	3.78 2	.....	*Fe*	3.82	pr	1.0	− 1d?	1	.....
					V+	3.8	....	1.7	.....	.....	.....
6616	.....	6.57 1	6.44 1	6.95 1	*Co*	7.04	6	4.5	− 2d?	.....	.....
6618	8.68 1	8.54 1	8.81 1	.....	.....	.....	.....	.....	.....	.....	.....
					Zr	*0.62*	5	2.3	.....	.....	.....
6620	.....	0.56 1	.....	.....	⊙	1.12	...	...	.....	2	.....
6622	.....	2.69 1	2.06 1	.....	.....	.....	.....	.....	.....	.....	.....
					⊙	4.78	...	...	.....	0	.....
					V	4.85	5	1.2	− 3N	1	A
6624	4.94 6N	4.88 4	4.82 3	.....	*Fe*	5.05	1	1.0	0	2d	B
					TiO	*6.08*	2	...	.....	.....	B*
6627	.....	7.7 0	7.71 1	.....	*Fe*	7.57	3	4.5	1	0	B
6630	9.91 1	0.10 1	9.97 1	.....	*Cr*	0.04	4	1.0	− 2	4	A
6632	1.78 1	.....	2.26 1	.....	*Co?*	2.48	15	2.3	− 1N	− 1	.....
6633	3.78 1	3.72 2	3.73 3	3.51 1	*Fe*	3.77	7	4.5	2	1	A
6634	4.7 3N	.....	.....	.....	*TiO*	*4.30*	2	...	.....	.....	A
6635	6.14 1	.....	5.91 1	.....	.....	.....	.....	.....	.....	.....	.....
6639	9.68 2	9.79 2	9.67 1	.....	*Fe*	9.73	pr	4.6	0	.....	.....
6640	.....	.....	.....	0.32 1	.....	.....	.....	.....	.....	.....	.....
6643	3.63 4	3.72 3	3.54 3	3.45 2	*Ni*	3.65	20	1.7	5	6	A
6646	7.54 2	7.66 2	6.94 1	.....	*Fe*	6.98	1	2.6	− 1	0	A
6648			8.38 1	8.16 1	*Fe?*	8.13	pr	1.0	− 2	− 1	.....
6651	1.66 5	1.34 2N	1.59 1	.....	*TiO*	*1.46*	5	...	.....	.....	A*
6653	.....	.....	3.94 1	.....	*Fe?*	3.92	....	4.1	− 1	− 2	.....
6656	.....	6.77 2N	.....	.....	.....	.....	.....	.....	.....	.....	.....
6657	.....	.....	7.24 1	.....	.....	.....	.....	.....	.....	.....	.....

* *TiO* does not contribute to this line in Arcturus.

TABLE III—*Continued*

Wave-Length Obs.	Betel-geuze	Alde-baran	Arc-turus	Pro-cyon	Identification				Sun		Con-trib-utor
					El.	W.-L.	Int.	E.P.	Dk.	Sp.	
6660		0.81 2	0.96 1		Cb	0.76	150				B
					Cr	1.09	12	4.2	− 1	1d	B
6663	3.33 3	3.39 4	3.32 3	3.28 2	Fe	3.26	1	4.5	1	0	C
					Fe	3.47	8	2.4	3	4	A
					Ti?	6.55	2	1.5	− 2N		
6667	7.32 2N	7.16 3N	7.75 1N		Fe	7.46	pr	2.4	− 2		
					Fe	7.75			− 1		
6677	7.99 5	8.09 5	7.97 5	7.88 2	Fe	8.01	12	2.7	5	5	A
6681			1.39 1								
6681	1.62 5N	1.58 2N			TiO	1.06	6				A
6683			3.32 1								
6684			4.99 1		Co	4.90	5		− 3		
6685	5.61 1	5.86 2n			TiO	5.97	1				B
6687		8.04 2n	7.81 1		V	7.57	25	0.0		0	
6689			9.33 1								
6696		6.23 2	6.28 2		Al	6.04	3	3.1	1N	2	A
					⊙	6.33			0		B
6698		8.82 1	8.63 1		Al	8.68	3	3.1	0	0	A
6701		1.37 1	1.06 1		Ni?	0.93		4.2	− 3		
					⊙	1.39			− 2		
6703		3.63 1	3.49 2		Fe	3.59	2	2.7	1	2	A
6705		4.96 1	5.09 1		Fe	5.12			1	0	A
					⊙	7.46			− 2		
6707		7.43 2	7.26 1		Li	7.77		0.0		2N	
					Li	7.94		0.0		1N	
6710	0.50 2	0.26 2	0.41 2		Fe	0.33	1	1.5	0	1	A
6713			3.24 1		Fe	3.05	3	4.6	1	ob	B
					Fe	3.75	1	4.8	1	0	B
6715	4.84 5	5.42 1n			TiO	4.37	6				A
6715			5.77 1		Fe	5.40	3	4.6	1	1	
6717	7.69 4	7.77 3	7.66 4	7.61 2	Ca	7.70	30	2.7	5	8	A
6721			1.45 1								
6722		2.73 1n	2.19 1	2.23 1							
6723				3.98 1							
6726	6.15 1	6.16 2n	6.23 2n		Fe	6.68	3	4.6	2	1	
6728				8.31 1							
6728		8.9 0			Fe	9.03			− 1	0	
6730		0.4 0	9.9 0		⊙	0.32			− 2N		
6733			3.35 1n		Fe	3.16	3	4.6	1	0	B
6734	4.45 1	4.59 1									
6737		7.24 1									
6739	9.72 3	9.64 2n	9.39 2		Fe	9.53	1	1.6	0	1	A
6743	3.27 2	3.17 2	3.13 3		Ti	3.14	10	0.9	1	4	A
6743				3.52 1−	S	3.58	6	7.8	− 2N	− 2N?	A
					⊙	5.56			− 2N	2	
6745	6.3 0	5.9 1N	6.0 0n		⊙	5.99			− 1	1	
6748	8.04 3n	8.1 1n			TiO	7.80	5				A
6748				8.69 1	S	8.79	8	7.8	− 2		A
6750	0.21 2	0.15 2	0.12 2	0.20 1	Fe	0.17	6	2.4	3	4	A
					Zr	2.73	10	1.0			A
6753	3.22 3	3.00 4	2.94 3		Fe	2.73	3	4.6	1	1d	B
					V?	3.02		1.1	− 2N		A
6755	6.1 0	6.1 0	5.83 1		Fe	5.61			0	0	C
6757				7.25 1+	S	7.20	10	7.8	− 1d	− 1	A
6757	7.9 0	7.6 0			Cr	7.76	4				
6762	2.30 1	2.35 2			Cr	2.42	5				
					Zr	2.41	20	0.0	− 2		
6764		4.45 1d									
6766		6.40 3	6.0 0		V	6.53	3				
6767	6.98 2n	7.74 2	7.85 3	7.66 1	Ni	7.79	20	1.8	4	5	A
6771	0.87 1	1.01 2	1.20 2		Co	1.07	50	1.9	0d	1d	A
6772	2.5 0	2.25 1	2.52 1	2.53 1	Ni	2.33	5	3.6	2	2	A
6774	4.1 0	4.30 1			La	4.28	6				
6775	5.2 0	5.89 1									
6777	7.4 0	7.66 2			⊙	7.78			− 3N		
6780				0.48 1							
6781	1.81 10	1.93 1n			TiO	1.93	5				A
6783	4.62 8	3.59 3	3.80 2		Fe	3.72	1	2.6	− 1		C
					V	5.02	2				
6784		5.10 2	4.75 1		TiO	5.81	4				C

TABLE III—*Continued*

Wave-Length Obs.	Betelgeuze	Aldebaran	Arcturus	Procyon	Identification				Sun		Contributor
					El.	W.-L.	Int.	E.P.	Dk.	Sp.	
6786	.....	6.94 2	6.55 2	.....	*Fe*	6.87	2	4.2	1	0	B
6789	9.7 0	9.96 1n	9.62 1	.....	*Sa+*	9.97	.....	.....	− 2	.....	.....
6791	1.5 0		1.15 1	.....	*Zr*	*0.89*	10	.....	.....	.....	.....
6793	4.05 3	3.70 3	3.49 2	.....	*V*	3.64	.....	0.1	0N	1	B
6796	6.36 2	6.29 3	6.18 1	.....	*Fe*	6.14	.....	.....	0	1d	A
6798	8.55 2	8.65 3	8.82 1	.....	*Ni?*	8.48	1	4.5	− 1	2	B
6801	1.18 2	1.26 1	.....	.....	⊙	1.21	.....	.....	− 3N	.....	.....
6804	3.83 2	3.95 2	4.30 1	.....	*Fe*	4.02	.....	4.6	0	1	A
					Fe	4.31	.....	.....	0	− 2	C
6806	7.07 3	7.02 3	6.85 2	.....	*Fe*	6.87	2	2.7	1	1d	A
6810	0.09 2	0.24 2	9.96 2	.....	*Fe*	0.28	4	4.6	3	2	A
					Zr	*1.32*	2	.....	.....	.....	.....
6812	2.55 2	2.58 2	0	.....	*V?*	2.37	.....	1.0	− 2N	.....	C
					Zr	*2.66*	3	.....	.....	.....	.....
6814	.....	.....	4.96 2	.....	*Co*	4.97	40	1.9	0	1d	A
6815	5.42 4	5.18 3	.....	.....	*TiO*	*5.27*	5	.....	.....	.....	A
					Fe−	9.61	pr	4.1	− 1d?	2	.....
6820	0.51 1	0.32 2	0.41 2	.....	*TiO*	*0.17*	3	.....	.....	.....	.....
					Fe	0.39	.....	.....	2	0	B
6821	.....	.....	.....	1.27 1+	.....	.....	.....	.....	.....	.....	.....
6824	4.61 1	.....	.....	.....	⊙	4.87	.....	.....	− 2N	.....	.....
6825	.....	.....	.....	5.14 1	.....	.....	.....	.....	.....	.....	.....
6825	5.85 1	.....	.....	.....	.....	.....	.....	.....	.....	.....	.....
6827	7.62 1	.....	.....	.....	*Mn*	*7.21*	.....	.....	− 2	.....	.....
					⊙	7.97	.....	.....	− 2	.....	.....
6828	8.67 1	8.35 3n	8.45 1	8.37 2	*Fe*	8.61	4	4.6	2	2	A
					Zr	*8.82*	10	1.4	.....	.....	C
6830	0.52 2	0.37 2n	.....	.....	.....	.....	.....	.....	.....	.....	.....
					V	*2.47*	2	.....	.....	.....	C
6832	2.85 3	2.87 4	.....	2.7 0	*V+?*	2.49	.....	1.6	− 3	.....	C
					Zr	*2.03*	12	0.1	.....	.....	B
					Fe	3.26	1	4.6	− 1	− 2	.....
6833	3.64 1	3.9 0	3.3 0	.....	*Mn*	*3.02*	4	.....	.....	.....	.....
					Zr	*3.69*	4	1.4	.....	.....	.....
6835	.....	5.3 0	.....	.....	.....	.....	.....	.....	.....	.....	.....
6837	7.14 2	7.06 1	.....	.....	*Fe*	7.03	.....	.....	0	− 1	C
					⊙	8.74	.....	.....	− 1	1d	.....
6839	9.29 2	9.76 1	9.59 1	.....	*Fe*	8.85	.....	.....	0	0	.....
					V	*0.59*	2	.....	.....	.....	.....
					Fe	9.85	2	2.5	1	2d	.....
					Fe	1.36	4	4.6	3	3	A
6841	1.93 2	1.65 2	1.55 2	.....	*Ti?*	1.05	.....	2.7	− 3N	.....	.....
					V	*1.90*	2	.....	.....	.....	C
					Ni	2.05	8	3.6	0	− 1	C
6843	.....	.....	3.38 2	.....	*Fe*	2.70	2	4.6	1	1d	.....
6843	.....	.....	.....	3.89 1	*Fe*	3.07	4	4.6	3	2	A
6844	4.29 1	4.4 0n	.....	.....	*Fe*	4.70	pr	1.6	− 3	.....	.....
					Zr	*5.30*	5	.....	.....	.....	.....
6846	6.69 2	6.83 2	6.81 1	.....	*Zr*	*6.42*	5	0.6	.....	.....	C
					Zr	*7.03*	18	1.5	.....	.....	A
6847	.....	.....	.....	7.16 1	.....	.....	.....	.....	.....	.....	.....
6848	.....	.....	8.95 1	.....	⊙	8.57	.....	.....	0Nd	1	.....
					Zr	9.31	8	1.5	− 2N	.....	.....
6850	0.21 3n	9.95 2n	.....	.....	*TiO*	*0.23*	5	.....	.....	.....	A
					Ni	0.45	2	.....	− 1N	.....	.....
6851	.....	.....	1.97 1	.....	*Fe*	1.66	pr	1.6	− 2	.....	.....
6852	2.16 3n	2.15 2	.....	.....	*TiO*	*2.33*	6	.....	.....	.....	A
6855	5.16 3n	5.09 3n	5.16 3	5.18 2	*Fe*	5.18	5	4.5	3	2	A
					Fe	7.27	.....	.....	0	1	B
6857	7.97 1n	8.14 1	7.87 1	7.62 2	*TiO*	*8.06*	4	.....	.....	.....	.....
					Fe	8.17	3	4.6	2	2	A
6859	.....	.....	.....	9.22 1	.....	.....	.....	.....	.....	.....	.....
6860	0.35 1	0.63 1	0.30 1	.....	*Fe?*	0.34	1	2.6	− 2	.....	.....
					Fe?	0.97	pr	2.8	− 2	.....	.....
					Ti	1.52	6	2.3	− 2	2	.....
6861	1.99 3	1.88 3	1.81 4N	.....	*Fe*	1.96	2	2.4	0	1d	.....
					Fe	2.51	2	4.5	1	0	.....
6881	.....	.....	.....	1.46 1+	⊙	1.47	.....	.....	− 1	.....	.....

TABLE III—*Continued*

Wave-Length Obs.	Betel-geuze	Alde-baran	Arc-turus	Pro-cyon	Identification				Sun		Con-tribu-tor
					El.	W.-L.	Int.	E.P.	Dk.	Sp.	
					Cr	1.73	2	3.4	o	3d	†
6881	.....	.....	1.72 1	.....	*Fe*	1.73	1	4.5	1	1d	.....
					Cr	2.53	5	3.4	1	od	.....
					Cr	3.07	10	3.4			.....
6910	0.30 1	.....	.....	.....	⊙	0.02	.....	.....	— 3N	.....	.....
6910	.....	.....	.....	0.81 1	⊙	0.74	.....	.....	— 3	.....	.....
6911	.....	.....	1.45 1	.....	*Fe*	1.54	1	2.4	— 1N	od	.....
6914	4.57 2	4.54 2	.... ×	.....	*Ni*	4.58	50	1.9	4	3	A‡
6916	.....	.....	6.78 1	.....	*Fe*	6.69	3	4.1	2	1	.....
6921	.....	1.43 2N	.....	.....		.....	.....	.....	.....	.....	§
					Cr	4.16	10	3.4	9	.....	A‖
6924	.....	4.42 2	.....	.....	*Cr*	5.29	6	3.4	1	2d	C
6926	6.07 1	5.99 2	6.27 2	6.08 1	*—Ti*	6.11	2	3.6	o	1d	.....
6928	8.07 1	×	.....	.....		.....	.....	.....	.....	.....	¶
6930	0.68 1	0.69 1	.....	.....		.....	.....	.....	.....	.....	.....
6931	.....	.....	1.21 1	1.30 1	*Mn*	1.13	5	.....	.....	.....	.....
					Fe	3.05	pr	4.2	oN	— 1	.....
6933	3.38 4	3.30 3	3.49 4	3.28 3	*Mn*	3.58	4	.....	.....	.....	.....
					FeAt	3.63	2	2.4	2	3	A
6935	.....	.....	.....	5.06 1	⊙	4.90	.....	.....	— 3	.....	.....
6945	5.58 4	5.42 4	5.16 2	5.26 2	*Fe*	5.22	4	2.4	4	4d	A**
6951	.....	.....	1.02 3	0.98 2	*Fe*	1.26	3	4.5	1	od	.....
					Fe	1.65	pr	4.3	— 2	.....	††
6951	1.78 3	1.32 3	.....	.....	*TiO*	1.5	.....	.....	.....	.....	.....
6953	.....	.....	3.40 3	.....	*Zr*	3.87	20	0.6	.....	.....	A
6954	4.30 5n	4.48 5	.....	.....	*At*	3.59	.....	.....	.....	.....	‡‡
6957	7.87 2	.....	.....	.....		.....	.....	.....	.....	.....	.....
6959	9.69 2	9.67 2	.....	.....		.....	.....	.....	.....	.....	.....
6962	2.81 2n	2.80 2n	.....	.....		.....	.....	.....	.....	.....	§§
6964	.....	.....	.....	4.12 2		.....	.....	.....	.....	.....	.....
6965	5.2 o	6.04 3n	5.16 2	.....	*Ni*	.....	.....	.....	.....	.....	.....
6966	6.59 3	.....	.....	.....	*Zr*	6.49	12	1.6	.....	.....	A
6967	.....	.....	.....	7.83 1	*Mn*	8.00	3	.....	.....	.....	.....
6969	.....	.....	.....	9.94 2		.....	.....	.....	.....	.....	.....
6971	1.10 5N	1.28 3N	1.30 2N	.....	*Fe*	1.95	1	3.0	— 1	1	C
6973	.....	.....	.....	3.07 1		.....	.....	.....	.....	.....	.....
6974			4.5 o			.....	.....	.....	.....	.....	.....
6976	4.90 2n	5.07 3n	6.88 1	6.41 2N	*Fe*	6.28	1	4.6	— 2N	.....	.....
					Si	6.53	4	.....	1	— 2	A
					At	7.48	.....	.....	.....	.....	.....
					Cr?	8.42	15	3.4	1N	2d	B
6978	8.77 7	8.79 6	8.77 4	8.94 2	*Fe*	8.88	3	2.5	2	3	A
					Cr	9.81	7	3.4	1	1d	C
6981	1.58 1	1.5 o	1.69 2	.....		.....	.....	.....	.....	.....	.....
6982	.....	.....	.....	2.68 1		.....	.....	.....	.....	.....	.....
6984	4.33 1	4.5 o	4.5 o	.....		.....	.....	.....	.....	.....	.....
6986	6.58 1	6.76 1	6.26 2	6.06 2	*At*	6.59	.....	.....	.....	.....	.....
					TiO	8.51	1	.....	.....	.....	C
6988	8.76 4	8.46 1	.....	.....	*Fe*	8.54	2	2.4	o	2	A
6990	0.49 4	0.44 1n	.....	.....	*Zr*	0.86	18	0.6	1	.....	A
6994	4.56 3	4.63 2	.....	.....	*Zr*	4.39	12	0.7	— 3	.....	A
6996	6.91 2	.....	.....	.....	*Ti*	6.68	1	2.3	.....	.....	B ‖ ‖
6999	9.75 4	9.80 2n	.....	.....	*Fe*	9.91	3	4.1	1	1	C
7001	1.63 2	1.50 1	1.69 1	.....	*Ni*	1.56	1	1.9	— 1	.....	C

† This line is too near the tail of the atmospheric B band for study.

‡ Blended with Atm 6913.6 in Arcturus.

§ Blended with Atm 6923.75.

‖ Separated from the atmospheric line at this wave-length by the large positive radial-velocity shift in Aldebaran.

¶ Blended with Atm 6929 in Aldebaran.

** Blended with Atm 6947.55 in Aldebaran and Betelgeuze.

†† On plates of Aldebaran and Betelgeuze this line is blended with Atm 6953.8. In Arcturus and Procyon the blend is with Atm 6950.7. Bobrovnikoff lists a *TiO* band at 6951.9 in α_1 Herculis.

‡‡ Blended with Atm 6956.4 in Betelgeuze and Aldebaran.

§§ On one plate of Betelgeuze two lines are barely resolved.

‖ ‖ Blend Atm 6998.98.

TABLE III—*Continued*

Wave-Length Obs.	Betel-geuze	Alde-baran	Arc-turus	Pro-cyon	Identification				Sun		Con-trib-utor
					El.	W.-L.	Int.	E.P.	Dk.	Sp.	
7004	4.31 3	4.18 2	.....	.....	.....	.....	.....	.....	.....	.....	.....
7008	8.13 2	8.19 2	8.20 1	.....	*Fe*	7.99	2	4.2	o	1d	.....
					Ti	*8.32*	1	.....	.....	.....	B
7011	1.06 3	1.15 2	1.05 3	.....	*Ti*	*0.94*	1	.....	.....	.....	B
					At, Fe	1.34	.....	.....	2	.....	.....
7012	.....	.....	2.87 1	.....	.....	.....	.....	.....	.....	.....	.....
7014	.....	.....	4.88 1	.....	.....	.....	.....	.....	.....	.....	.....
7016	6.21 3	6.39 4	.....	.....	*Fe*	6.08	.....	4.6	1	.....	.....
					Fe	6.45	.....	4.1	3	.....	.....
					At	6.45	.....	.....	.....	.....	.....
					Co	*6.59*	35	.....	.....	.....	.....
7019	.....	.....	9.10 1	.....	.....	.....	.....	.....	.....	.....	.....
7020	0.36 1	.....	0.04 1N	.....	.....	.....	.....	.....	.....	.....	.....
7022	2.90 2	2.8 o	3.01 2	3.00 2	*Fe*	2.97	3	4.2	2	2	A
7024	4.59 2	4.80 2	4.43 2	.....	*Fe*	4.65	2	4.5	1	od	.....
					Ni	4.89	3	4.5	o	.....	.....
7027	7.22 1	7.37 1	.....	.....	*Zr*	*7.40*	15	0.6	.....	.....	A¶¶
7029	.....	9.03 1	9.35 1	.....	⊙	9.00	.....	.....	o	.....	.....
					⊙	9.13	.....	.....	− 1	.....	.....
7030	.....	0.77 1	.....	.....	.....	.....	.....	.....	.....	.....	.....
7032	.....	2.3 o	2.53 1	.....	⊙	2.33	.....	.....	1	1	.....
7033	3.12 2N	3.4 o	.....	.....	*Ni*	4.41	1	3.5	− 3N	.....	.....
7034	.....	4.9 1	4.91 1	.....	*Fe*	4.92	.....	2.8	2N	1	.....
					Si	*4.92*	7	5.8			.....
7034	.....	.....	.....	4.55 1+	.....	.....	.....	.....	.....	.....	.....
7037	8.46 6	8.51 6n	7.08 2	.....	*At, Ni*	7.21	2	5.5	o	.....	.....
					Fe	8.24	3	4.2	1	1d	.....
7039			9.02 4	9.20 2	*Fe*	8.79	1	4.2	o	.....	.....
					Ti	*8.83*	3	.....	.....	.....	B
7041	.....	.....	1.75 1	.....	.....	.....	.....	.....	.....	.....	.....
7042	2.34 1	.....	.....	.....	⊙	2.48	.....	.....	− 3	.....	.....
7044	5.05 4n	4.98 2n	4.69 1	.....	*Fe?*	4.69	.....	4.9	− 1	− 1	C
7047	6.97 1n	7.3 o	7.09 1	.....	.....	.....	.....	.....	.....	.....	.....
7048	×	8.91 1	.....	.....	⊙	9.01	.....	.....	− 3	.....	.....
7049	.....	.....	.....	9.91 1	.....	.....	.....	.....	.....	.....	.....
7050	0.36 2	0.71 1	0.68 2	.....	*Ti*	*0.68*	1	.....	.....	.....	B
7051	.....	.....	.....	1.90 1	.....	.....	.....	.....	.....	.....	.....
7052	2.72 2	2.80 3	2.81 3	.....	*At*	2.79	.....	.....	1	o	.....
					Co?	2.93	60	1.9	o	—	.....
7054	4.29 10	4.76 5n	.....	.....	*TiO*	*4.51*	8	.....	.....	.....	A
7056	.....	.....	6.41 1	6.36 1	⊙	6.48	.....	.....	− 3	.....	.....
7058	.....	.....	8.79 1	.....	.....	.....	.....	.....	.....	.....	.....
7060	9.92 4	0.12 2	0.31 2	.....	*Ba*	*9.94*	400	1.2	—	—	.....
					TiO	*0.01*	3	.....	.....	.....	.....
					At−	0.45	.....	.....	1N	o	.....
7063	2.85 1	3.14 1	3.00 1	.....	*Ni*	2.99	4	1.9	− 2N	.....	A
7066	6.11 1	6.15 2n	5.95 2	.....	*La+*	6.23	300	0.0	− 2d	.....	C
7068	8.73 2n	8.75 3	8.77 2	.....	*Fe*	8.42	3	4.9	2	1	B
					Ti	9.09	2	3.2	− 3N	− 1	B
7072	2.0 o	.....	.....	.....	.....	.....	.....	.....	.....	.....	.....
	2.9 o	2.5 o	2.21 1n	.....	*Fe*	1.87	1	4.6	oN	− 3	B
7074	4.89 1	4.4 o	4.81 1n	.....	.....	.....	.....	.....	.....	.....	.....
7076	6.86 1	6.49 1	8.45 2N	.....	.....	.....	.....	.....	.....	.....	.....
7079	9.24 1	9.28 1			.....	.....	.....	.....	.....	.....	.....
7082	3.13 1	2.67 1	.....	.....	.....	.....	.....	.....	.....	.....	.....
7084	4.77 3	4.72 5	4.86 4	.....	*Co*	4.99	100	1.9	2N	3	A
7087	7.15 10	7.88 5	.....	.....	*TiO*	*7.89*	12	.....	.....	.....	A
					Zr	*7.35*	20	0.6	.....	.....	C
7088	.....	.....	8.07 1	7.89 1	.....	.....	.....	.....	.....	.....	.....
7090	0.05 4	0.30 1	0.46 2	.....	*Fe*	0.40	3	4.2	2	2	B
7090	.....	.....	.....	0.71 1	.....	.....	.....	.....	.....	.....	.....
7092	2.97 5n	3.07 1	2.92 1	.....	*TiO*	*3.17*	4	.....	.....	.....	A***
					Zr	*4.61*	7	1.5	.....	.....	A
7095	5.18 3	5.40 1n	5.37 1	.....	*Fe*	5.42	2	4.2	o	− 1	B
					Zr	*5.66*	8	1.5	.....	.....	A
7097	7.60 2	7.74 1	7.76 1	.....	*Zr*	*7.78*	25	0.7	.....	.....	A
7099	9.41 2	9.4 o	9.9 o	.....	.....	.....	.....	.....	.....	.....	.....

¶¶ Separated from Atm 7027.49 by radial velocity shift.

*** Not due to *TiO* in Arcturus.

TABLE III—*Continued*

Wave-Length Obs.	Betel-geuze	Alde-baran	Arc-turus	Pro-cyon	Identification				Sun		Con-trib-utor
					El.	W.-L.	Int.	E.P.	Dk.	Sp.	
7100	0.99 2	1.3 0									
7103	3.10 3n	3.32 4n	2.85 2n		*Zr*	2.95	20	0.6			A
					Zr	3.77	18	0.0			A
7105				5.66 1							
7107	7.66 2	7.28 2n	7.35 1		*Fe*	7.48	1	4.6	0	1	A
					Ni	0.92	3	1.9	1	1d	B
7111	1.47 4n	1.44 4n	1.14 2n		*Zr*	1.71	12	0.5			A
					Fe	2.19	1	3.0	0	1	B
7115	5.09 2n	5.05 1	4.96 1n								
7117	7.22 1	7.49 1	7.66 1N								
7119	9.82 1	0.13 1	9.72 1N								
7122	2.63 1	2.39 2	2.34 2	1.99 2	*Ni*	2.22	100	3.5	4	6	A
7125	5.14 9	6.01 5n			*TiO*	5.61	14				
7127			7.42 1								
7130		0.91 3n	0.71 2n	0.86 1	*Fe*	0.94	4	4.2	3	4	
7131	1.64N				*TiO*	1.34	5				
7133		3.39 2	3.51 1n								
7135	5.66 1	5.69 2	5.96 1		*Ti*	5.54	1				B
7139	9.61 1	9.20 4n	9.20 2N		*At, Ti*	8.95	1	1.4	− 2	2	B
7142		2.35 1	2.68 1	2.36 1	*Fe*	2.53			0	− 2	A
7143		3.7 0									
7145		5.39 1	5.29 1		*Fe*	5.32	1	4.6	1	− 1	A
7148	8.4 0	8.35 3	8.06 4	8.10 2	*Ca*	8.16	10	2.7	3N	7	A
					Mn	1.28	3				
7151	1.39 1	1.25 2	1.02 2		*Fe*	1.48	1	2.5	− 1		
7153		3.1 0									
7155	5.4 2	5.33 3	5.45 2		*Fe*	5.65	1	5.0	0N	0	
7155				5.97 1N							
7158	9.72 4N	8.87 2	8.69 1	8.47 1N	*TiO*	9.03	6				B
7160		0.38 2	0.56 1								
7161				1.67 1N							
7163				3.92 1							
7164	5.17 1	4.44 2	4.48 4		*TiO*	4.31	4				†††
					Fe	4.45	4	4.2	2	4	A
7165				5.48 1	*Si*	5.57	15	5.8	1N	− 2	A
7169		9.02 3			*Zr*	9.14	40	0.6			A‡‡‡
7174	4.61 2				*Mn*	4.46					
7177	7.93 1										
7180	0.00 2				*Fe*	0.01		1.5	− 2		
7181	1.17 2				*Fe*	1.21	2	4.2	0	1	
7187	6.96 1	7.30 1			*Fe*	7.39	5	4.1	5N		A§§§
7188	8.78 2N										
7190	0.16 2				*Ti*	9.92	2	2.6			B
7197	7.47 4	7.16 2			*Ni*	7.02	5	1.9	0	1	A||||
					TiO	7.67	3				A
7203	3.74 1				*TiO*	3.64	4				A
7207	7.69 2	7.49 4	7.46 1		*Fe*	7.41	3	4.1	1	0	C¶¶¶
					Ti	9.51	5	1.5	3	6	A****
7209	9.53 4	9.59 4	9.43 4		*At*	9.51					
7211				1.05 1							
7213	3.66 3N	3.65 4N									
7214				4.96 1							
7216	6.48 3	6.40 2	6.37 3n		*Ti*	6.19	5	1.4	− 2	3	A††††
					At	6.54			2		
7217				7.86 1							
7219	9.37 1	9.49 1			*TiO*	9.40	6				B
7221	1.47 1	1.41 3			*Fe*	1.22	1	4.5	0	− 2	C

††† Blended with Atm 7167 in Aldebaran.

‡‡‡ Blend with Atm 7170.3.

§§§ Listed as due to *Fe*-Atm in *Revised Rowland*. The stellar component is clearly separated in Aldebaran by velocity shift.

|||| The *Ni* line 7197.02 is separated from Atm 7197.23 by radial velocity shift in Aldebaran. May be blended with Atm 7198.4.

¶¶¶ Blended with Atm 7206.43 in Arcturus. Blended with Atm 7209.51 in Aldebaran and Betelgeuze.

**** Blended with Atm line at same wave-length in Arcturus. The stellar component is clearly separated in Aldebaran.

†††† Blended with Atm 7216.54 in Arcturus. Separated in Aldebaran and Betelgeuze.

TABLE III—*Continued*

Wave-Length Obs.	Betel-geuze	Alde-baran	Arc-turus	Pro-cyon	Identification				Sun		Con-trib-utor
					El.	W.-L.	Int.	E.P.	Dk.	Sp.	
7223	3.763	3.732	3.415	.....	*Fe*	3.65	2	3.0	3	.....	.....
					At	3.65	....	....	3	.....	‡‡‡‡
7228	9.023	8.763	8.412	.....							
7236	6.803n	6.391	.....	.....							
7240	0.253n	.....	.....	.....							
7244	4.855	4.863	.....	.....	*Ti*	4.87	4	1.4	− 1	4	A
					Fe	4.87	2	4.9			
7245	.....	.....	5.342	.....							
7246	6.831	.....	.....	.....							
7248	.....	.....	.....	8.51							
7251	1.685	1.633	.....	.....	*Ti*	1.73	4	1.4	− 2N	3	A§§§§
7254	3.981	4.07 1n	.....	.....	*Ti*	*3.76*	1	....	.....	.....	.....
7258	9.011	8.811	.....	.....							
7259	.....	.....	.....	9.95 1n							
7261	1.275	1.595	1.524	1.69 1n	*Fe*	1.52	....	....	− 1N	.....	‖‖‖‖‖
					Ni	*1.93*	....	....	.....	.....	.....
					At−	2.01	....	....	1	.....	.....
7264	.....	.....	4.702	.....							
7266	6.272	6.251	.....	.....	*Ni*	6.15	....	....	− 3N	.....	.....
					TiO	*9.05*	6	....	.....	.....	A
7271	1.315	×	.....	.....	*At*	2.99	....	....	5N	.....	.....
					TiO	*3.93*	5	....	.....	.....	A
7278	8.122N	8.561n	.....	.....							
7280	.....	.....	.....	0.402						..	
7280	.....	0.951n	.....	.....							
7281	1.625n	.....	.....	.....							
7282	.....	2.242n	2.181n	.....							
7284	4.323	.....	.....	.....	*Mn*	3.81	6	4.4	− 3N	.....	.....
					Fe	4.85	....	....	− 1	− 1	.....
7285	.....	5.343n	.....	.....	*Fe*	5.28	....	2.9	− 2	− 3	.....
7288	8.624	.....	.....	.....	*Fe*	8.76	3	4.2	− 1	− 1	.....
					Si	9.20	500	5.6	0Nd?	− 3	.....
7291	1.115	1.253	.....	.....	*TiO*	*0.80*	5	....	.....	.....	A
					Ni	1.46	1	1.9	− 1	0	A
7292	.....	.....	.....	2.331							
7293	3.042	3.153	2.872	.....	*Fe*	3.06	1	4.2	− 2N	.....	.....
7295	5.052	5.311	.....	.....	*Fe*	5.05	....	....	1	.....	A
7297	7.503	7.882	.....	.....	*TiO*	*7.01*	3	....	.....	.....	A
7299	9.434	9.642	.....	.....	*Ti*	9.65	2	1.4	0N	.....	A¶¶¶¶
7302	2.794	2.73n	.....	.....	*Mn*	2.87	6	4.4	− 3	.....	C*****
7307	7.904	8.063	.....	.....	*Ti*	*8.18*	1	....	.....	.....	A
7310	0.653	.....	0.672	0.501	*Fe*+	0.21	pr	3.9	− 1	.....	C
					Fe	1.10	2	4.3	0Nd?	− 1	C
7311	.....	1.193	.....	.....	*Fe*	1.10	2	4.3	0Nd?	− 1	.....
7312	2.541	.....	.....	.....							
7315	5.364	.....	.....	.....							
7318	.....	8.323	.....	.....	*Ti*	*8.43*	2	....	.....	.....	A
7319	9.982	.....	.....	.....							
7320	.....	0.881	0.691	0.482	*Fe*	0.69	0	3.9	1	1	B
					Fe+	0.69	....	4.9			
7322	2.915	.....	.....	.....							
7323	.....	3.872	.....	.....							
7325	5.474	.....	.....	.....							
7326	.....	6.124	6.423	6.534	*Ca*	6.18	2	2.9	0	5	B
					Mn	*6.50*	7	4.4	− 2	.....	B
7337	.....	7.671	7.471	.....							
7338	8.541	.....	.....	.....	*V*	*8.93*	3	....	.....	.....	.....
7339	.....	9.181	.....	.....							
7344	4.308	4.545	4.305	.....	*Ti*	*4.74*	3	1.5	− 2	.....	A††††
7346	6.641	.....	.....	.....							
7350	.....	.....	0.292N	.....							
7351	0.893	1.173n	.....	.....	*Ni*	*1.16*	....	....	.....	.....	.....

‡‡‡‡ Separated from Atm line at same wave-length in Aldebaran and Arcturus.

§§§§ Separated from Atm 7252.9 by velocity shift in Aldebaran.

‖‖‖‖‖ Blend with Atm 7262.01.

¶¶¶¶ The titanium line is separated from the terrestrial component in Aldebaran.

***** Blended with Atm 7304.19 in Aldebaran.

†††† May be blended with Atm 7343.95 and 7344.76 in Arcturus.

TABLE III—*Continued*

Wave-Length Obs.	Betel-geuze	Alde-baran	Arc-turus	Pro-cyon	Identification				Sun		Con-trib-utor
					El.	W.-L.	Int.	E.P.	Dk.	Sp.	
7355	5.94 5	5.95 3	5.89 3	6.00 1	*Cr*	5.89	10	2.9	1	5	A
7357	7.81 5	7.76 2	7.60 2	.....	*Ti*	7.76	3	1.4	− 1	.....	A
7360	.....	.....	0.21 1	0.17 1	.....	.....	.....	.....	.....	.....	.....
7361	.....	.....	1.65 1	1.48 1	*Al*	1.58	6	.....	.....	.....	C
					Al	2.32	10	.....	.....	.....	C
7362	2.16 3	2.01 4	.....	.....	*Fe*	2.32	0	1.6	.....	.....	C
7363	.....	.....	.....	3.38 1	.....	.....	.....	.....	.....	.....	.....
7364	4.17 4	4.05 3	4.02 3	.....	*Ti*	4.04	2	1.4	− 2	.....	A
7365	.....	.....	.....	5.18 1	.....	.....	.....	.....	.....	.....	.....
7366	6.64 3	6.70 3	6.41 3	6.45 1	*Fe*	6.41	.....	.....	.....	.....	A
					Ti	6.58	1	1.4	.....	.....	B
7368	.....	.....	.....	8.31 1	.....	.....	.....	.....	.....	.....	.....
7369	9.80 3n	9.58 2n	.....	.....	*Fe*	0.18	.....	.....	− 1N	.....	.....
7370	.....	.....	.....	0.99 1	.....	.....	.....	.....	.....	.....	.....
7372	2.59 1	.....	.....	.....	.....	.....	.....	.....	.....	.....	.....
7373	.....	3.00 1n	3.31 1	3.11 1	⊙	3.06	.....	.....	− 1	.....	.....
7374	.....	.....	4.74 1	.....	.....	.....	.....	.....	.....	.....	.....
7375	.....	.....	.....	5.56 1n	.....	.....	.....	.....	.....	.....	.....
7376	6.71 2n	6.56 1n	6.42 1	.....	.....	.....	.....	.....	.....	.....	.....
7377	.....	.....	.....	7.32 1	.....	.....	.....	.....	.....	.....	.....
7382	2.20 4	2.30 3n	2.57 2n	2.55 2n	*Ni*	2.00	.....	.....	− 1	.....	.....
					Ni	5.30	1	.....	1	.....	.....
7385	5.65 4	5.74 2n	5.38 1N	.....	*Ni*	6.24	.....	.....	− 2	.....	.....
					Fe	6.37	.....	.....	1N	.....	.....
7386	.....	.....	.....	6.77 2N	⊙	7.74	.....	.....	1N	.....	.....
7389	9.88 5	9.48 4	9.31 2	9.53 2	*Fe*	9.39	3	4.3	2	1	B
7390	.....	.....	0.84 1	0.88 2	.....	.....	.....	.....	.....	.....	.....
7393	3.66 3	3.63 3	3.55 2	3.49 1	*Ni*	3.61	10	3.6	2	1	A
7396	.....	.....	6.36 2	6.24 1	.....	.....	.....	.....	.....	.....	.....
7397	.....	7.81 1n	.....	.....	.....	.....	.....	.....	.....	.....	.....
7400	0.39 5	0.23 3	0.17 2	0.34 2n	*Cr*	0.18	10	2.9	1	4	A
7401	.....	1.64 1	1.66 1	.....	*Ni*	1.12	4	5.6	.....	.....	.....
7403	.....	.....	.....	3.13 1	.....	.....	.....	.....	.....	.....	.....
7405	.....	.....	5.81 2	5.81 2	*Si*	5.79	200	.....	1	− 1	A
					Si	5.95	200	5.6			
7406	6.21 3	6.09 1	.....	.....	.....	.....	.....	.....	.....	.....	.....
7409	9.27 3	9.15 2	9.22 2	9.23 2	*Si*	9.11	100	5.6	0	.....	B
					Ni	9.35	8	5.5 3.8	1	0	B
7411	1.27 3	1.23 2	1.05 2	1.17 1	*Fe*	1.16	3	4.3	1	1	A
7414	4.71 4	4.69 3	4.65 2	4.36 1	*Ni*	4.51	2	2.0	1	1	A
7415	.....	.....	.....	5.88 3n	*Si*	5.96	250	5.6	1	− 2	A
7417	8.00 3d	7.38 2	7.73 1	7.5 0	*Co*	7.39	10	.....	.....	.....	B
7418		8.76 1	9.20 1	9.0 0	*Fe*	8.67	.....	.....	0	− 1	B
					Ni	2.29	15	3.6	1	0	A
7422	3.35 1on	3.30 6n	2.19 3	3.30 3n	*Si*	3.51	400	5.6	1	− 3	A
7423			3.87 3		*Si*	4.65	20	5.6	− 1	.....	A
					Ti	3.12	2	1.4	.....	.....	.....
7430	1.11 3	0.76 3n	1.01 2n	.....	*Fe?*	0.87	.....	.....	− 1	.....	.....
7432	2.94 3	2.82 3	.....	2.63 1	*V?*	1.61	.....	.....	− 2	.....	.....
7433	.....	.....	3.48 1	.....	*Ni*	3.48	.....	.....	− 2	.....	.....
7435	.....	5.66 1	.....	.....	⊙	5.61	.....	.....	− 1	.....	.....
7437	.....	7.21 1	.....	.....	.....	.....	.....	.....	.....	.....	.....
7440	0.35 5	0.37 4	0.66 2	.....	*Zr*	0.89	20	0.5	.....	.....	A
					Ti	0.58	3	.....	− 2	.....	A
					Fe?	0.92	.....	.....	1	0	.....
					Fe	3.04	.....	.....	0	.....	.....
7442	2.99 2	2.96 1	3.02 1	.....	*Mn*	3.49	.....	.....	.....	.....	.....
7445	5.71 3	5.78 3	5.70 2	5.75 1	*Fe*	5.76	3	2.3	2	3	A
7448	.....	.....	8.99 1	.....	.....	.....	.....	.....	.....	.....	.....
7450	.....	.....	0.29 1	.....	.....	.....	.....	.....	.....	.....	.....
7451	.....	.....	1.66 1	.....	.....	.....	.....	.....	.....	.....	.....
7456	6.80 3	6.59 2	6.63 1	.....	⊙	5.43	.....	.....	− 2	.....	.....
					Co	7.35	.....	.....	− 2	.....	.....
7458	.....	.....	8.69 1	.....	⊙	8.40	.....	.....	− 2?	.....	.....
7462	2.12 6	2.10 5	2.00 3	2.26 2	*Cr*	2.34	10	2.9	2	5	A
					Fe+	2.34	pr	3.9			
7469	9.91 1	0.67 2n	.....	.....	.....	.....	.....	.....	.....	.....	.....
7471	1.53 1										

TABLE III—*Continued*

Wave-Length Obs.	Betel-geuze	Alde-baran	Arc-turus	Pro-cyon	Identification				Sun		Con-trib-utor
					El.	W.-L.	Int.	E.P.	Dk.	Sp.	
7475	5.55 2	4.99 1	5.58 1	.....	*Ti*	*4.93*	1	1.7	.....	.....	B
					⊙	*5.25*	....	....	− 2N	.....	.....
7479	9.42 1	.....	.....	.....	⊙	*9.73*	....	....	− 2	.....	.....
7481	1.90 1	1.95 2N	1.55 1	.....	*Ni*	*1.50*	2	....	− 2	.....	B
7482	.....	.....	.....	2.53 1s	.....	...	...	...	.....	.....	.....
7483	3.66 3	4.06 2N	.....	.....	.....	...	...	...	.....	.....	.....
7483	.....	.....	.....	3.89 1s	.....	...	...	...	.....	.....	.....
7489	9.39 2	9.42 2	9.41 1	.....	*Ti*	*9.60*	2	....	− 2	.....	B
7491	.....	.....	.....	1.25 1	.....	...	...	...	.....	.....	.....
7491	1.71 2	1.76 2	1.69 2	.....	*Fe*	1.65	2	4.3	1	1	A
7495	5.19 6	5.02 4	5.02 2	5.18 2	*Fe*	5.08	3	4.2	2	3	A
7498	.....	8.53 1	.....	.....	*Fe*	*8.56*	....	....	− 1	.....	.....
7505	7.08 1	7.22 2n	5.96 2	.....	⊙	*6.06*	....	....	− 1	.....	.....
7507			7.97 2	.....	*Fe*	7.28	....	4.4	1	1	.....
7511	1.09 3	1.07 3	0.98 3	1.01 3	*Fe*	1.03	4	4.2	2	3	A
7522	.....	.....	2.73 2	2.85 1	*Ni*	2.78	3	3.6	1	0	A
7523	3.01 2	3.06 3	.....	.....	.....	...	...	...	.....	.....	.....
7525	5.32 1	5.25 2	5.37 1	5.15 1	*Ni*	5.12	2	3.6	1	0	A
7528	.....	.....	8.72 1	.....	.....	...	...	...	.....	.....	.....
7531	1.05 1	1.11 2	1.16 3	1.02 1	*Fe*	1.15	....	4.4	2	2	A
7536	.....	.....	6.73 1	.....	.....	...	...	...	.....	.....	.....
7537	.....	.....	.....	7.95 1	.....	...	...	...	.....	.....	.....
7540	0.20 1	0.19 2	0.33 2	.....	⊙	*0.46*	....	....	− 2	.....	.....
7543	.....	3.60 1	.....	.....	.....	...	...	...	.....	.....	.....
7546	6.40 3	6.45 3	6.71 3	.....	*Fe*	*6.19*	....	....	1	.....	B
7550	.....	0.51 1n	.....	.....	⊙	*9.11*	....	....	− 2	.....	.....
					⊙	*1.13*	....	....	− 2	.....	.....
7554	.....	4.6 0	.....	.....	*Zr*	*4.73*	10	0.6	.....	.....	.....
					⊙	*4.86*	....	....	− 1	.....	.....
7555	5.16 3	5.31 2d	5.38 3	5.58 2	*Ni*	5.61	5	3.8	2	2	B
7558	.....	.....	8.34 1	.....	.....	...	...	...	.....	.....	.....
7559	×	9.43 2	.....	.....	*NiFe*	*9.71*	....	....	0	.....	B
7560	.....	.....	0.60 1	.....	.....	...	...	...	.....	.....	.....
7563	.....	3.32 1	2.94 1	.....	*Fe*	*3.02*	....	....	− 1	.....	A
7568	9.02 3	8.84 2	9.09 3	8.57 2	*Fe*	8.91	2	4.3	1	0	A
7574	4.47 3	4.43 3	4.19 3	4.20 2	*Ni*	4.05	1	3.8	1	0	A
7583	3.75 2	3.63 2	3.75 3	.....	*Fe*	3.80	2	3.0	1	2	A
7586	6.27 2	6.33 2	6.23 2	6.12 1	*Fe*	6.03	....	4.3	2	2	A
7589	9.79 3	9.09 1n	.....	.....	*TiO*	*9.62*	8	....	.....	.....	A

DISCUSSION OF STELLAR LINES BETWEEN 6562 A AND 7593 A

Hydrogen (*1*).—Hydrogen is represented by the line *Hα*, which has been taken as the starting-point for this investigation. The line is present on all spectrograms, with an intensity too strong for calibration.

Helium (*2*).—Since no B stars are included in this study, it is not to be expected that the helium lines would be evident. A number of plates of various B-type stars show quite strongly the line 6678 A. The lines 7065 A and 7281 A should also be present in B-type stars.

Lithium (*3*).—The ultimate doublet of lithium at 6707.83 A has an intensity of 4 in the sun-spot spectrum. It should be present in

Aldebaran and Betelgeuze. A line at 6707.43 A, intensity 2, in Aldebaran may be due to lithium, but the discrepancy in wave-length is rather high. It may be blended with a line of shorter wave-length,

TABLE IV

LINES IN VEGA AND SIRIUS, 6562–7593 A

Wave-Length Obs.	Vega Int.	Sirius Int.	Identification				Sun		Contributor
			El.	W.-L.	Int.	E.P.	Disk	Spot	
6562.8	20	20	*H*	2.82	.....	10.155	40	20	A
6586.8	0	1n	.....	.....	.....	.....	.....	.....	*
6588.3	1n	.....	.....	.....	.....	.....	.....	.....	.....
6591.4	1n	.....	*Fe*	1.35	.....	.....	− 1	− 2	.....
6594.1	1n	.....	.....	.....	.....	.....	.....	.....	.....
6717.5	1	.....	*Fe*?	7.54	.....	4.587	− 2	.....	.....
6719.7	1	.....	.....	.....	.....	.....	.....	.....	.....
6772.8	1	.....	.....	.....	.....	.....	.....	.....	.....
6794.6	2	0	⊙	4.63	.....	.....	− 2	.....	.....
6932.4	2	.....	⊙	2.51	.....	.....	− 3	.....	.....
6973.9	1	.....	.....	.....	.....	.....	.....	.....	.....
7001.7	1	1	.....	.....	.....	.....	.....	.....	.....
7042.0	1	.....	.....	.....	.....	.....	.....	.....	.....
7043.1	1	.....	.....	.....	.....	.....	.....	.....	.....
7044.6	1	.....	*Fe*	4.69	.....	4.934	− 1	− 1	.....
7078.7	2	.....	.....	.....	.....	.....	.....	.....	.....
7080.6	1	.....	.....	.....	.....	.....	.....	.....	.....
7161.3	1	.....	.....	.....	.....	.....	.....	.....	.....
7162.9	2	.....	.....	.....	.....	.....	.....	.....	.....
7167.3	1	.....	.....	.....	.....	.....	.....	.....	.....
7212.5	2	.....	*Fe*	2.44	.....	4.934	− 1	.....	.....
7306.5	1	.....	*Fe*	6.58	.....	4.160	− 1	− 2	.....
7321.2	.....	1	.....	.....	.....	.....	.....	.....	.....
7341.7	1	.....	.....	.....	.....	.....	.....	.....	.....
7354.8	1	.....	.....	.....	.....	.....	.....	.....	.....
7356.7	.....	1	.....	.....	.....	.....	.....	.....	.....
7360.7	.....	1	.....	.....	.....	.....	.....	.....	.....
7363.8	1	.....	*Fe*	3.97	.....	4.934	− 2	.....	.....
7372.3	1	.....	.....	.....	.....	.....	.....	.....	.....
7379.0	1	.....	.....	.....	.....	.....	.....	.....	.....
7389.5	1	.....	*Fe*	9.39	3	4.283	2	1	B
7406.3	.....	1	.....	.....	.....	.....	.....	.....	.....
7408.1	.....	1	.....	.....	.....	.....	.....	.....	.....

* A line is present at this wave-length on plates of Rigel, γ Orionis, and γ Pegasi.

but even the partial identification of the measured line in Aldebaran with the lithium line must be considered doubtful.

Carbon (6).—No strong neutral carbon lines occur in this region. *C* II 6578 A and 6582 A appear on plates of Rigel, γ Orionis, and other B-type stars.

Nitrogen (*7*).—The line 7468.7 A is not observed on spectrograms of Vega or Sirius, possibly because the spectra are of slightly inferior quality at this point. Merrill[5] reports this line as present in α Cygni, intensity 2. He also records *N* I 7423.88 A, intensity 0, and 7442.56 A, intensity 0.

Oxygen (*8*).—A line at 7001.7 A in Vega and Sirius may be *O* I 7002.2, although the discrepancy in wave-length is rather large.

Fluorine (*9*).—Most of the strong lines of neutral fluorine listed by Miss Moore in her compilation, "A Multiplet Table of Astrophysical Interest," are in the spectral region under consideration. They do not occur on any of the plates studied. They should be looked for in early-type stars because of their high excitation potentials, 12–13 volts.

Neon (*10*).—Recently some of the strong neon lines in the red were reported[6] by Miss MacCormack to be present in Rigel and γ Pegasi. When spectrograms of these stars in the extreme red become available, they should be examined for the strong neon lines of this region.

Magnesium (*12*).—Neither *Mg* I 7193 A nor 7387 A occurs on any of the plates examined.

Aluminum (*13*).—Two lines of neutral aluminum at 6696.04 A and 6698.68 A appear on plates of Arcturus and Aldebaran.

Silicon (*14*).—Practically all of the neutral silicon lines listed by Miss Moore are slightly weakened in the sun-spot spectrum. Consequently it is anticipated that the lines will be relatively weak in Betelgeuze and Aldebaran as compared with Arcturus and Procyon. Table V illustrates this.

Sulphur (*16*).—The case for neutral sulphur in the sun has recently been presented by Miss Moore and Babcock.[7] In their discussion they state:

> The presence of the group at λ 6743 is more doubtful, if the spot intensities in this region are considered. Two of the lines, λ 6743 and λ 6757, have each been assigned a spot intensity of −2N which precludes their identification as *S*, of excitation potential 7.8 volts, since lines of this excitation would be completely obliterated. The absence of this multiplet makes the presence of the later series members extremely doubtful.

[5] *Ap. J.*, **79**, 183, 1934.

[6] *Pub. A.S.P.*, **46**, 64, 1934.

[7] *Ap. J.*, **79**, 492, 1934.

On the basis of the present work,[8] this group may now be unqualifiedly identified as due chiefly to sulphur since the lines are present in Procyon and absent from all the other stars considered. The fact that two lines of the group, 6757 A and 6743 A, are not obliterated in the spot spectrum indicates a blend with some other element, as pointed out by Miss Moore and Babcock.

Attention is further called to the fact that Dunham in his work on α Persei[9] records three lines which agree so well in wave-length with the sulphur group at 4696 A as to leave little doubt as to their source.

TABLE V

LINES OF *Si* I

Wave-Length*	Int.	E.P.	Sun		Betelgeuze	Aldebaran	Arcturus	Procyon	Notes, Blends	
			Disk	Spot						
6976.80	10	.....	1	−2	.....	.....	1	2N	Atm	7.48
									Fe	6.28
7034.92	50	5.846	2N	1	.....	1	1	1+	*Fe*	4.92
7405.94	300	5.589	1	−1	.....	.....	2	2		
7409.14	100	5.591	0	.....	3	2	2	2	*Ni*	9.35
7416.08	250	5.591	1	−2	.....	.....	.....	3n		
7423.64	500	5.595	1	−3	10n	6n	3	3n	*Ni*	2.28
7424.70	20	5.594	−1	.....						

* Laboratory data from Kiess, *Bur. of Stand. J. of Research*, **11**, 775, 1933.

A well-exposed three-prism plate of Procyon taken at the Yerkes Observatory was examined for the group at 4696 A. The lines are unquestionably present. They do not appear in Albrecht's[10] table of lines in Procyon, doubtless because his plates are rather weak in this region. The data for sulphur are assembled in Table VI.

The presence of *S* II lines in the sun was recently suggested by Bartelt and Eckstein.[11] In the paper by Miss Moore and Babcock they show quite conclusively that the coincidences are due to chance. As they point out, the high ionization potential of *S* is wholly inconsistent with the presence of *S* II lines in the sun. Sometime ago the

[8] Announced in *Science*, **80**, 73, 1934.

[9] *Pub. of the Princeton Obs.*, No. 9, 1929.

[10] *Ap. J.*, **80**, 86, 1934.

[11] *Zs. f. Ap.*, **7**, 272, 1933.

writer[12] found that these lines come to a maximum of intensity at about B5. They persist in some of the early A-type stars, but are not strong even at their maximum and hence cannot be expected as late as G0. The one ionized sulphur line in the region studied in this paper is a weak one at 6981.65 A. It is not observed in Vega.

TABLE VI

LINES OF *S* I

LABORATORY			SUN		α PERSEI (DUNHAM)	PROCYON
Wave-Length	Int.	E.P.	Disk	Spot		
4694.13	10	6.50	0N	0b?	4.11 2	4.03 1+
4695.45	8	6.50	0N	0Bd	5.44 1	5.32 1−
4696.25	6	6.50	−1N	.....	6.25 1	6.47 0
6743.58	6	7.83	−2N	−2N?	.....	3.52 1−
6748.79	8	7.83	−2	.....	.....	8.69 1
6757.16	10	7.84	−1d?	−2N	.....	7.25 1+

TABLE VII

LINES OF *Ca* I

Wave-Length (Sun)	Int.	E.P.	Disk	Spot	Betelgeuze	Aldebaran	Arcturus	Procyon	Vega
6572.804	8	0.000	1	6	3	3	2	.....	.....
6717.697	30	2.697	5	8	4	3	4	2	1
7148.163	10	2.697	3N	7	0	3	4	2	.....
7202.211	3	2.697	1N	5	.....	.....	.....	.....	*
7326.176	2	2.920	0	5	4	4	3	4	†

* Masked by Atm lines.

† Blended with Atm 7327.38 A and *Mn* 7326.53 A (Procyon). The line in Betelgeuze is shifted about half an angstrom toward the violet, indicating another contributor.

Chlorine (*17*).—Two lines of chlorine of excitation potential 8.9 are found in the laboratory at 7256.65 A and 7547.09 A. No evidence for their presence in either Procyon or Vega has been found.

Argon (*18*).—The argon lines in the extreme red have too high an excitation potential to occur in stars of spectral classes later than A. Evidence of the presence of argon lines is lacking on the plates of Vega considered here. The presence of ionized argon in *υ* Sagittarii (B8p) was recently demonstrated by W. W. Morgan.[13]

[12] *Ap. J.*, **72**, 191, 1930. [13] *Ibid.*, **79**, 513, 1934.

Calcium (*20*).—Five strong calcium lines are observed in the laboratory in the extreme red. Their occurrence on the plates measured is indicated in Table VII.

TABLE VIII

Ti I LINES, 6562–7593 A

WAVE-LENGTH	INT.	E.P.	SUN		BET.	ALD.	ARC.	PROC.	NOTES, BLENDS
			Dk.	Sp.					
6599.13	3	0.896	−1	4	4	3	3	1	*Ni* 8.62
6666.60	2n	1.454	−2N	od	2N	3N	1N	.....	Blend at longer wave-length
6743.15	2	0.896	1	4	2	2	3	.....	
6861.47	2	2.258	−2	2	3	3	4N	.....	*Fe* 1.95; *Fe* 2.51
6926.11	2	3.567	0	1d	1	2	2	1	
6996.69	1	2.324	−3	−1	2	.....	.....	.....	
7008.32	1	.....	.....	.....	2	2	1	.....	*Fe* 7.99
7010.94	1	.....	.....	.....	3	2	3	.....	*Fe*; Atm 1.34
7038.83	3	.....	.....	.....	6	6	.....	.....	*Fe* 8.24
7050.68	1	.....	.....	.....	2	1	2	.....	
7069.11	2	3.166	−3N	−1	2n	3	2	.....	*Fe* 8.42
7138.92	1	1.437	−2	2	1	4n	2N	.....	Atm and *Ti* lines separated in Bet. and Ald.
7189.92	2	2.567	−2	.....	2	.....	.....	.....	
7209.44	5	1.454	3	6	4	4	4	.....	
7216.19	3	1.437	−2	3	3	2	3n	.....	Atm 6.54 in Arc.
7244.82	4	1.437	−1	4	5	3	2	.....	Atm 5.69 in Arc.
7251.74	4	1.424	−2N	3	5	3	.....	.....	
7253.76	1	.....	.....	.....	1	1n	.....	.....	
7299.67	2	1.424	cN	.....	4	2	.....	.....	
7308.18	1	.....	.....	.....	4	3	.....	.....	
7318.43	2	.....	.....	.....	.....	3	.....	.....	
7344.69	3	1.454	.....	.....	8	5	5	.....	
7357.73	3	1.437	−1	.....	5	2	2	.....	
7364.11	2	1.424	−2	.....	4	3	3	.....	
7366.58	1	1.424	.....	.....	3	3	3	1	*Fe* 6.41
7423.12	2	1.437	.....	.....	10n	6n	.....	.....	
7440.58	3	.....	.....	.....	5	4	2	.....	*Zr* 9.89
7474.93	1	1.741	.....	.....	2	1	1	.....	
7489.61	2	.....	.....	.....	2	2	1	.....	

Scandium (*21*).—The stellar line at 6604.27 A in Arcturus and Procyon is tentatively assigned to ionized scandium, 6604.609 A. The behavior of the observed line is satisfactory, since it is absent from Betelgeuze and Aldebaran.

Titanium (*22*).—The behavior of the titanium lines is shown in Table VIII. In general, their intensities increase in the cooler stars.

Bands of titanium oxide.—A number of *TiO* bands appear on the spectrograms of α Orionis and α Tauri. In the case of the former the three strong bands at 7054, 7087, and 7125 A are the most prominent features of this part of the spectrum.

The red infra-red system of *TiO* was recently discussed by N. T. Bobrovnikoff[14] for the star α_1 Herculis. This system, $^3\Sigma - {}^3\Pi$, has been measured in the laboratory by Miss Lowater[15] and by A. Christy.[16] Practically all of the bands found by Bobrovnikoff in α_1 Herculis are present, with about equal intensity in α Orionis. There is a definite weakening of these bands in α Tauri, as is to be expected.

In this study the plates were measured by setting the crosswire on the approximate center of the line. If there could be no question of the band nature, the setting was made on the head. In general, the measures give a wave-length a little high, since most of the bands appeared like diffuse lines.

The data for the *TiO* bands are assembled in tables according to sequence. The α_1 Herculis data are from Bobrovnikoff's paper. Laboratory figures are due to Miss Lowater.

There is no evidence for the presence of the *TiO* bands in Arcturus, type Ko. If they were present with Rowland intensity 1 or greater, they would doubtless have been detected. The absence of the three strongest *TiO* bands from the spectrum of Arcturus indicates definitely that any coincidences of measured lines in Arcturus with the weaker bands of *TiO* are accidental.

It appears that the bands of the red infra-red system of *TiO* first appear between Ko and K5. Hale and Adams[17] found the strongest band heads in the spectra of sun-spots. Their published illustration is quite convincing, especially for the band heads at 7054 A, 7088 A, and 7125 A. The sun-spot spectrum is usually considered to be of spectral class K2.

Professor A. Fowler[18] was the first to associate these bands in M-type stars with the bands of an oxide of titanium. In Richardson's

[14] *Ibid.*, **78**, 211, 1933.

[15] *Proc. of the Phys. Society*, **41**, 557, 1929.

[16] *Ap. J.*, **70**, 1, 1929.

[17] *Ibid.*, **25**, 75, 1907.

[18] *Proc. R. Soc.*, *A*, **73**, 219, 1904; **79**, 509, 1907.

study of molecular spectra in sun-spots[19] he concludes that the *TiO* bands which he examined were present in the sun-spot spectrum and were probably absent from the disk spectrum. The bands which

TABLE IX

TiO BANDS, SEQUENCE +1

v′, v″	LABORATORY		α_1 HERCULIS	BETELGEUZE	ALDEBARAN	NOTES, BLENDS
	W.-L.	Int.				
	R-Heads					
a 1, 0	6651.5	5	3	5	2N	
b	6681.1	6	4	5N	3n	
c	6714.4	6	3	5	1n	
a 2, 1	6719.3	6	3	.....	.....	*
b	6747.8	5	2	3n	1n	
c	6781.9	5	6	10	1n	
a 3, 2	6785.8	4	6	8	2	*Fe* 3.72
b	6815.3	5	4	4	3	*Co* 4.97
c	6850.2	6	2	3n	2n	*Zr* 9.31; *Ni* 0.45
a 4, 3	6852.3	6	1	3n	2	
b	6883.8	3	.....	.....	.....	In B band
c	6919.5	4	3	.....	.....	In B band
b 5, 4	6951.5	.....	2	2	3	*Fe* 1.25
c	6988.6	1	3	4	1	*Fe* 8.54
	Q-Heads					
a 1, 0	6657.7	2	1	.....	.....	
b	6686.0	1	1	1	2n	†
b 2, 1	6724.0	5	1	.....	.....	

* Band masked by *Ca* 6717.8.

† Probably not due to *TiO* in Aldebaran.

he studied were 4954 A and 5167 A, members of the blue-green system $^3\Pi - {}^3\Pi$.[20]

The blue-green system and the red infra-red system have the same lower electronic level. It would be of interest to determine

[19] *Ap. J.*, **73**, 216, 1931.

[20] Cf. Christy, *Phys. Rev.*, **33**, 701, 1929.

TABLE X

TiO BANDS, SEQUENCE o

v′, v″	Laboratory W.-L.	Laboratory Int.	α_1 Herculis	Betelgeuze	Aldebaran	Notes, Blends
	R-Heads					
a o, o	7054.5	8	10	10	5n	
b	7087.9	12	10	10	5	
c	7125.6	14	10	10	6	Also *Ra* 1, 1
b 1, 1	7159.0	6	2	4N	.....	
c	7197.7	8	.....	4	2	*Ni* 7.02; also *Ra* 2, 2
b	7230.4	4	.....	.....	.....	
c	7269.05	6	.....	5	.....	Blend with *Qa* 3, 3 and *Qa* 2, 2; also *Ra* 3, 3
b 3, 3	7303.04	5	.....	4	3N	Atm 3.80
	Q-Heads					
a o, o	7060.0	3	2	2	2	*Ba* 9.94
b	7093.2	4	2	5n	1	
c	7131.3	5	2	4N	.....	Also *Qa* 1, 1; *Fe* 0.94
b 1, 1	7164.3	4	.....	1	2	*Fe* 4.45
c	7219.4	6	.....	1	1	
a 2, 2	7203.6	4	.....	1	.....	
c	7273.9	5	.....	5	.....	Also *Qa* 3, 3; blend with *TiO* 7269.05

TABLE XI

UNCLASSIFIED *TiO* BANDS

Laboratory W.-L.	Laboratory Int.	α_1 Herculis	Betelgeuze	Aldebaran	Blends, Notes
6626.08	2	2	6N	.....	*Fe* 5.05, *V* 4.85, α(9, 12) *Ra*
6634.30	2	2	3N	.....	Unclassified
7290.80	5	.....	5	3	Unclassified *Ni* 1.46
7297.01	3	.....	3	2	Unclassified

which of the two systems first appears along the stellar sequence. According to the Draper classification,[21] the blue-green system becomes faintly visible at K5. On our spectrograms of the K5 star α Tauri, the bands of the red infra-red system are quite strong and, although absent from Arcturus K0, might be anticipated at about K2.

Vanadium (*23*).—For three lines in this region vanadium seems to be unblended. There is a general tendency for the observed vanadium lines to increase in intensity, proceeding in the direction of the

TABLE XII

V I LINES, 6562–7593 A

LABORATORY			SUN		BETELGEUZE	ALDEBARAN	ARCTURUS	NOTES, BLENDS
Wave-Length	Int.	E.P.	Disk	Spot				
6565.85	2	1.178	−3	−1?	?	2	1	Betelgeuze, line at 6566.62, *i* = 2
6578.97		1.039		−2	0	1		
6605.93	5	1.190	2N	2	2	2	1	
6607.90		1.345		−1	1	1		Blend *Fe* 6608.05
6624.84	5	1.213	3N	1	6N	4	3	*TiO*, 6626.08 in Bet. and Ald. *Fe* 6625.02
6753.02		1.076	2N		3	4	3	*Fe* 6752.72
6812.36		1.039	−2N		2	2	0	

cooler stars. Thus none of the lines listed in Table XII is visible in Procyon. In all cases the lines are stronger in Aldebaran than in Arcturus.

Chromium (*24*).—Chromium lines contribute to a number of blends. The three unblended lines listed in Table XIII show how rapidly the intensities increase in the cooler stars.

Manganese (*25*).—Although it is suspected that manganese may be a contributor in a few cases, there are no good identifications.

Iron (*26*).—Iron lines are fairly numerous in this part of the spectrum. About 150 lines are recorded, a number of which are unblended. Because of the wide range of excitation potential represented, the unblended lines were examined to note how the relative intensities of the lines in the four stars vary with the excitation potential.

[21] Cf., for instance, R. H. Curtiss, *Handbuch der Astrophysik*, **5**, Part I, 47, 1932.

In Figure 2 the ordinates are differences in intensity on my scale, all reduced to zero for Arcturus. The general trend is for the high-

TABLE XIII

Cr I LINES

Sun			E.P.	Betelgeuze	Aldebaran	Arcturus	Procyon
Wave-Length	Disk	Spot					
6630.04.....	−2	4	1.026	1	1	1	.....
7355.89.....	1	5	2.877	5	3	3	1
7400.22.....	1	4	2.887	5	3	2	2n

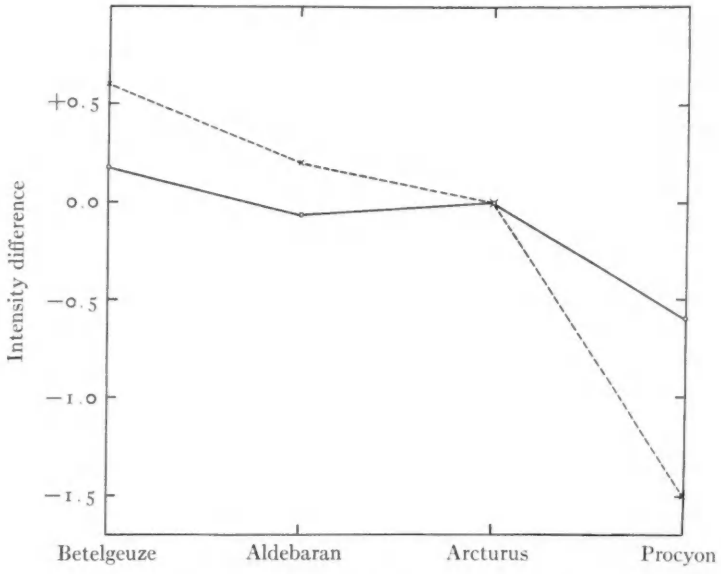

FIG. 2.—Comparison of iron lines of low and high excitation potentials. Dotted curve is based on twelve lines of average excitation potential 2.3 volts; solid curve on twenty-one lines of average excitation potential 4.4 volts.

excitation lines to be relatively stronger in Procyon than those of low excitation potential. The low-excitation lines are strengthened in Aldebaran and Betelgeuze relative to Arcturus and Procyon. The dotted curve is based on twelve lines whose average excitation po-

tential is 2.3 volts; the solid curve on twenty-one lines of average excitation potential 4.4 volts.

These stars cannot be considered homogeneous. For instance, between Betelgeuze and Procyon there is a difference in luminosity of

TABLE XIV

LINES OF *Zr* I

Wave-Length*	Betel-geuze	Alde-baran	Arc-turus	Pro-cyon	Laboratory		Sun		C.	Notes, Blends
					Int.	E.P.	Dk.	Sp.		
6603.27	3.11 1	.....	.....	.....	8	1.524	.....	.....	....	
6620.02	.....	0.56 1	.....	.....	5	2.313	.....	.....	....	
6752.73	3.22 3	3.00 4	2.94 3	.....	10	0.995	.....	.....	B	*Fe* 2.73; *V* 3.02
6762.38	2.30 1	2.35 2	.....	.....	20	0.000	−2	....	A	*Cr* 2.42
6828.82	8.67 1	8.35 3n	8.45 1	8.37 2	10	1.390	.....	.....	C	*Fe* 8.61
6832.93	2.85 3	2.87 4	.....	.....	12	0.070	.....	.....	A	
6846.42	6.69 2	6.83 2	6.81 1	.....	5	0.620	.....	.....	C	
6847.03					18	1.524	.....	.....	A	
6849.29	0.21 3n	9.95 2n	.....	.....	8	1.524	−2N	....	C	*TiO* 0.23; *Ni* 0.45
6953.87	4.30 5n	5	.....	.....	20	0.648	.....	.....	A	Atm 3.586
6966.49	6.59 3	6.04 3n	.....	.....	12	1.575	.....	.....	B	
6990.86	0.49 4	0.44 1n	.....	.....	18	0.620	.....	.....	B	
6994.38	4.56 3	4.63 2	.....	.....	12	0.684	−3	....	A	
7027.40	7.22 1	7.39 1	.....	.....	15	0.601	.....	.....	A	
7087.35	7.15 10	7.88 5	.....	.....	20	0.601	.....	.....	C	*TiO* 7.89
7094.61	5.18 3	5.40 1n	5.37 1	.....	7	1.524	.....	.....	A	
7095.66					8	1.524				
7097.78	7.60 2	7.74 1	7.76 1	.....	25	0.684	.....	.....	A	
7102.95	3.10 3n	3.32 4n	2.85 2n	.....	20	0.648	.....	.....	A	
7103.77					18	0.000				
7111.71	1.47 4n	1.44 4n	1.14 2n	.....	12	0.517	.....	.....	B	*Ni* 0.92; *Fe* 2.19
7169.14	Atm	9.02 3	.....	.....	40	0.620	.....	.....	A	Atm 7170
7439.89	0.35 5	0.37 4	0.66 2	.....	20	0.540	.....	.....	A	*Ti* 0.58; *Fe* 0.92

* Laboratory data from C. C. Kiess and H. K. Kiess, *Bur. of Stand. J. of Research*, **6**, 621, 1934.

about 7 mag. Consequently, the difference of intensity of the iron lines of either group among the four stars is not significant. The point of interest is the behavior of the two groups, *inter se*.

Strontium (*38*).—The strongest line of *Sr* I in this region, 6617.28 A, is absent from all spectrograms.

Yttrium (*39*).—A line at 6793.65 A has intensities of 3, 3, and 2 in Betelgeuze, Aldebaran, and Arcturus, and has been identified as partially due to *Y* I 6793.64. The identification is not considered

very strong because the equally intense laboratory line at 6687.57 A is very doubtfully present in these stars. The strongest *Y* I line, at 6435.02 A, is out of the range of this study. It has a disk intensity of -3 and a spot intensity of 3.

Y II 6613.8 may contribute to the stellar line at 6613.79 A. *Y* II 6795.41 is not observed on my plates.

Zirconium (*40*).—Twenty-four laboratory lines have been attributed to neutral zirconium. In a large number of these lines zirconium is considered an "A" contributor. In the list are the two resonance lines 6762.38 A and 6832.93 A. The absence of the strong line 6769.16 A is unexplained. The lines become stronger from Arcturus to Betelgeuze, which is consistent with the fact that the lines are strengthened in the spot spectrum.

Only two weak ionized zirconium lines are recorded in the laboratory spectrum of this region, consequently no test can be made on the basis of the present study.

Barium (*56*).—At 7060 A is a stellar line to which *Ba* I 7059.94 A may contribute. In the case of Betelgeuze the close agreement in wave-length is fortuitous, since on the two plates of this star the determinations are 7059.60 A and 7060.24 A. This line is just to the red of the strong *TiO* band head at 7054 A and is consequently difficult to set on.

Lanthanum (*57*).—Ionized lanthanum is represented by a line at 7066 A. In Betelgeuze and Aldebaran the identification seems fairly probable.

ACKNOWLEDGMENTS

This study was made possible by the co-operation of the Yerkes and the Perkins Observatories. It is a pleasure to acknowledge my indebtedness to the officials of these two institutions. Dr. H. T. Stetson and Dr. N. T. Bobrovnikoff generously placed the equipment of the Perkins Observatory at my disposal. I have also profited by numerous discussions with Dr. Bobrovnikoff. The problem was suggested by Dr. Otto Struve, director of the Yerkes Observatory, and developed under his active encouragement. To him I am deeply grateful for granting to me the opportunity of carrying on this work.

YERKES OBSERVATORY
July 30, 1934

THE ANALYSIS OF NOVA EMISSION BANDS*

By O. C. WILSON

ABSTRACT

It is assumed, following Gerasimovič and Chandrasekhar, that nova emission bands originate in spherical expanding gaseous envelopes having internal velocity gradients; also that the matter in the envelope is transparent to its own radiation and that Chandrasekhar's occultation effect may be neglected.

A method is then developed by which the velocity gradient can easily be found from the observed band shapes; all that is required is a simple integration.

The analysis is applied to the hydrogen emission contours recently measured in the spectrum of RS Ophiuchi.

In two very interesting papers Gerasimovič[1] and Chandrasekhar[2] have recently laid the foundations for the interpretation of nova and Wolf-Rayet emission bands in terms of expanding gaseous envelopes of non-uniform velocity. Essentially, their method is to make certain assumptions as to the physical properties of the envelope and to deduce the corresponding band shapes, which are then compared with the observations. From the practical standpoint, it would evidently be more satisfactory to reverse this procedure, and, beginning with the observed band shapes, deduce directly from them the properties of the gaseous envelope. In this paper we develop a means for doing this.

It will be well to state clearly at the outset what assumptions are made. These are: (1) the nova possesses complete spherical symmetry; (2) the nebular matter is entirely transparent to its own radiation; (3) Chandrasekhar's occultation effect is negligible; (4) matter is ejected from the star at a constant rate.

Numbers 1 and 2 are common to all work thus far done on this subject. As to assumption 4, we mean simply that if N be the number of atoms ejected over the whole star per unit time, then for $-\infty < t < t_1$, $N = 0$; for $t_1 \leq t \leq t_2$, $N = \text{Const.}$; and for $t_2 < t < +\infty$, $N = 0$. This assumption doubtless could be modified without great difficulty.

* *Contributions from the Mount Wilson Observatory, Carnegie Institution of Washington*, No. 500.

[1] B. P. Gerasimovič, *Zs. f. Ap.*, **7**, 335, 1933.

[2] S. Chandrasekhar, *M.N.*, **94**, 522, 1934.

Assumption 3 requires a little discussion. In the first place, the occultation effect does not appear naturally in our method as it does in Chandrasekhar's, and we have been forced to abandon it in order to gain advantages elsewhere. Second, there does not as yet seem to be any observational evidence to indicate that it is of sufficient magnitude to be important in real novae. In fact, we may recall that this effect demands a shift of the centers of gravity of all bands to the violet of the normal positions, while measurements of nova bands show that, in general, they are shifted to the red, in some cases by considerable amounts. Last of all, even though the occultation effect were important, our method would still be applicable to the violet sides. Thus, in what follows, where we compare our results with those of Chandrasekhar, it will be understood that we are referring to the violet sides of his theoretical contours. In any event, it is clear that the inclusion of assumption 3 will not seriously affect the usefulness of our method.

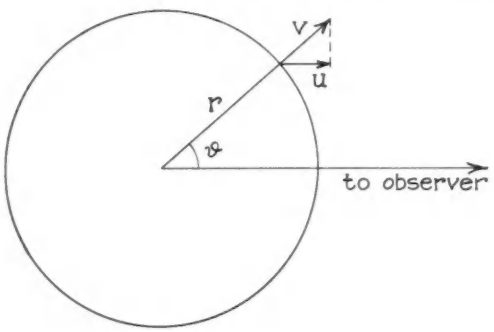

FIG. 1

The calculation starts with an obvious extension of the original work of Beals.[3] Consider a star surrounded by a spherical gaseous envelope. Measuring r and ϑ as shown in Figure 1, we have

$$u = -v \cos \vartheta. \tag{1}$$

The minus sign is inserted on the right-hand side of (1) to accord with the usual convention regarding the sign of a radial velocity. The zonal element of area on the sphere corresponding to r and ϑ to $\vartheta + d\vartheta$ is

$$dS = 2\pi r^2 \sin \vartheta d\vartheta \ ;$$

the element of volume within this zone between r and $r + dr$ is

$$d\tau = 2\pi r^2 \sin \vartheta d\vartheta dr \ .$$

[3] C. S. Beals, *ibid.*, **91**, 966, 1931.

Generalizing a trifle more than Chandrasekhar, we suppose that the emission dE due to the matter in $d\tau$ is given by

$$dE = k\rho^{\alpha}v^{\beta}d\tau \,, \tag{2}$$

or

$$dE = 2\pi kr^2\rho^{\alpha}v^{\beta} \sin\vartheta d\vartheta dr \,, \tag{2'}$$

where ρ and v are, respectively, the density and outward velocity at distance r. By assumption 1, both are functions of r only.

From equation (1), $du = v \sin\vartheta d\vartheta$, and, substituting in equation (2'), we have

$$dE = 2\pi kr^2\rho^{\alpha}v^{\beta-1}drdu \,. \tag{3}$$

But since

$$dE = dI(u)du \,,$$

$$dI(u) = 2\pi kr^2\rho^{\alpha}v^{\beta-1}dr \,. \tag{4}$$

This relation is, of course, merely Beals's result applied to a thin spherical element of the nebular envelope.

Now consider for a moment how an emission contour is built up. It is clear that we may think of the total contour due to an expanding envelope of finite thickness as consisting of a large number of elementary contours, originating in infinitesimal shells, superimposed on each other. Thus, the intensity at the value of u corresponding to point a in Figure 2 will be given by an integration of (4) along the strip ab. The only question is that of the limits of integration. The widest elementary contour will originate in the fastest-moving shell. This shell corresponds to point a. Clearly, b corresponds to that shell for which $u = v$. Thus the complete solution of the problem, subject to our assumptions, is given by

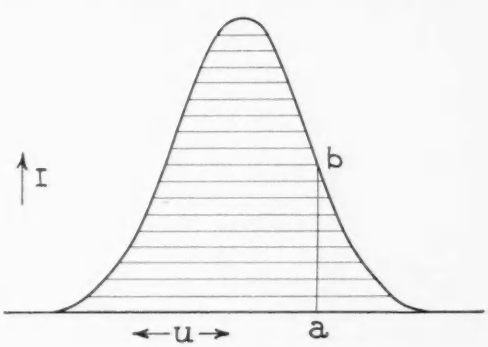

FIG. 2

$$I(u) = 2\pi k \int_{r(v_{\max})}^{r(u)} r^2\rho^{\alpha}v^{\beta-1}dr \,. \tag{5}$$

This formula would enable us to predict $I(u)$ readily enough, provided we knew ρ and v as functions of r. But we wish to turn the procedure around.

Differentiating (5) with respect to u, we get

$$\frac{dI(u)}{du}=I'=2\pi k\frac{dr}{du}r^2\rho^{\alpha}v^{\beta-1}. \tag{6}$$

On the right-hand side of (6) it must be remembered that $\rho=\rho(r[u])$ and $v=v(r[u])$, and, since we have specified that $r(u)$ is that value of r for which $u=v$, it is clear that $v(r[u])=u$. Thus we have

$$I'=2\pi k\frac{dr}{du}r^2\rho^{\alpha}u^{\beta-1}. \tag{7}$$

Since I' in this equation is a known function of u obtained from the measured band shape, (7) is a simple differential equation, the solution of which will give a relation between r and u. But, by the preceding argument, this is the same as the relation between r and v. Hence the solution of (7) and the substitution of v for u yields the desired velocity distribution in the nebular envelope as deduced from the observed contour $I=I(u)$. For the moment we may write (7) as

$$2\pi k\int r^2dr=\int I'u^{1-\beta}\rho^{-\alpha}du. \tag{8}$$

We now make use of assumption 4. The time required to traverse dr at distance r is $dt=dr/v(r)$. During this interval Ndt atoms are ejected, which will all be found between r and $r+dr$. Thus the density at r is

$$\rho(r)=\frac{Ndt}{4\pi r^2dr}=\frac{N}{4\pi r^2v(r)}. \tag{9}$$

Inserting (9) in (8) and remembering to put $u=v$, we have

$$K\int r^{2-2\alpha}dr=\int I'u^{1-\beta+\alpha}du, \tag{10}$$

with $K=2^{1-2\alpha}\pi^{1-\alpha}kN^{\alpha}$.

Equation (10) is the final solution of the problem, but, before applying it, attention must be called to one more point. Suppose that

we are dealing with a mechanism of ejection in which the velocity is a maximum at the inner boundary of the envelope. Then (5) and (10) are evidently correct as they stand. But, if we suppose that the maximum velocity occurs at the outer boundary, we must interchange the limits of integration in (5), resulting in a factor of -1 on the right-hand side of (10). These remarks indicate how Chandrasekhar's mechanisms A[4] and B are handled by this method. It is merely that, if we postulate A, we must insert a -1 on the right-hand side of (10). Then, for either A or B, we determine the integration constant at the inner boundary.

To illustrate, let us apply (10) to the observed contour for Nova Aquilae presented by Gerasimovič. Following him, we assume that we are dealing with a point source from which the matter is ejected and subsequently decelerated, and that $\alpha=2$, $\beta=0$. The measures show that, to a close approximation, we may take $I'=\text{Const.}=-\sigma$, say. Since this is a case of mechanism B, we use (10) as it stands. Thus (10) becomes

$$K\int r^{-2}dr=-\sigma\int u^3du\ ,\ \text{or}\ \frac{1}{r}\propto u^4+C\ .$$

We now replace u by v and, noting that $C=0$, we get $v\propto r^{-\frac{1}{4}}$, which is Gerasimovič's result as corrected by Chandrasekhar.

Now consider Chandrasekhar's interpretation. He wishes the velocity to be zero at the surface of the star ($r=1$) and to increase outward (mechanism A). So, putting $\alpha=\beta=2$, (10) gives

$$K\int r^{-2}dr=\sigma\int udu\ ,\ \text{or}\ \frac{1}{r}=-K'u^2+C\ .$$

Setting $u=v$ and adopting proper units to eliminate K', we have $C=1$, since $v=0$ at $r=1$, and thus arrive at $v^2=1-(1/r)$ or $v=\sqrt{1-r^{-1}}$, in agreement with Chandrasekhar.

These examples show the practical advantages of the present method. We have made the observed contour our starting-point and

[4] In this paper we take the liberty of generalizing the terms "mechanism A" and "mechanism B" to mean processes in which ejection is followed by any acceleration or deceleration, respectively. Chandrasekhar has applied them only to specific cases in which the acceleration or deceleration is a particular function of r.

deduced from it the necessary velocity distribution in the envelope for either of the possible mechanisms of ejection. Furthermore, the calculations are surprisingly simple. Of course, in the case of Chandrasekhar's interpretation, we happened to know beforehand the proper value of β. But even had this not been so, it clearly would not have been a very arduous task to experiment with (10) and determine β so as to yield the velocity distribution demanded by him. His other results can readily be verified by putting the I''s predicted by him into (10) and working back to reproduce the assumed velocity distributions with which he started.

Thus far we have been concerned only with the sloping sides of the bands. The interpretation of flat central portions has been discussed by Chandrasekhar, but it may not be amiss to say a few words about this phase of the matter from the present point of view.

The whole thing is contained in the fundamental equation (5). Consider mechanism A first. The atoms are expelled with velocity v_1, say, and are thereafter accelerated outward. Then, at any instant, $r(v_{\max})$ is the outer boundary of the envelope. Starting with $u=v_{\max}$, we have $I(u)=0$. Then, as we let $u\to v_1$, the lower limit of the integral approaches $r(v_1)=r_1$, the inner boundary, and $I(u)$ increases steadily. $I(u)$ reaches its maximum at $u=v_1$. Then, for $v_1>u\geq 0$, the right-hand side of (5) is not a function of u, and thus

$$I(v_1>u\geq 0)=2\pi k\int_{r(v_1)}^{r(v_{\max})} r^2\rho^{\alpha}v^{\beta-1}dr=\text{Const.}$$

Moreover, it is obvious that

$$I(u=v_1+dv)\to I(u=v_1-dv)\text{ as }dv\to 0\ ;$$

hence there is no discontinuity in $I(u)$, as, of course, there should not be. Thus we see that, if $v_1\neq 0$, mechanism A requires that there be always a flat central region of width $2v_1$ on the contour, and that this width remains constant so long as v_1 does. Only if $v_1=0$ are the contours peaked or rounded.

This last result is not in agreement with Chandrasekhar. He states that his equation (20) will hold for all values of u, provided that $v_1=1$, and that the contour has no flat portion in this case.

Mathematically this is quite true, but we note from his equation (15) that $v_1 = 1$ requires r_1, the radius of the inner boundary, to be infinite. Therefore this case is not of physical interest, and the situation is as stated above.

Now suppose that we are dealing with an example of mechanism *B* in which the atoms are ejected with a common large velocity v_1 and are subsequently decelerated. In this case $r\ (v_{max}) = r_1$, the inner boundary, and, by (5), we integrate outward from r_1.

To make the argument applicable to a real nova, we must consider changes in the bands in the course of time. Let us begin a short time after the first ejection, before the envelope has grown very large, and while the atoms on its outer edge are still moving rapidly outward. Then, from (5), $I(u)$ increases steadily from $u = v_1$ to some maximum value at $u = v_2$, where v_2 is the velocity of the outer boundary at the moment. As before, $I(u)$ is constant for $v_2 > u \geq 0$ and there is no discontinuity. Thus, whether v_1 exceeds the velocity of escape or not, the nova bands should show flat tops in the beginning.

Suppose that $v_1 < v_{escape}$. Then v_2 steadily decreases in time and the flat part of the band grows narrower, disappearing when $v_2 = 0$.

If, on the other hand, $v_1 > v_{escape}$, $v_2 \to v_\infty$, the limiting velocity at great distances, and the width of the flat part should decrease at first and approach $2v_\infty$ as a limit.

These remarks indicate the possibility of distinguishing between mechanisms *A* and *B* and between $v_1 \gtrless v_{escape}$ by merely noting qualitatively the time sequence of band shapes.

We conclude this work by applying equation (10) to the study of the hydrogen emission-band contours recently measured on spectrograms of RS Ophiuchi taken during its 1933 outburst.[5] For simplicity, we confine ourselves to the later stages in which it was found that the band shapes could be represented fairly well by the simple exponential $I(u) = e^{-\frac{u}{u_0}}$. For this case, (10) becomes

$$K \int r^{2-2\alpha} dr = -\frac{1}{u_0^\gamma} \int e^{-\frac{u}{u_0}} u^\gamma du\,, \tag{11}$$

[5] O. C. Wilson and E. G. Williams, *Mt. Wilson Contr.*, No. 501; *Ap. J.* (in press).

where we have put $\gamma = 1 - \beta + \alpha$. Considering mechanism A first, we must multiply the right-hand side of (11) by -1. If γ is a positive integer, we find

$$K \frac{r^{2-2\alpha+1}}{2-2\alpha+1} = \frac{1}{u_0}\left[-u_0 u^{\gamma} e^{-\frac{u}{u_0}} + u_0 \gamma \int e^{-\frac{u}{u_0}} u^{\gamma-1} du \right], \tag{12}$$

or, if γ is a negative integer and $\gamma < -1$, we get

$$K \frac{r^{2-2\alpha+1}}{2-2\alpha+1} = \frac{1}{u_0}\left[\frac{1}{-\gamma-1}\left(-\frac{e^{-\frac{u}{u_0}}}{u^{-\gamma-1}} - \frac{1}{u_0} \int \frac{e^{-\frac{u}{u_0}}}{u^{-\gamma-1}} du \right) \right]. \tag{13}$$

Equation (13) will clearly lead to an infinite series for all negative integral values of γ and so, to minimize complexity, we must take $\gamma \geq 0$ and use (12). From (12) we see that the simplest result will be arrived at by taking $\gamma = 0$. Doing this, we find (setting $u = v$)

$$K \frac{r^{2-2\alpha+1}}{2-2\alpha+1} = -e^{-\frac{v}{u_0}} + C . \tag{14}$$

Now $\gamma = 1 - \beta + \alpha$; hence, if we assume a recombination spectrum, $\alpha = 2$ and $\beta = 3$, and (14) then becomes

$$\frac{K}{r} = e^{-\frac{v}{u_0}} + C . \tag{15}$$

Since we are assuming mechanism A and the bands are observed to be rounded, we infer that $v = 0$ at the inner boundary. Thus $C = (K/r_1) - 1$, and (15) may be written

$$K\left(\frac{1}{r} - \frac{1}{r_1}\right) = e^{-\frac{v}{u_0}} - 1 .$$

Last of all, we adopt units such that $K/r_1 = 1$ and, solving for v, we obtain the velocity distribution

$$v = u_0 \log r . \tag{16}$$

This is the simplest result possible for mechanism A and $\alpha = 2$. While it may well be correct, the fact must be emphasized that it is cer-

tainly not unique. One would rather be inclined to favor $\beta=0$ for hydrogen; but if $\beta=3$ can be justified in any way, (16) would thereby receive support. If we put $\beta=0$, i.e., $\gamma=3$, in (12), the result is more complicated than (16), but perhaps not impossibly so.

While it is generally assumed that in novae we have to do with recombination rather than mere excitation, it is just as well to look into the latter also. This would mean $\alpha=1$ and, for $\gamma=0$, $\beta=2$. Inserting these values into (12), we find

$$Kr=-e^{-\frac{v}{u_0}}+C\,. \tag{17}$$

As before, $v=0$ when $r=r_1$, and we find, with proper units,

$$v=-u_0\log(2-r)\,. \tag{18}$$

In this equation we note that while r is supposed to range from 1 to ∞, v is of physical interest only for $1\leq r\leq 2$. That is, the acceleration is so great that the velocity has increased from zero to infinity while the atoms have moved from r_1 to $2r_1$. This conclusion has about it an air of improbability, and we might naïvely regard the superiority of (16) over (18) as evidence for $\alpha=2$ as against $\alpha=1$.

There remains now only the consideration of mechanism B. Still retaining $\gamma=0$ for simplicity, we have in place of (15) and (17)

$$\frac{K}{r}=-e^{-\frac{v}{u_0}}+C\,, \qquad (\alpha=2) \tag{19}$$

and

$$Kr=e^{-\frac{v}{u_0}}+C\,. \qquad (\alpha=1) \tag{20}$$

For mechanism B the velocity is a maximum, v_1, at $r=r_1$. Hence we find, from (19),

$$v=-u_0\log\left(e^{-\frac{v_1}{u_0}}+1-\frac{1}{r}\right), \tag{21}$$

and from (20),

$$v=-u_0\log\left(e^{-\frac{v_1}{u_0}}-1+r\right). \tag{22}$$

In (21) and (22) we note that v goes to zero for a finite value of r. This behavior is what we should have expected from the fact that the bands are not flat topped. We find from (21) and (22), respectively,

$$r_{\max}=e^{\frac{v_1}{u_0}} \text{ and } r_{\max}=2-e^{-\frac{v_1}{u_0}}.$$

Between these two results there seems to be no preference.

To summarize: In analyzing the emission contours of RS Ophiuchi we have been guided, first of all, by the supposition that the simplest possible solutions are also the most probable. If this be true, then the most likely velocity distributions are

1. Mechanism *A*: $\alpha=2$, $\beta=3$; $v=u_0 \log r$.

2. Mechanism *B*: $\alpha=2$, $\beta=3$; $v=-u_0 \log\left(e^{-\frac{v_1}{u_0}}+1-\frac{1}{r}\right)$,

or $\alpha=1$, $\beta=2$; $v=-u_0 \log\left(e^{-\frac{v_1}{u_0}}-1+r\right)$.

It must be remembered that, so far as our analysis goes, there is nothing unique about any of these solutions. There are, in fact, an infinite number of possible solutions, if we are willing to let α be unrestricted. A complete physical theory of these matters would doubtless define α exactly, or, at least, within narrow limits. Until this is done, however, we seem to have exhausted the possibilities of the simple theory.

In conclusion, we point out two ways in which the theory might conceivably be improved without undue effort. First, assumption 4 should probably be modified by supposing that N starts from zero at $t=t_1$, rises without discontinuity to a maximum between t_1 and t_2, and then falls in the same way to zero again at the latter time. Second, we have implicitly assumed in writing equation (4) that the excitation in $d\tau$ is independent of the distance of $d\tau$ from the star. The independence is doubtless only approximate, and, if need be, allowance can be made for the variation of excitation with distance by letting k in equation (4) be a function of r.

CARNEGIE INSTITUTION OF WASHINGTON
MOUNT WILSON OBSERVATORY
August 1934

PHOTOGRAPHIC DETERMINATION OF MASS RATIOS OF VISUAL BINARIES

By RALPH C. HUFFER

ABSTRACT

By means of plates taken with the 40-inch refractor at epochs separated by fourteen to twenty-eight years, the mass ratios of seventeen visual binaries have been determined. The masses of these and of all others with known mass ratios are computed and plotted on a mass-luminosity diagram. In general there is agreement with the Eddington curve, both in the positions of the points on the chart and in the mass ratios as indicated by the slopes of the lines joining the two components of the pairs.

The values of the mass ratios are plotted as functions of spectral type, period, total mass of the system, and difference of magnitude of the components.

The photographic determination of the mass ratio of a visual binary requires plates of large scale covering a long period of time. During the interval the orbital motion must have been such that the components show measurable departure from uniform rectilinear motion.

In 1916 G. Van Biesbroeck, recognizing the need and value of mass ratios, added a number of binaries to the regular parallax program of the Yerkes Observatory. At that time he outlined[1] the various cases in which a determination could be made and presented four illustrations of the methods of solution.

The test of the theory of A. S. Eddington[2] on the relationship between stellar masses and luminosities, published in 1924, depended in the region of the dwarf stars on a very limited number of visual binaries. Of these the mass ratios were uncertain or unknown in all but four. The present investigation covers all stars for which suitable plate material is now at hand.

According to the data available, one of three methods was used. The first was in the case of stars of approximately equal magnitude in which the separation was sufficient to insure against the interference of the images. Here the measures alone, corrected for annual parallax, were sufficient for the completion of the solution. The second procedure was used in the cases of stars of unequal magnitude in which only the brighter appeared on the plates. Here wide separa-

[1] *A.J.*, **29**, 173, 1916.

[2] *M.N.*, **84**, 308, 1924.

tion was not necessary, but in this case the position of the fainter component had to be computed from a satisfactory orbit, if available. The third method was used when no orbit covered the time of the plates sufficiently well. Then micrometric measures over the entire interval were used as a basis for interpolating the polar co-ordinates of the pair. Plates at three epochs were always available and solutions depending on catalogue values of the proper motions were not necessary.

In two cases it seemed desirable to compute new orbital elements, as existing ones were not in agreement with recent micrometric meas-

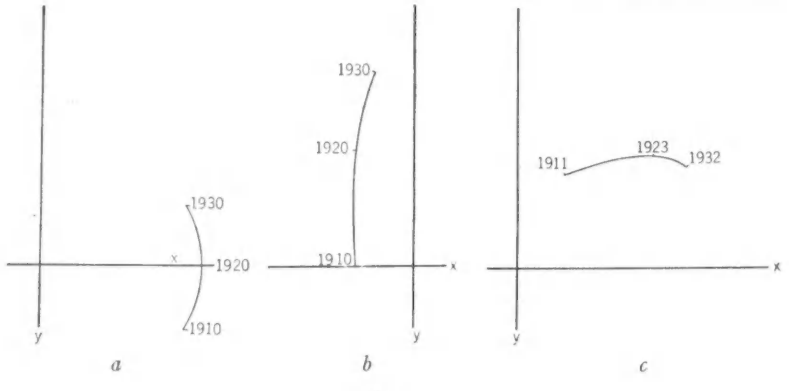

FIG. 1

ures and gave poor determinations of the mass ratios. The following elements for 26 Draconis were computed by Van Biesbroeck in September, 1933, and have been previously unpublished: P, 80.6 years; T, 1873.2; e, 0.10; Ω, 153°.18; ω, 330°.0; i, 73°.8; a, 1″.51. In October of the same year the writer computed the following elements for β 648: P, 61.8 years; T, 1911.2; e, 0.25; Ω, 48°.7; ω, 281°.4; i, 65°.0; a, 1″.24. In both pairs the motion is retrograde.

In the majority of stars measures were made in both rectangular co-ordinates x and y, corresponding to the directions of α and δ at the binary. In the case of ζ Herculis, however, the motion was such that the measures in only one direction were justified. As an example of the bases for decision as to the direction of measure, consider a star moving in the apparent orbit as shown in Figure 1*a*. Here the curvature is such that measures in x would show a considerable de-

viation from uniform motion, while measures in y would indicate practical uniformity. In Figure 1*b* the deviation in y, caused largely by retarded motion, would be about 60 per cent greater than that in x, caused by curvature. In the case of a star moving with an inclination of 90° and node of 0°, the change in x would be zero and hence would add nothing to the solution, while under certain conditions a determination from y-measures, using the deviation from uniform velocity, would be easily possible. Figure 1*c* shows the part of the orbit of 70 Ophiuchi covered by the plates in the present determination. The weight of the solution in x, dependent largely on velocities, is 1.6 times that in y, which uses mainly curvature. The results in the case of this star and of others indicate that the suggestion of H. L. Alden[3] that measures should always be made in the direction perpendicular to the arc at the middle point of the apparent orbit needs to be altered to make use of variations in velocity as well as of curvature.

The data and results for seventeen binaries are given in Table I. The plates were measured and reduced by the method used at this observatory in the determination of parallaxes. Conditional equations of the type

$$\mu_x t + k_x - r_x B = m_x$$

were formed, where μ_x is the proper motion in x, k_x a constant, r_x the separation of the two components, t the time at which the plate was made, B the ratio $m_2/(m_1+m_2)$ or mass of the companion in terms of total mass, and m_x the measured position of the brighter star after correction for parallax. Measures in y gave rise to similar equations. Solutions were usually first made in x and y together. If residuals in this solution indicated disagreement in x or y, separate solutions were made in each direction. Where this was not done, the residuals indicated that better results could not be expected from separate solutions. Results are given in the last two columns of Table I as obtained from least-squares solutions for B from the equations in x, in y, and in x and y together. Some previous determinations are given for each star when such have been made. The sources are des-

[3] *Pop. Astr.*, **33**, 164, 1925.

TABLE I

DETERMINATIONS OF MASS RATIOS

STAR	APPARENT VISUAL MAGNITUDES	PARALLAX IN SECONDS OF ARC; SOURCE OF ORBIT	NO. OF PLATES; INTERVAL (YEARS)	$m_2/(m_1+m_2)$	
				From x; from y	From x and y; from Other Sources
η Cas	3.64	0.180	6	.....	.24 ± .01
0^h43^m	7.9	Doberck	27	.....	VB, .21; M, .25; B, .43
48 Cas	4.8	0.028	6	.....	.50 ± .08
1^h54^m	7.2	Bennot	22	.....	.....
Procyon	0.48	0.310	7	.....	.26 ± .01
7^h34^m	13.5	Jones	16	.....	J, .24; B, .25
ϵ Hya AB	4.0	0.024	7	.....	.26 ± .09
8^h42^m	5.5	Aitken	14	.....	M, .50; R, .40
ξ Boo	4.7	0.155	6	.37 ± .12	.49 ± .05
14^h47^m	6.7	None	15	.51 ± .06	B, .47
ι Boo	5.2	0.078	6	.....	.54 ± .14
15^h0^m	6.0	None	17	.39 ± .06	.....
γ CrB	4.0	0.020	6	.....	.50 ± .16
15^h39^m	7.0	None	21	.....	.....
ζ Her	3.0	0.106	6	.....	.....
16^h37^m	6.5	Silbernagel	13	.51 ± .04	B, .30
26 Dra	5.3	0.062	7	.....	.47 ± .05
17^h34^m	9.3	V. Biesbroeck	21	.....	.....
70 Oph	4.1	0.198	7	.49 ± .02	.50 ± .03
18^h0^m	6.1	None	21	.51 ± .05	VB, .47; M, .44; B, .45
99 Her	5.2	0.053	9	.....	.30 ± .13
18^h3^m	9.7	None	14	.....	K, .04
β 648	5.2	0.072	7	.91 ± .08	.....
18^h54^m	8.7	Huffer	14	.35 ± .03	K, .17
61 Cyg	5.6	0.300	8	.49 ± .27	.69 ± .13
21^h2^m	6.3	None	27	.77 ± .09	.....
τ Cyg	3.8	0.051	6	.....	.40 ± .04
21^h11^m	8.0	V. Biesbroeck	22	.....	VB, .47
ζ Aqr	4.4	0.028	6	.57 ± .20	.15 ± .11
22^h24^m	4.6	None	14	−.22 ± .09	.....
Kr 60	9.3	0.257	6	.....	.37 ± .01
22^h24^m	10.8	None	27	.....	M, .46; Alden, .46

TABLE I—*Continued*

Star	Apparent Visual Magnitudes	Parallax in Legends of Arc; Source of Orbit	No. of Plates; Interval (Years)	$m_2/(m_1+m_2)$	
				From x; from y	From x and y; from Other Sources
π Cep	5.2	0.015	6	$.28 \pm .09$	$.09 \pm .22$
23^h5^m	7.5	Lauritzen (II)	14		
85 Peg	5.8	0.090	7	$.31 \pm .04$	$.47 \pm .04$
23^h57^m	11.0	V. Biesbroeck	21	$.57 \pm .03$	B, .64; VB, .64
85 Peg				$.30 \pm .07$	$.42 \pm .03$
23^h57^m		Allen		$.48 \pm .02$	Allen, .64

ignated as follows: B, Lewis Boss;[4] VB, G. Van Biesbroeck;[5] M, S. A. Mitchell;[6] J, H. S. Jones;[7] and K, P. Van de Kamp.[8]

The relevant facts about all the stars for which mass ratios are known have been collected in Table II. The parallaxes are taken from F. Schlesinger's "Catalogue of Bright Stars"[9] and "Catalogue of Parallaxes."[10] The absolute magnitudes are computed from apparent magnitudes from the same sources or from R. G. Aitken's "New General Catalogue of Double Stars."[11] Masses of the separate components have been assigned on the basis of the mass ratios listed. Six of the stars have given some evidence of multiplicity. The three stars ι Bootis B, γ Coronae Borealis A, and σ Coronae Borealis A are spectroscopic binaries with two spectra that are much alike in structure and intensity. Each has been treated as a single star of half the mass and half the luminosity that would otherwise be assigned to it. The other three—λ Ophiuchi A, τ Cygni A, and π Cephei A—show only single spectra. Because of uncertainty of duplicity, or at least because of a fair assurance that one component is relatively faint, each has been treated as a single star possessing the entire luminosity and mass of the visual component.

[4] *Preliminary General Catalogue, Carnegie Institution of Washington*, 1910.

[5] *Op. cit.*

[6] *Pub. Leander McCormick Obs.*, **3**, 661, 1920.

[7] *M.N.*, **88**, 432, 1928.

[8] *Pop. Astr.*, **38**, 478, 1930.

[9] *Pub. Yale Univ. Obs.*, 1930.

[10] *Ibid.*, 1924.

[11] *Carnegie Institute of Washington*, 1932.

TABLE II

DATA ON VISUAL BINARIES WITH KNOWN MASS RATIOS

Star ADS No.	Parallax	Abs. Vis. Mags.	$m_2/(m_1+m_2)$	Spectra	Computer of Orbit and of Mass Ratio	a'' P (Yrs.)	Masses (Sun=1)
η Cas	0.180	4.9	.24	F8	Doberck	12.21	.91
671		9.2		M1	Huffer	508	.30
48 Cas	.028	2.0	.50	A3	Bennot	0.66	1.62
1598		4.4			Huffer	63.3	1.65
o Eri BC	.203	10.7	.31	A2n	V. d. Bos	6.89	.44
3093		12.7		M6e	V. d. Bos	248	.20
80 Tau	.021	3.6	.31	Fo	V. d. Bos	1.04	3.79
3264		6.1			V. d. Bos	148.3	1.67
α Aur	.075	0.2	.44	gGo	Merrill	0.054	4.20
3841		0.2			Merrill	0.285	3.30
α CMa	.376	1.3	.32	A2s	Aitken	7.57	2.22
5423		11.3		F	Auwers	50.04	1.04
α Gem	.077	2.1	.44	A2s	Doberck	6.57	1.53
6175		3.1		A2s	Russell	477	1.20
α CMi	.310	3.0	.26	∓ 5	Jones	4.26	1.20
6251		16.0			Huffer	40.2	.41
ϵ Hya AB	.024	0.6	.26	gF9	Aitken	0.23	2.79
6993		2.1		F5	Huffer	15.3	.97
ξ UMa	.146	4.8	.32	Go	V. d. Bos	2.54	1.37
8119		5.7			V. d. Bos	59.9	.63
γ Vir	.073	2.3	.50	Fo	Lohse	3.62	1.30
8627		2.3		Fo	Boss	178	1.30
α Cen	.760	4.7	.46	Go	Finsen	17.66	1.06
		6.1		K5	Alden	80.1	.92
ξ Boo	.155	5.7	.49	G5	Doberck	4.87	.70
9413		7.7		K5	Huffer	151	.66
ι Boo	.078	4.7	.54	Go	Doberck	3.58	1.05
9494		6.3		G2p	Huffer	205	.62
γ CrB	.020	1.3	.50	Ao	Comstock	0.62	.72
9757		3.5			Huffer	101	1.47
σ CrB	.048	4.8	.32	Go	Doberck	6.00	.85
9979		5.1			Boss	900	.80
λ Oph	0.028	1.2	.50	Ao	Rabe	0.94	1.04
10087		3.3			Boss	135.3	1.04

TABLE II—*Continued*

Star ADS No.	Parallax	Abs. Vis. Mags.	$m_2/(m_1+m_2)$	Spectra	Computer of Orbit and of Mass Ratio	a'' P (Yrs.)	Masses (Sun=1)
ζ Her	0.106	3.1	.51	Go	Silbernagel	1.35	.86
10157		6.6			Huffer	34.5	.88
β 416	.143	7.2	.43	K2	Voute	1.83	.4
		9.2			Voute	42.2	.3
26 Dra	.062	1.3	.47	F8	V. Biesbroeck	1.51	1.18
10660		5.3			Huffer	80.6	1.04
μ Her BC	.111	7.1	.50	M5	Aitken	1.30	.44
10786		10.3			Hertzsprung	43.23	.44
70 Oph	.198	5.6	.50	K1	Pavel	4.50	.67
11046		7.6		K5	Huffer	88	.67
99 Her	.053	3.8	.30	F8	Makemson	1.03	1.64
11077		8.3			Huffer	56	.70
β 648	.072	4.5	.35	Go	Huffer	1.24	.87
11871		8.0			Huffer	61.8	.47
61 Cyg	.300	8.0	.69	K8	Baise	32.8	.71
14636		8.7		Mo	Huffer	756	1.58
τ Cyg	.051	2.3	.40	Fo	Aitken	0.96	1.64
14787		6.5			Huffer	49.2	1.12
κ Peg	.025	1.9	.36	F1s	Luyten	0.22	3.3
15281		2.4		Ko	Luyten	11.52	1.9
ζ Aqr	.028	1.6	.57	F2s			
15971		1.8		F1s	Huffer		
Kr 60	.257	11.3	.37	M3	Huffer	2.36	.25
15972		12.8		M4	Huffer	44.5	.14
π Cep	.015	1.1	.28	gG5	Lauritzen	0.92	5.20
16538		3.4			Huffer	178	2.07
85 Peg	0.090	5.6	.45	Go	V. Biesbroeck	0.82	.60
17175		12.8			Huffer	26.3	.49

In Figure 2 the absolute visual magnitudes have been plotted as ordinates against the logarithms of the masses. The Eddington mass-luminosity curve, adjusted to visual magnitudes, has also been drawn. While the scatter is considerable, as is to be expected from the uncertain orbits, parallaxes, and mass ratios entering into the solution for mass, there is, however, a very definite clustering about

the curve and the lines joining the pairs in the main tend to be parallel to the curve.

Figure 2 was originally plotted, using bolometric magnitudes as in Eddington's original article. The conversion from visual to bolometric magnitudes depends, however, on spectral type, and since for most of the faint components of the binaries in Table II the types are unknown or uncertain, it seemed wiser to use the visual magni-

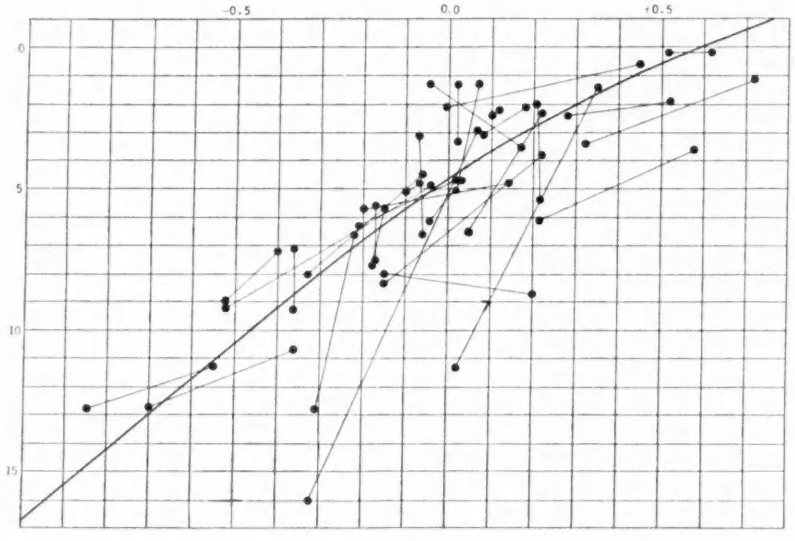

FIG. 2.—The ordinates are absolute magnitudes and the abscissas are logarithms of masses. The curve is Eddington's mass-luminosity law. The straight lines join the two components of a binary.

tudes in preference to reducing the number of stars. While this procedure might introduce serious difficulties into an analytic discussion of the problem, it makes apparently little difference in the agreement with reference to the graph.

In Table III the logarithms of the observed masses are compared with the values as read from the curve of mass luminosity, and the differences are listed. Of the sixty stars plotted, the twelve which show a disagreement of more than 0.25 in the logarithms of the masses are considered individually in the following paragraphs.

Both components of 80 Tauri lie below the mass-luminosity curve in Figure 2, although the line joining them is essentially parallel to

the curve. The chief weakness here is in the parallax. Aitken gives the parallax as -0".011 as obtained trigonometrically, and calls it "very uncertain." The cluster value is 0".026, which is also the value

TABLE III

COMPARISON OF COMPUTED MASSES WITH VALUES FROM THE MASS-LUMINOSITY CURVE

Star	Log Mass of Primary			Log Mass of Companion		
	Observed	Computed	O−C	Observed	Computed	O−C
η Cas	−0.04	−0.02	−0.02	−0.52	−0.40	−0.12
48 Cas	+ .21	+ .31	− .10	+ .22	+ .04	+ .18
o_2 Eri	− .36	− .52	+ .16	− .52	− .68	+ .16
80 Tau	+ .58	+ .10	+ .48	+ .22	− .14	+ .36
α Aur	+ .62	+ .57	+ .05	+ .52	+ .57	− .05
α CMa	+ .35	+ .39	− .04	+ .02	− .57	+ .59
α Gem	+ .18	+ .30	− .12	− .08	+ .18	− .10
α CMi	+ .08	+ .20	− .12	− .39	− .94	+ .55
ϵ Hya	+ .45	+ .51	− .06	− .01	+ .30	− .31
ξ UMa	+ .14	.00	+ .14	− .20	− .10	− .10
γ Vir	+ .11	+ .27	− .16	+ .11	+ .28	− .17
α Cen	+ .04	+ .01	+ .03	− .03	− .14	+ .11
ξ Boo	− .16	− .10	− .06	− .18	− .28	+ .10
ι Boo	+ .03	+ .01	+ .02	− .21	− .16	− .05
γ CrB	− .14	+ .40	− .54	+ .17	+ .27	− .10
σ CrB	− .07	.00	− .07	− .10	− .03	− .07
λ Oph	+ .02	+ .41	− .39	+ .02	+ .16	− .14
ζ Her	− .07	+ .19	− .26	− .06	− .19	+ .13
β 416	− .40	− .23	− .17	− .52	− .40	− .12
26 Dra	+ .07	+ .40	− .33	+ .02	− .06	+ .08
μ Her BC	− .36	− .22	− .14	− .36	− .47	+ .11
70 Oph	− .17	− .09	− .08	− .17	− .27	+ .10
99 Her	+ .22	+ .10	+ .12	− .16	− .33	+ .17
β 648	− .06	+ .03	− .09	− .33	− .30	− .03
61 Cyg	− .15	− .30	+ .15	+ .20	− .36	+ .56
τ Cyg	+ .22	+ .28	− .06	+ .05	− .18	+ .23
κ Peg	+ .52	+ .32	+ .20	+ .28	+ .26	+ .02
Kr 60	− .55	− .56	+ .01	− .85	− .64	− .21
π Cep	+ .72	+ .43	+ .29	+ .32	+ .14	+ .18
85 Peg	−0.22	−0.09	−0.13	−0.31	−0.64	+0.33

given in Schlesinger's "Catalogue of Bright Stars." An adopted value of 0".029 would give points very near the curve.

The well-known white dwarf α Canis Majoris B, with its uncertain magnitude and probable high density, would hardly be expected to lie near the mass-luminosity curve. It is about 7 mag. fainter than its mass would indicate.

Like the companion of Sirius, α Canis Minoris B is probably a white dwarf, is of uncertain magnitude, and is about 7 mag. fainter than the curve would predict on the basis of its observed mass.

ϵ Hydrae B, with an orbit of mean distance $0''.23$, a parallax uncertain between $0''.015$ and $0''.060$, and a mass ratio of $0.26 \pm .09$, is not farther from the curve than might be anticipated.

The spectroscopic binary γ Coronae Borealis A lies far off the curve. Its small parallax of $0''.022$ and its very uncertain mass ratio, as well as the uncertainty of the semi-major axis of the orbit, point to a very low weight of the observed value of the mass.

The trigonometric parallax of λ Ophiuchi A is given by Schlesinger as $0''.000$, although he adopts $0''.028$ in the "Catalogue of Bright Stars." The orbit is still very uncertain and the mass ratio is doubtful. In addition, the radial velocity is variable, introducing possible duplicity into the problem. A parallax of $0''.022$ would bring it into fair agreement.

ζ Herculis A lies above the curve, while its companion lies below, about half as far. If instead of the mass ratio of 0.51 of the present paper the value of 0.30 as given by Boss is adopted, both components will lie slightly above the curve with a difference of about one-tenth between observed and computed logs of the masses.

The orbit of 26 Draconis, because of the difficulty of measuring with the micrometer a close pair, of magnitudes 5 and 10, is the weakest part of its mass determination. Both the period and the semimajor axis are uncertain at the present time.

The slow-moving pair 61 Cygni has covered so little of its orbit that its period, mean distance, and mass ratio are little more than guesses. It is included in this paper as an interesting test of the method rather than as a reliable determination of a mass ratio.

The parallax of π Cephei is uncertain according to Aitken, who gives the trigonometric value as $0''.000$ and the spectroscopic as $0''.011$ or $0''.026$. Since the line joining the two components is nearly parallel to the curve, it appears that an adopted parallax of $0''.018$ would bring the star into agreement with the Eddington theory.

The faint member of the unusual system 85 Pegasi has repeatedly been shown to be the heavier of the two in various determinations of mass ratio. The results of the present paper from a number of dif-

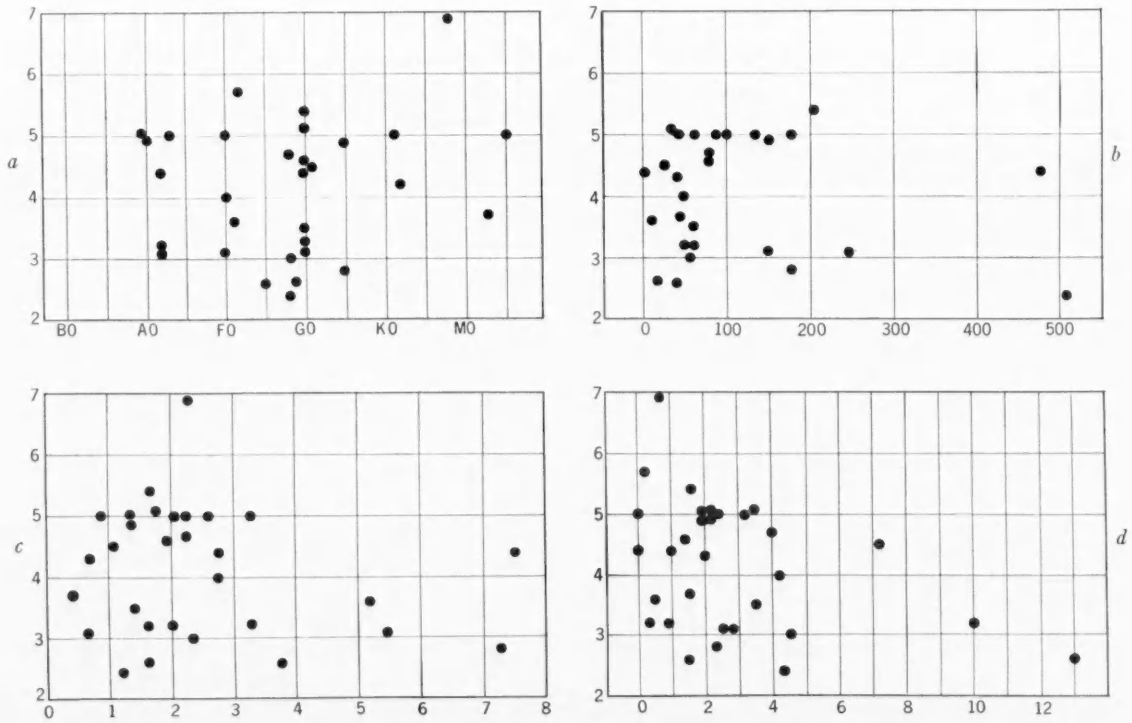

FIG. 3.—Mass ratio as a function (*a*) of spectral type; (*b*) of period in years; (*c*) of total mass of the system; and (*d*) of difference in magnitudes of the components.

ferent analyses are not conclusive. Since the companion is about 5 mag. fainter than its mass would indicate that it should be, and since its spectrum is not available, the suggestion that this star of absolute magnitude 12.8 is a white dwarf may not be out of place.

Of the sixty stars on the diagram in Figure 2, the remaining forty-eight show fair agreement with the Eddington theory. Of the twelve aberrant ones, six have uncertain parallaxes of less than 0".028, three are suspected white dwarfs, one can be brought into agreement by adoption of Boss's value of the mass ratio, and the remaining two are stars of very uncertain orbital elements. With the exception of the three suspected white dwarfs, it appears that there is no star on the list which can be said to be sharply in disagreement with the Eddington theory.

The thirty-one mass ratios of visual binaries given in Table II may throw some light on the changes in the relative masses of these systems during their life-histories and may make some contribution to the explanation of their origin. With this in mind, Figure 3 has been prepared in which the mass ratio is plotted as a function of various variables which might be expected to undergo systematic changes in the period of existence of the star.

Figure 3*a* shows the mass ratio plotted against the spectral type of the primary star. No correlation is evident. In Figure 3*b* a graph of mass ratio against period shows a wide scatter in the stars of short period, while the data on the slower binaries are too uncertain and too sparse to justify any conclusions. In Figure 3*c* the scatter of points on the graph of mass ratio against the total mass of the system is obvious. In Figure 3*d* mass ratio is shown as a function of the difference in magnitude between the components of the binary. It shows a tendency for the masses to become more unequal with increasing differences in magnitude, as is indicated by the curve of mass luminosity. The scatter is large, however, for any given magnitude difference, which is indicative of differing relations between these quantities in stars of different luminosities.

The writer wishes to acknowledge his obligation to Dr. Edwin B. Frost and Dr. Otto Struve for their kindness in making the equipment of the observatory available to him and to Dr. G. W. Moffitt

for his help at the telescope, at the computing machine, and in the darkroom. And especially are his thanks given to Dr. G. Van Biesbroeck, whose many suggestions in mapping out and solving the problem, and whose foresight in starting many of the series of plates for mass-ratio determinations, have made the work possible.

YERKES OBSERVATORY
AND
BELOIT COLLEGE
August 22, 1934

THE URSA MAJOR GROUP

By J. J. NASSAU and LOUIS G. HENYEY

ABSTRACT

An expedient method is developed for finding stars which have a given common motion. It is essentially based on the stereographic projection of the circles of equal radial velocity and equal cross-motion in declination. The method is applied in an examination of all stars in the *Yale Bright Star Catalogue* having complete data (radial velocity, proper motion, and parallax) for possible membership in the Ursa Major group. This examination yielded 126 stars, each of which differed from the assumed velocity of the group by a vector whose magnitude was less than 9.5 km/sec. The mean velocity of the group in galactic co-ordinates, with solar motion excluded, was found to be $l = 1°.4$, $b = -6°.0$, $V = 29.5$ km/sec. The space distribution of the stars is more or less spherical.

A study of the spectral and parallactic distributions shows that the selection is not at random. As compared with the spectral frequency of stars having complete data, the Ursa Major stars exhibit a gradual increase in number from M to A with half of them A types, and a complete absence of B-type stars. The Russell diagram shows all the characteristics of a type *2a* open cluster in Trumpler's classification.

The stars in space are divided into two groups by a gap 18 parsecs wide and passing through the sun.

1. INTRODUCTION

In the following discussion we shall understand that a collection of stars forms a group when the motions of the stars are more or less parallel and their velocities are approximately equal. The upper limit of the difference between the individual motion of any star of the group and the mean motion of the group is more or less arbitrary and depends only on the particular problem under consideration. No attempt is made to assign to the members of a group any kinship other than common motion. There are, however, various known groups whose members are regarded as having a closer relationship than merely equality of motion; such groups are known as moving clusters. Many of these systems are suspected of being very similar to galactic clusters and should therefore possess properties which are found in such clusters. It has been pointed out by Eddington[1] and others that the stars in moving clusters, to be recognized as members of the system, must adhere to their common motion with extreme exactness. In such a case the deviation from the mean motion is wholly due to errors of observation, in contrast with the more general case of a group whose members have actual deviations of motion besides those due to observational errors.

[1] *Stellar Movements and the Structure of the Universe*, p. 56.

In examining a number of stars for possible membership in a given stellar group, it is naturally desirable to base the examination of each star and the criteria for selection directly on the data given for such star, that is, position, proper motion, radial velocity, and parallax. The purpose of the first part of this report is to give a method for the selection of those stars in a catalogue which satisfy the criteria, within specified limits, for belonging to a known group. The second part is devoted to the application of the method in finding new members of the Ursa Major group, and a study of the characteristics of these stars together with the already known members.

2. FUNDAMENTAL CONSIDERATIONS

If (A, D) are the co-ordinates of the apex of a group and V is the velocity of the system with respect to the sun, the corresponding components of the velocity (x, y, z) in rectangular equatorial co-ordinates are given by the equations

$$\left.\begin{aligned} x &= V \cos A \cos D , \\ y &= V \sin A \cos D , \\ z &= V \sin D . \end{aligned}\right\} \tag{1}$$

For a point (α, δ) in the sky the components of V in the direction of radial velocity (ρ), proper motion in right ascension (Q), and proper motion in declination (P) are given in terms of (x, y, z) by the following three equations:

$$\left.\begin{aligned} \rho &= x \cos \alpha \cos \delta + y \sin \alpha \cos \delta + z \sin \delta , \\ P &= -x \cos \alpha \sin \delta - y \sin \alpha \sin \delta + z \cos \delta , \\ Q &= -x \sin \alpha + y \cos \alpha . \end{aligned}\right\} \tag{2}$$

When x, y, and z from (1) are substituted in (2), we get the equivalent equations:

$$\rho = V[\sin \delta \sin D + \cos \delta \cos D \cos (\alpha - A)] , \tag{3a}$$

$$P = V[\cos \delta \sin D - \sin \delta \cos D \cos (\alpha - A)] , \tag{3b}$$

$$Q = -V \cos D \sin (\alpha - A) . \tag{3c}$$

Equation (3*a*) is readily reduced to the familiar form

$$\rho = V \cos \lambda , \tag{4}$$

where λ is the angular distance from the apex to the point (α, δ).

The quantities (ρ, P, Q) measure the velocity that a star with co-ordinates (α, δ) must have in order to belong to a group with velocity (V, A, D). Observational values of P and Q (which we shall denote by P_0 and Q_0) are computed from the following formulae:

$$P_0 = 4.74 \frac{\mu_\delta}{\pi} , \tag{5a}$$

$$Q_0 = 4.74 \frac{\mu_\alpha}{\pi} , \tag{5b}$$

$$Q_0 = 71.1 \frac{\mu'_\alpha \cos \delta}{\pi} . \tag{5b'}$$

The use of (5*b*) or (5*b'*) depends on whether the data used give the proper motion in right ascension in seconds of arc or rate of change of right ascension in seconds of time.

3. EVALUATION OF ρ, P, AND Q

a) *Radial velocity.*—Equation (4) shows that ρ is constant along any circle with its center at the apex. This property is utilized in a stereographic projection of the celestial sphere, since in such a projection the circles on the sphere remain circles after projection. Figure 1 shows the projection used in the study of the Ursa Major group. The light lines are the co-ordinate lines while the heavy lines are the circles for ρ, given for every 5 km/sec. on either side of zero. The northern hemisphere was projected from the south pole. For the southern hemisphere the same figure is used by changing the right ascension by twelve hours and changing the sign of ρ.

Let the equator be the plane of projection and the south pole the point of projection. Points on the unit sphere then transform into points on the plane and have for polar co-ordinates

$$\theta = \alpha$$

and

$$r = \tan \tfrac{1}{2}(90^\circ - \delta)$$

or

$$r = \sec \delta - \tan \delta .$$

The contour circles for the radial velocity are all concentric on the sphere but go into a coaxial system on the plane. These circles cut

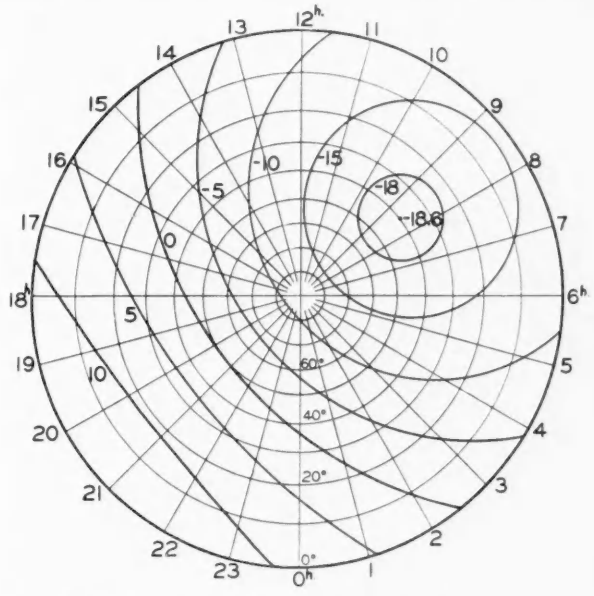

FIG. 1.—ρ-function for the Ursa Major group

the hour circle through the apex at points on the sphere with declinations

$$\delta_1 = D + \lambda ,$$

$$\delta_2 = D - \lambda .$$

The corresponding points on the plane therefore have radius vectors

$$r_1 = \sec (D+\lambda) - \tan (D+\lambda) ,$$

$$r_2 = \sec (D-\lambda) - \tan (D-\lambda) .$$

By declinations numerically greater than 90° we mean points beyond the pole on the same hour circle. The center of the projected circles are then located by

$$r_0 = \frac{r_1 + r_2}{2} .$$

The radius is

$$a=\frac{|r_1-r_2|}{2}.$$

b) *P-function.*—The value of this function is readily obtained from the ρ-diagram. We see from (3) that

$$P(\alpha, \delta)=\rho(\alpha+180^\circ, 90^\circ-\delta).$$

In other words, the value of P at any point is the same as the value of ρ at a point 90° toward the north (beyond the pole for the northern hemisphere). While this statement holds for the southern hemisphere, it is more convenient here to make use of the fact that the values of P are the same at diametrically opposite points on the sphere. Therefore in either case the magnitude of P is determined at a point on the ρ-diagram 90° from the point at which ρ is found, beyond the north pole and on the same hour circle. We recall in this connection that for the southern hemisphere ρ is found at the diametrically opposite point.

c) *Q-function.*—Equation (3*c*) shows that Q is a function only of right ascension. It can therefore be calculated for suitable intervals of right ascension. In our case it was calculated approximately once for each page of the catalogue.

The foregoing method is equally applicable for obtaining corrections for ρ, P, and Q. Let $d\rho$, dP, and dQ denote these corrections and dx, dy, and dz the corresponding corrections for x, y, and z. Since the relations given in equation (2) are linear, an identical equation may be written for $d\rho$, dP, and dQ in terms of dx, dy, dz, and hence equation (3) may be written with these new variables. The latter equation, of course, is used for the derivation of the diagrams. The new values of A, D, and V which are necessary in the actual construction of the diagrams are obtained from equation (1) by substituting dx, dy, and dz for x, y, and z.

It is readily seen that the method of determining ρ, P, and Q is applicable to the determination of the corresponding components of solar motion.

As an auxiliary method of getting ρ, one may use an alignment chart similar to that given by A. F. Dufton[2] for the radial component

[2] *MN*, **92**, 688, 1932.

of solar motion. The correspondence of the ρ-function and the P-function suggests an alignment chart for the latter similar to that of Dufton.

4. APPLICATION OF THE METHOD

In proceeding through a catalogue, only those stars are examined which have proper motions that appear promising. With a little experience one can readily recognize a star which may satisfy the criteria.

The following procedure has been found to work well:

a) The radial velocity (ρ_0) given in the catalogue is compared with ρ obtained from Figure 1.

b) The value of P is also obtained from the same diagram and is compared with the value of P_0 computed from (5*a*).

c) The computed value of the Q-function for the page of the catalogue is compared with Q_0 ,which is found according to (5*b*) or (5*b'*).

d) The sum of the squares of the residuals is found, that is:

$$R^2=(\rho_0-\rho)^2+(P_0-P)^2+(Q_0-Q)^2\,. \tag{6}$$

If R^2 is less than some assigned upper limit, the star is accepted. It is evident that the foregoing procedure is well adapted in cases where the stars under consideration have incomplete data.

5. THEORETICAL PARALLAX

Assuming that the stars form a cluster, we may obtain a value of the parallax of each star from a weighted mean of the two observational equations

$$\left.\begin{aligned}\pi&=4\cdot74\,\frac{\mu_\alpha}{Q}\,,\\ \pi&=4\cdot74\,\frac{\mu_\delta}{P}\,.\end{aligned}\right\} \tag{7}$$

If the weight of the first equation is taken as $|Q|$ and that of the second as $|P|$, we have

$$\pi_c=4\cdot74\,\frac{\mu_\alpha\dfrac{|Q|}{Q}+\mu_\delta\dfrac{|P|}{P}}{|P|+|Q|}\,. \tag{8}$$

In the case where either P or Q is zero, the non-zero value is of course used in determining the parallax. A more rigorous formula might be

$$\pi_c = 4.74 \frac{\mu_\alpha Q + \mu_\delta P}{P^2 + Q^2}, \tag{9}$$

which yields results not materially different from the previous one. In the case where the rate of change in right ascension is given for μ_a, the foregoing formulae are modified, as equation ($5b'$) shows.

A modification of the well-known equation for determining theoretical parallaxes

$$\pi_c = 4.74 \frac{\mu}{V \sin \lambda} \tag{10}$$

may be effected by means of equation (4), that is:

$$\pi_c = 4.74 \sqrt{\frac{\mu_\alpha^2 + \mu_\delta^2}{P^2 + Q^2}} \tag{11}$$

or

$$\pi_c = 4.74 \sqrt{\frac{\mu_\alpha^2 + \mu_\delta^2}{V^2 - \rho^2}}. \tag{12}$$

Since $\rho^2 + Q^2 + P^2 = V^2$.

A comparison of the results obtained by means of equation (8) and the foregoing will be considered in paragraph 11. Equation (10), or its equivalent (11) or (12), does not discriminate between the positive and negative signs of μ_α and μ_δ; this is particularly true when either P or Q is small.

6. THE URSA MAJOR GROUP

In 1921 N. Rasmuson,[3] summarizing the work of all previous investigators, assigned 28 stars to the Ursa Major group. Twenty-six of the stars were of spectral type A, one of F, and one of K. The ellipsoidal distribution of the stars in space gave one short axis with a direction approximately parallel to the motion of the group. In 1930 J. M. Mohr,[4] assuming approximately Rasmuson's direction of

[3] *Meddelanden från Lunds Observatorium* (2d ser.), No. 26, 1922.

[4] *B.A.*, **6**, III, 1930.

motion but not limiting the magnitude of the velocity, added to the group 77 members, mostly of type A, with a few F stars. Ch. Bertaud,[5] after an examination of 526 A-type stars, and assuming an upper limit for $R = 10$ km/sec., confined the group to 79 stars. Of these stars, all are of type A with the exception of 3, which are of type F.

The method explained in the preceding paragraphs was employed in the search for new stars in the Ursa Major group. The assumed direction and velocity of the system was taken from the work of Rasmuson, namely,

$$A = 307°.6; \quad D = -39°.9; \quad V = 18.6 \text{ km/sec.},$$

which agrees well with the work of other investigators.

The material examined for new members consisted of the stars having complete data in the *Yale Catalogue of Bright Stars*. Of the 9110 stars in the collection, some 2900 were given with complete data. With few exceptions the data were used as given in the catalogue, no correction being applied to radial velocities or proper motions.

All stars having the value of R less than 10 km/sec. were temporarily considered as members of the group. Rasmuson's list of stars yields an upper limit for R of 10 km/sec. Bertaud, as referred to above, uses a value of 10 km/sec., while Wilson,[6] investigating the Taurus group, allows a still higher limit. Using this temporary list, the values of ρ, Q, and P for each star were actually computed and hence a more accurate value for R was secured. All stars having $R > 9.5$ km/sec. were then rejected. Some half-dozen stars were thus eliminated. This was thought advisable since the estimated values of ρ and P made from the diagrams are somewhat inaccurate.

Table I gives the data for 126 stars in our final selection, of which the majority of A- and F-type stars have already been given by Rasmuson and Bertaud. Column 1 gives the *Bright Star Catalogue* number; column 2, the spectral type; column 3, the absolute magnitude; and column 4, the observed parallax. The computed parallax is given in column 5, having been obtained by means of equation (8). The

[5] *Ibid.*, **8**, II, 1932.

[6] *A.J.*, **42**, 7, 1932.

TABLE I

B.S.	Sp.	M	π_0	π_c	v_x	v_y	v_z	R	X	Y	Z	Group
68	A2	0.4	15	22	38.6	−1.0	− 3.1	9.0	6.2	59.8	− 28.9	I
180	Ko	0.4	14	17	25.9	−6.8	− 4.7	7.8	0.5	− 22.9	− 67.6	I
196	Ao	1.1	13	7	25.4	0.0	4.3	9.3	− .7	8.4	− 8.0	I
378	A2	1.5	17	14	29.6	4.9	− 2.2	5.1	− 8.2	30.5	− 49.7	I
497	Ko	1.2	15	20	33.5	−1.5	− 5.6	4.3	− 14.2	− 6.5	− 65.0	I
531	Fo	2.5	35	48	38.3	− .6	− .2	9.4	− 7.8	8.1	− 26.1	I
569	A5	1.8	25	22	32.9	8.3	− .9	9.4	− 10.3	14.3	− 3.1	I
647	Fo	3.2	28	33	26.6	−2.9	− 7.1	5.2	− 9.1	33.7	− 7.6	I
710	A2	2.2	19	21	27.5	−1.5	− 6.9	3.9	− 21.6	9.0	− 47.3	I
797	Ao	1.3	10	11	27.0	4.4	− 8.2	6.6	− 48.1	56.1	− 67.5	I
872	K2	0.6	15	16	32.2	8.6	− 5.1	9.0	− 8.0	− 50.5	− 42.6	I
892	A2	1.8	16	18	28.8	−8.0	− 1.5	8.5	− 34.3	21.2	− 47.5	I
1002	A2	1.0	16	17	30.3	7.4	− 4.0	7.3	− 28.5	54.3	− 11.5	I
1143	K2	1.3	22	31	30.7	−5.2	−10.7	8.5	− 25.4	− 12.5	− 35.7	*p*
1195	Ko	0.2	16	19	32.0	−2.0	− 3.3	3.2	− 36.5	− 16.6	− 48.1	*p*
1327	Go	−0.4	7	7	31.7	−3.7	− 7.2	5.2	− 48.4	131.1	28.1	I
1381	A2	0.1	10	7	25.1	8.0	− 2.4	9.4	− 80.4	41.0	− 43.2	*p*
1383	A2	1.5	18	20	28.1	−1.4	− 5.2	2.4	− 45.2	11.6	− 30.0	*p*
1448	Ao	1.5	14	8	26.1	.5	3.0	7.9	− 59.8	23.9	− 30.9	*p*
1666	A3	1.5	52	35	30.8	2.9	2.4	7.1	− 17.4	2.2	− 7.7	*p*
1872	A2	1.3	16	11	35.1	1.9	2.2	8.4	− 59.4	12.6	− 14.9	II
1982	G5	7.0	135	133	33.2	3.6	− 1.7	5.5	− 6.6	− 1.6	− 2.8	*p*
1983	F8	4.4	135	134	32.5	2.3	− 1.9	4.2	− 6.6	− 1.6	− 2.8	*p*
1995	Ko	0.2	13	22	27.6	−6.9	− 7.0	7.8	− 57.7	50.0	9.6	*p*
2029	A2	0.9	16	8	28.2	−1.1	3.1	7.3	− 34.3	49.5	17.1	*p*
2047	F8	4.6	102	87	30.3	2.2	− 1.9	3.2	− 9.0	4.0	− .2	*p*
2088	Aop	−0.4	29	26	31.2	−2.7	− 3.4	3.2	− 23.9	23.9	6.9	*p*
2296	G5	0.7	22	18	29.0	4.8	− 1.1	5.7	− 37.7	− 20.5	− 15.0	II
2487	Ko	0.9	13	6	23.5	3.4	1.5	8.9	− 50.6	51.0	27.3	II
2491	Ao	1.2	375	409	28.1	− .7	− 4.4	1.8	− 2.7	− 0.7	− 0.4	*p*
2585	A2	1.5	22	15	25.7	1.6	− 2.0	4.8	− 32.0	28.0	16.4	II
2753	A3	0.8	10	11	28.7	1.4	− 3.0	2.0	− 74.8	53.3	39.8	II
2763	A2	1.4	35	40	27.7	2.0	− 4.2	2.9	− 27.1	5.4	7.3	II
3131	A2	0.7	17	14	31.9	3.7	− 2.0	4.8	− 53.0	− 24.5	7.2	II
3221	Fo	1.8	12	15	25.5	.4	− 7.4	5.4	− 37.8	56.9	47.4	II
3391	Go	4.9	70	42	25.4	3.2	− .9	6.2	− 5.2	10.2	8.5	*p*
3441	Ko	2.5	31	31	22.3	−3.5	− 1.7	8.5	− 27.2	− 14.8	9.3	II
3450	A3–G	2.2	20	9	34.6	6.0	− .5	8.4	− 42.4	− 1.2	26.5	II
3485	Ao	−0.6	30	31	28.5	− .8	1.2	5.4	− 16.6	− 28.5	− 4.0	II
3512	G5	1.5	18	16	29.5	3.0	− .4	4.7	− 40.7	− 37.8	7.6	II
3572	A3	1.8	31	40	30.0	.6	2.4	6.6	− 30.8	2.7	9.6	II
3587	A2	1.7	15	0	25.9	3.3	− 2.8	5.3	− 46.7	17.2	44.5	II
3595	Ao	0.2	9	4	30.6	3.2	− 3.9	3.4	− 83.2	14.5	72.0	II
3615	A5	2.5	45	23	21.7	− .7	− 2.1	8.4	− 7.4	− 20.4	− 4.9	II
3676	Ao	1.1	12	28	30.3	2.5	5.0	9.4	− 44.7	37.7	59.2	II
3800	G5	1.0	19	44	24.5	−3.1	− .1	7.3	− 31.2	14.8	39.6	II
3894	A2	0.2	14	6	23.4	5.0	− .9	8.7	− 28.7	37.2	53.7	II
3903	Ko	0.0	14	11	31.8	6.8	− 1.6	7.5	− 47.4	− 39.3	36.1	II
3974	A5	1.6	26	40	33.3	.0	− 1.0	4.7	− 19.9	8.6	31.9	II
3998	F5	3.6	27	35	32.6	− .3	− 2.6	3.3	− 22.3	− 5.3	29.1	II
4031	Fo	−0.5	15	16	29.8	1.1	− .8	3.4	− 36.9	1.3	55.7	II
4101	Ao	1.1	11	6	28.3	6.1	1.1	8.1	− 49.5	− 20.5	73.5	II
4141	Fo	3.2	40	43	29.0	2.1	.2	4.8	− 7.2	13.4	19.9	*p*

TABLE I—*Continued*

B.S.	Sp.	M	π_o	π_c	v_x	v_y	v_z	R	X	Y	Z	Group
4216	G5	0.0	28	22	26.3	−3.8	3.8	9.4	.5	9.5	− 11.6	II
4295	Ao	0.6	43	47	30.0	1.1	− 2.0	2.4	− 5.5	11.9	19.3	*p*
4299	Ma	1.4	19	14	27.6	4.6	− 5.1	5.2	− 22.8	− 23.8	40.8	II
4357	A3	1.9	72	91	33.2	−1.6	−11.9	8.8	− 5.1	− 1.2	13.0	II
4399	F5	2.8	57	63	31.7	.8	2.1	6.5	− 5.9	− 4.6	15.7	II
4418	Ko	0.6	12	9	28.1	3.5	− .6	5.1	− 27.5	− 32.5	71.5	II
4514	G5	1.1	17	15	29.1	2.4	− .9	4.0	− 14.5	− 41.3	39.2	II
4554	Ao	0.6	41	42	29.3	1.8	− .4	4.1	− 3.2	11.0	21.6	*p*
4660	A2	1.6	44	47	30.3	− .8	− 5.4	1.7	− 1.6	11.4	19.7	*p*
4716	Ko	0.2	11	1	22.7	5.5	− 5.8	9.1	− 11.5	3.7	− 7.9	II
4842	Ko	1.6	24	37	37.3	−2.0	− 7.6	8.6	0.0	− 41.7	1.1	II
4859	A5	2.1	18	5	22.8	−5.3	− 7.0	9.1	.3	32.2	45.4	*p*
4865	Ao	0.6	10	16	35.5	−6.3	− 4.4	8.5	1.7	− 22.9	97.4	II
4867	F5	3.8	38	35	29.0	2.5	− 1.5	3.6	0.2	14.3	22.1	*p*
4905	Aop	0.0	45	43	29.2	2.0	− 1.4	3.4	0.5	10.6	19.4	*p*
4931	Fo	2.5	34	40	31.0	2.4	2.6	7.2	1.1	14.2	25.8	*p*
4955	Ko	0.3	10	7	24.5	7.4	− 5.1	8.9	9.8	− 61.6	78.2	II
5009	G5	0.2	6	5	21.5	2.7	− 4.9	8.7	3.6	133.3	100.0	I
5054	A2p	0.6	43	46	30.3	1.2	− 2.2	2.3	2.2	10.8	20.7	*p*
5055	A2	2.2	43	49	31.0	.3	− 2.9	1.7	2.2	10.8	20.7	*p*
5062	A5	2.0	40	43	30.6	.7	− 4.3	1.2	2.5	11.7	22.1	*p*
5105	A2p	0.9	16	15	28.1	4.8	− 7.6	6.2	13.0	− 24.5	56.0	II
5214	A2	1.6	10	11	27.9	−2.0	− 7.4	4.3	23.4	14.3	96.1	II
5329	A5	1.1	20	20	29.1	.6	−10.9	6.9	11.7	21.7	43.5	*p*
5365	Fo	2.4	26	29	35.5	5.4	− 3.4	7.9	15.0	− 8.2	34.5	II
5373	A2	1.0	10	9	25.7	−2.0	− 7.4	5.6	31.5	22.6	92.4	II
5477–8	A2	0.4 0.0	13	16	33.7	4.9	−10.4	8.9	36.1	− 14.0	66.5	II
5634	Fo	3.9	59	73	27.9	−2.6	−10.8	7.4	8.8	0.6	14.4	*p*
5727–8	Go	4.6 5.1	63	65	25.8	−4.5	− 5.0	6.0	8.7	2.2	13.1	*p*
5793	Ao	0.5	44	43	33.3	1.8	2.0	7.2	13.7	2.1	18.0	*p*
5840	G5	1.4	12	9	29.3	2.9	1.3	6.1	55.5	− 6.2	61.8	*p*
5843	Aop	1.3	16	12	27.3	4.6	− 1.4	5.8	42.3	− 7.9	45.3	*p*
5867	A2	0.8	26	25	26.6	2.6	− 6.3	4.7	26.4	− 3.0	27.8	*p*
5886	A2	1.6	20	21	30.6	−2.4	2.8	7.3	16.6	31.8	34.9	I
5888	Ko	1.5	17	18	22.4	−1.8	− 7.7	8.4	42.2	− 16.8	37.1	*p*
6110	A2	0.7	8	7	25.3	1.6	− 3.2	4.8	86.1	31.1	85.5	I
6117	Aop	1.1	21	22	22.2	−1.5	− 8.3	8.8	37.9	3.0	28.9	I
6146	Mb	−0.7	7	8	35.1	5.9	− 3.8	8.1	87.9	56.9	97.0	I
6254	A2p	1.4	20	19	29.6	−4.2	0.9	6.6	30.4	24.1	31.7	I
6292	Ko	0.2	6	9	30.7	−7.3	− 8.5	8.5	133.0	32.0	95.8	I
6481	A2	1.4	14	13	32.7	2.7	− 1.3	4.9	64.4	6.7	30.1	I
6618	Ao	0.7	10	13	34.1	4.1	− 5.5	6.0	57.1	64.4	51.1	I
6917	A2	1.4	14	10	33.3	5.7	2.5	9.5	61.8	28.9	21.1	I
6993	Ao	0.8	10	6	29.9	−4.3	3.8	8.9	99.9	− 2.3	2.8	I
7267	F5	4.6	41	22	30.0	0.1	3.8	7.8	23.0	7.5	1.1	I
7312	Fo	2.3	27	43	36.6	4.6	− 6.9	8.7	8.7	32.1	15.8	I
7400	Ao	0.8	10	10	33.9	−7.8	− 0.6	9.5	97.9	11.6	− 15.3	I
7451	F5	3.7	39	55	35.6	−1.8	− 6.9	6.7	15.7	19.3	6.2	I
7545	Ao	0.7	9	11	25.4	6.3	− 6.5	7.9	38.1	97.0	39.3	I
7555	G5	−0.3	5	6	32.6	6.7	− 4.9	7.2	150.2	130.7	19.5	I
7781	Ao	0.7	10	4	23.7	0.5	2.9	9.2	52.3	83.3	18.0	I

TABLE I—*Continued*

B.S.	Sp.	M	π_0	π_c	v_x	v_y	v_z	R	X	Y	Z	Group
7822....	Fo	1.5	20	9	33.0	−0.2	− 1.9	4.0	42.8	− 4.2	− 25.5	I
7826....	Ao	1.2	14	16	34.9	−6.5	− 3.5	8.3	50.3	50.4	− 1.0	I
7928....	A5	0.8	18	23	29.3	−1.9	1.0	5.5	46.8	24.9	− 16.9	I
8039....	G5	−0.3	10	−16	27.5	5.5	− 8.0	7.0	70.1	− 25.7	− 66.6	I
8170....	F8	4.6	41	53	31.1	−3.2	− 9.6	6.6	14.5	19.5	− 3.1	I
8207....	Ko	1.9	15	30	35.5	−4.7	− 6.0	7.7	47.1	− 2.8	− 47.2	I
8252....	Ko	0.9	22	28	35.2	3.2	− 5.4	6.6	23.7	38.5	− 4.0	I
8263....	A2	0.8	8	12	35.5	−1.1	− 1.2	6.6	91.5	38.2	− 76.2	I
8287....	K5	1.0	11	5	24.6	4.6	− 1.8	7.3	65 1	30.9	− 55.2	I
8407....	Ao	0.9	12	10	26.4	0.5	− 3.2	3.5	38.6	72.4	− 13.0	I
8410....	A3	0.8	13	17	32.0	−2.3	− 9.6	6.3	49.4	26.1	− 52.9	I
8454....	F5	−0.2	12	8	24.5	2.4	1.3	7.8	43.6	65.5	− 27.3	I
8488....	G5	0.2	10	− 1	22.9	2.3	− 3.1	7.2	45.1	− 31.6	− 83.4	I
8573....	Ao	0.6	14	9	22.7	0.5	− 7.9	8.0	38.9	15.1	− 57.7	I
8641....	Ao	1.0	17	9	23.7	6.6	− 3.2	9.1	26.4	45.9	− 25.8	I
8649....	K5	0.1	11	16	32.1	−4.9	−10.9	8.8	43.6	7.9	− 79.4	I
8694....	Ko	1.5	37	39	29.0	−6.0	− 4.6	6.0	5.2	26.3	2.9	I
8695....	Ao	0.7	17	27	27.8	−5.7	− 3.6	6.1	23.3	− 8.2	− 53.4	I
8709....	A2	1.5	40	21	28.5	6.0	− 5.3	6.3	11.2	3.6	− 22.0	I
8821....	B8	0.3	10	7	23.6	2.2	− 4.2	6.5	39.6	56.7	− 71.9	I
8906....	K5	1.4	24	35	31.0	−4.7	− 5.0	4.9	13.2	3.9	− 39.4	I
9064....	Ma	0.1	12	15	32.7	−6.6	0.4	8.5	15.5	65.4	− 49.2	I

components of space velocity (v_x, v_y, v_z) refer to the galactic system of co-ordinates with the solar motion excluded. The pole of the galaxy was assumed to be at $\alpha = 190°$ and $\delta = 29°$, and the directions of the axes in the galactic system were taken as follows:

$+X$-axis $l = 0°$ and $b = 0°$,

$+Y$-axis $l = 90°$ and $b = 0°$,

$+Z$-axis toward $b = 90°$.

The solar apex was assumed to be at

$$\alpha = 270°,\ \delta = 30°, \text{ and } V = 20 \text{ km/sec.}$$

Throughout this paper the co-ordinates are given for the epoch of 1900. The positions of the stars in rectangular galactic co-ordinates are given in columns X, Y, and Z.

7. SPECTRAL DISTRIBUTION

In view of the fact that previous investigators have limited the Ursa Major membership to stars of early spectral type, and since we

have included other types, it was thought advisable to look for any distinction between stars of early and those of late types.

Inasmuch as the stars in the *Bright Star Catalogue* are brighter than magnitude 6.5, the distribution according to spectral class up

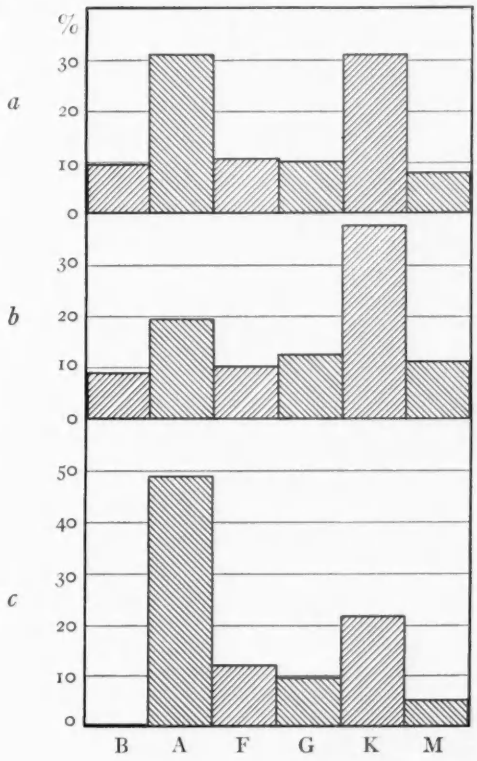

FIG. 2*a*.—Spectral distribution of all stars brighter than 6.5 mag.

FIG. 2*b*.—Spectral distribution of complete data stars in *Bright Star Catalogue*

FIG. 2*c*.—Spectral distribution of Ursa Major stars

to this magnitude was constructed (Fig. 2*a*) by slightly modifying the data given in the *Handbuch der Astrophysik*.[7] The groups B, A, F, G, K, and M are the same as those given in the *Handbuch* (p. 111).

Figure 2*b* gives a similar distribution of all stars with complete data in the *Bright Star Catalogue*, that is, all stars examined, while Figure 2*c* shows the distribution for the stars given in Table I. All

[7] Band V/1, Teil I, p. 112.

distributions are given in percentages. The marked difference between Figures *2a* and *2b* is undoubtedly due to the selection of stars for the determination of parallax and radial velocity, together with the great number of spectroscopic parallaxes present in the late types. The difference between Figures *2b* and *2c*, with which we are mostly interested, is also striking. Almost 50 per cent of the stars in the Ursa Major group are of type A, and while a proportionally large number of B-type stars have complete data, they are completely absent from the group. It is possible that the inaccuracies in the small parallaxes of the B's might explain their absence. In the Russell diagram the extremely abrupt dropping-off of stars earlier than B9 is further evidence of the fact that they are really absent.

TABLE II

1	2	3	4	5
B.....	0	11.1	12.1	0.0
A.....	62	24.7	38.8	2.5
F.....	17	12.7	13.4	1.3
G.....	12	15.6	13.0	0.8
K.....	29	47.7	38.8	0.6
M.....	6	14.2	10.0	0.4

Table II, column 2, gives the number of stars of the Ursa Major group for each spectral class, and column 3 the expected number, assuming that our selection from the 2900 stars was at random. For comparison purposes we give in column 4 the expected number of stars from the spectral distribution of all stars. The ratio of columns 2 and 3 given in column 5 shows a well-marked diminution of the number of stars from early to late types.

Table III shows the numerical Russell diagram. In spite of the fact that the number of stars is insufficient to give great confidence to our conclusions, we feel it is worth while to point out some characteristics. The main sequence is represented mostly by A and F stars, which is probably due to the fact that our investigation was confined to bright stars. This becomes most evident from the study of the K-type stars having complete data. The parallaxes of these stars are confined principally between $\pi = 0''.000$ and $0''.030$. Assuming the upper limit of absolute magnitude to be 4.0 for K0

dwarfs and using 6.5 for the limit of apparent magnitude, the smallest possible parallax for a Ko star becomes 0".032. For further confirmation of this point we have investigated the distribution in the various spectral classes of the parallaxes of the 2900 stars having complete data. This shows evidence of larger parallaxes in the F and

TABLE III

M	B8	Ao	A2	A3	A5	Fo	F2	F5	F8	Go	G5	Ko	K2	K5	Ma	Mb
−.6		1				1										1
−.3		1						1		1	2					
.0		1	2								1	1		1	1	
.3	1	1	2								2	6				
.6		9	3								1	1	1			
.9		4	6	2	1						1	2		1		
1.2		8	1		1						1	1	1			
1.5		1	11	1	1	1					2	3		1	1	
1.8			2	2	1	1						1				
2.1			2	1	2											
2.4					1	4						1				
2.7								1								
3.0																
3.3						2										
3.6								2								
3.9						1		1								
4.2																
4.5								1	3	1						
4.8										1						
5.1										1						
5.4																
5.7																
6.0																
6.3																
6.6																
6.9											1					

G stars, with an abrupt diminution in the K's. Among the giants in our selection we have an unusually large concentration of A types and a smaller concentration of K's, which is in definite contrast with a typical Russell diagram.

The isolation of the late-type giants from the rest of the stars, the absence of the B-type stars, the fact that stars are numerous where the giants and dwarfs meet, together with the suspected presence of the main sequence, indicate that the Ursa Major group is similar to Trumpler's[8] type *2a* open cluster.

[8] *P.A.S.P.*, **37**, 307, 1925.

8. PARALLAXES

To show again that our selection of stars is not at random, a study of the distribution of parallaxes was made. Figure 3*a* gives the distribution of parallaxes of approximately 2600 stars (here we do not

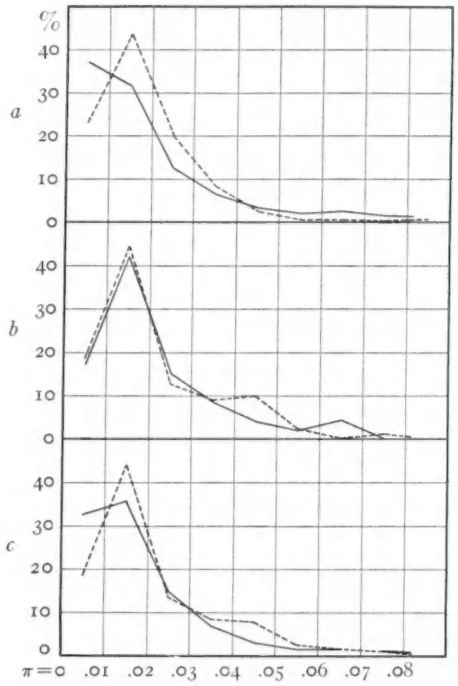

FIG. 3*a*.—Parallax distribution of early-type stars (dotted line) and of late-type stars (full line) having complete data. In this diagram the B-type stars are not included.

FIG. 3*b*.—Parallax distribution of early-type stars (dotted line) and of late-type stars (full line) in the Ursa Major group.

FIG. 3*c*.—Parallax distribution of stars with complete data (full line) and of Ursa Major stars (dotted line) showing diminution in small parallaxes for the latter. The B-type stars are not included.

include the B-type stars, as they are completely absent from the group), the broken line showing the early spectral classes (A and F) and the full line showing the late (G, K, and M). Figure (3*b*) shows similar distributions for the 126 stars of the Ursa Major group. The great number of small parallaxes in the late types of the 2600 stars does not affect the late types of the Ursa Major stars, but the late

PLATE IV

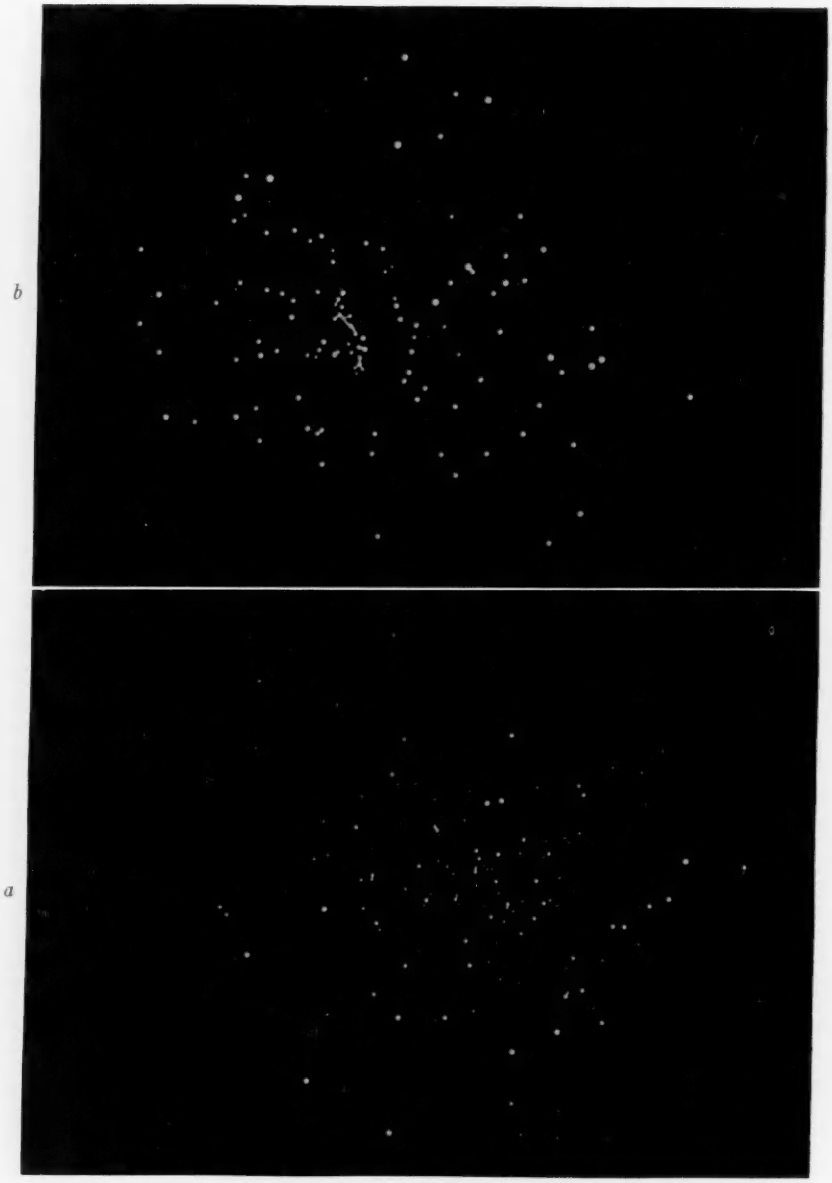

a. Photograph of the Model of the Ursa Major Group as Seen from a Point on the Equator at 0^h R.A.

b. Photograph of the Model of the Ursa Major Stars Showing the Gap in Space Distribution

Ursa Major stars yield a distribution similar to the distribution of early-type Ursa Major stars. This, we believe, shows that our selection was not at random.

9. SPACE DISTRIBUTION OF STARS

There is no evidence of systematic grouping of early- and late-type stars on the celestial sphere. About one-third of all the stars (especially A type) are clustered in the vicinity of the constellation Ursa Major, while an area about one-sixth of the celestial sphere, with its center in the direction of Scorpius, is free of any stars. This area has actually more stars with complete data than any other corresponding area below the plane of the equator.

The centroid of the group in parsecs and in equatorial co-ordinates is

$$\bar{x}=-4.31;\ \bar{y}=-15.42;\ \bar{z}=+8.80.$$

The relatively large negative value of y is no doubt due to the concentration of the stars near the constellation Ursa Major. The positive value of z is partly due to the same cause and partly to the fact that the stars examined are more numerous in the northern hemisphere.

A study of the stars in space yielded practically a spherical distribution with no marked difference between the distributions of early and late stars. If a_1, a_2, and a_3 denote the dispersion in the direction of the three axes of the ellipsoid for the 126 stars, we have in parsecs

$$a_1=42.9;\ a_2=35.6;\ a_3=39.9.$$

A photograph of the space model constructed for the 126 stars is shown in Plate IV (*a*).

10. MOTION OF GROUP

The computed apexes for the two subgroups and for the whole group are

Spectral Groups	*A*	*D*	*V*
For A and F stars	305°.6	−37°.3	17.3
For G, K, and M stars	307.5	−39.6	17.8
For all stars	306.3	−38.2	17.5

The motion of the Ursa Major group in galactic co-ordinates and with solar motion excluded is

$$v_x = 29.4 \; ; \; v_y = 0.7 \; ; \; v_z = -3.1 \, ,$$

the direction and velocity being

$$l = 1\overset{\circ}{.}4 \; ; \; b = -6\overset{\circ}{.}0 \; ; \; V = 29.5 \text{ km/sec.}$$

The stars in the group are moving approximately in the plane of the galaxy and in a direction about 36° from the galactic center.

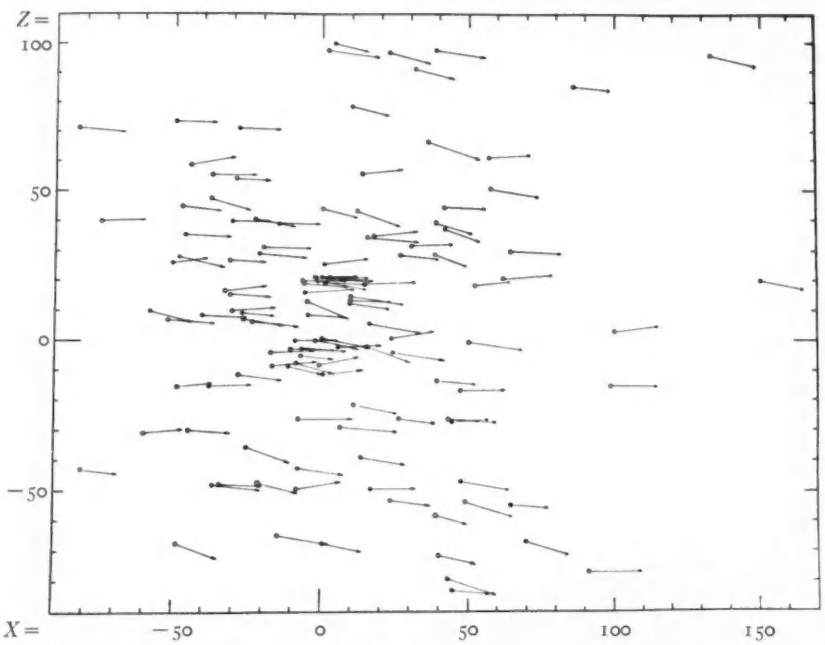

FIG. 4.—A projection of the Ursa Major stars and their velocities on the XZ-plane (galactic system). The lengths of the vectors are shown on the scale of 2 km/sec. per parsec. The open circles represent stars of early types while the full circles represent those of late types.

11. THEORETICAL PARALLAXES

Since the assumed apex and velocity differ from the corresponding computed values, it was thought advisable to correct the already computed values of P and Q before they were substituted in equa-

tion (8). By utilizing the method of paragraph 3, these corrections were obtained with little difficulty.

The distribution of the residuals in parallax ($\pi_o - \pi_c$), when plotted, shows a well-marked Gaussian curve. Thus we may compute the probable error in parallax; its value is $0''.0053$. This is reasonable, as the probable error of all observed parallaxes is certainly not smaller than $0''.006$. The residuals in parallax were also obtained by computing π_c from equation (12). This produced little change in individual parallaxes, one-third of them remaining the same. The new distribution was practically the same but yielded a somewhat smaller value for the probable error. Since in the results obtained there is little difference between the two formulae, and since the former is much easier to apply, the values of π_c shown in Table I were computed by means of equation (8).

12. THE GAP

An examination of the space model shows that the stars are completely divided into two groups by a gap passing through the sun. The boundaries of this gap are approximately two parallel planes about 18 parsecs apart. The photograph of the model given in Plate IV(*b*) was taken from the line of intersection of the equator and the gap ($\alpha = 16^h$). The stars to the right of the gap will be designated as group I and those on the left as group II.

There is no marked difference in spectral distribution or in absolute magnitude between the two groups. Their mean space velocities in galactic co-ordinates, with solar motion excluded, are

$$\text{Group I: } v_x = 29.9 \quad v_y = 0.1 \quad v_z = -3.6$$

$$\text{Group II: } v_x = 29.0 \quad v_y = 1.2 \quad v_z = -2.7$$

Although the difference in these velocities is not sufficiently great to have much significance, it is interesting to note that its direction is nearly parallel to the gap, with a magnitude of 1.7 km/sec.

The boundary of group II is so well marked as a plane and so well populated with stars that we thought it advisable to determine its position in space.

The normal to the plane has for direction

$$l = 46°.1 \; ; \; b = -31°.3 \, ,$$

and the plane is 3.1 parsecs from the sun. There are 33 stars in the plane, two-thirds of them being less than 2 parsecs from it. The tendency of these stars is to follow the main sequence branch of the Russell diagram. Professor Turner[9] in 1911, utilizing all the known stars (13) in the Ursa Major group, obtained practically this same plane.

The last column of Table I indicates the stars in each group, and those in the plane are marked by the letter *p*.

13. CONCLUSIONS

After an examination of all the stars in the *Yale Bright Star Catalogue*, 126 of them were assigned to the Ursa Major group, the criterion of selection being their common space velocities. On the basis of parallax and spectral distribution, which are distinctly different from those of the stars used in the selection, it appears that these stars form a related unit and are not chosen at random. The system may be regarded as a moving cluster, although it should be recalled that the strict adherence of its members to the common motion is not essential in view of the large dimensions of the group.

It is interesting to note that approximately one out of twenty-four of the stars in the *Bright Star Catalogue* having complete data belongs to the Ursa Major group. It is reasonable to assume that this is also true for all the stars near the sun. The space distribution of the stars is almost spherical, with an approximate diameter of 150 parsecs for the group.

A well-marked gradual increase in the number of stars from late to early types is the distinctive characteristic of the spectral distribution. The Russell diagram agrees well with type *2a* in Trumpler's classification of clusters.

The group is completely separated by a wide gap, the boundaries of which are planes. One-quarter of all the stars in the group are within 5 parsecs of one of these planes. There is no difference in distribution of spectral types or absolute magnitudes between stars on the two sides of the gap.

WARNER AND SWASEY OBSERVATORY
CASE SCHOOL OF APPLIED SCIENCE
June 1934

[9] *Observatory*, **34**, 246, 1911.

THE ACCURACY OF POSITIONS FROM PHOTOGRAPHIC PLATES TREATED BY THE NORMALIZING PROCESS

By P. VAN DE KAMP and A. N. VYSSOTSKY

ABSTRACT

Twenty photographs of the central part of the Praesepe cluster have been taken with the 26-inch McCormick refractor on Cramer Iso Presto plates. Half of these plates had been "normalized" before exposure by soaking them in water, followed by dehydration in alcohol.

The positions of 52 stars were measured. From a study of the 2080 residuals obtained with respect to the means of five plates, it is found that the normalizing process results in a considerable increase in positional accuracy for stars near the edge of the plates. For the remaining area of the plate, the process gives an appreciable increase in positional accuracy for one emulsion, but causes no improvement for the second emulsion. Investigations are being continued to ascertain the relative frequency of emulsions free from stress, among plates of the same brand.

It has been long recognized that the position of the latent image on a photographic plate may suffer a shift during the process of developing, fixing, washing, and drying, thus leading to a distortion or film error in the measured photographic position. Schlesinger[1] finds that the mean value of this distortion (for Cramer Instantaneous Isochromatic plates) is of the order of 0.001 mm. Attempts to reduce these distortions by soaking the plates in alcohol so as to secure rapid and uniform drying have led to conflicting results. Ross[2] finds, for example, that the distortions are materially reduced, at least on plates of small dimensions (27×37 mm). Coburn[3] finds no improvement whatever on a plate 5×7 inches. Littell and Phenix[4] find a decided improvement near the edge of the plate.

In 1930 D. and C. D. Cooksey,[5] of the Sloane Physics Laboratory, Yale University, showed that stresses in undeveloped gelatin emulsions can be relieved before plates are exposed, by soaking them in water, followed by dehydration in alcohol; the process was termed by them "normalizing." A plate so treated was found to have higher

[1] *Publications of the Allegheny Observatory*, **1**, No. 1, 1906.

[2] *The Physics of the Developed Photographic Image*, p. 194, 1924.

[3] *Astronomical Journal*, **42**, 75, 1932.

[4] *Ibid.*, **43**, 37, 1933.

[5] *Physical Review*, **36**, No. 1, 80, 1930.

positional accuracy than a non-treated plate. Apparently the gelatin stresses, which for the normalized plates are relieved before exposure, are relieved for the non-treated plates during the development process after exposure and thus cause so-called distortions. Clearly the process is entirely different from the alcohol drying process just mentioned; in the "normalizing" process the plates are treated with water and alcohol before the plates are exposed.

It was deemed of importance to test the value of the normalizing process for the case of photographic positions of stars obtained with a long-focus refractor. The accuracy of a measured position as determined by two exposures, on a plate taken with the McCormick 26-inch telescope, is represented by a probable error of about 0.0014 mm. Of this, 0.0008 mm is introduced by the process of measuring, leaving 0.0012 mm for the probable error inherent in the plate. Any process which might appreciably reduce the latter error should be considered and carefully tested.

It might be expected that the "normalizing" process would act differently on different brands of plates and on different emulsions of the same brand. At present, the plate in regular use here is the Cramer Iso Presto (5×7 in.). In the present investigation, we have limited ourselves to this brand of plates and have studied two different emulsions only, Nos. 286879 and 287416, here designated as "emulsion A" and "emulsion B."

In normalizing the plates we have followed the method used by Cooksey and Cooksey and described in their paper. The process consists in soaking the fresh non-exposed plates in clean water at 65° F. for approximately thirty minutes and then putting them in strong ethyl alcohol for about the same interval of time. The alcohol used was 94 per cent by weight as measured with a hydrometer. In order not to dilute the alcohol by transporting water with the wet plates, two successive baths of alcohol were used, the second being of maximum strength. The plates were then dried on edge in a humid atmosphere. After the plates were exposed and developed in the usual manner, they were again treated with alcohol in order to insure rapid and uniform drying. The developer used was Carbonal Hauff, 1:32, and the fixing bath contained chrome alum and sulphuric acid.

In order to make the results of the test directly applicable to as-

tronomical problems, it was decided to use images of stars obtained with the telescope under average observational conditions. The central part of the Praesepe cluster was chosen as a suitable test object. Twenty plates were taken on four nights, ten plates with emulsion A and ten with emulsion B. Each plate contains two exposures of six minutes each, separated about 2.5 mm in the approximate direction of right ascension. Half of the plates (five of each emulsion) had been "normalized." The non-treated plates were allowed to dry without the alcohol treatment. The normalized plates show no detectable difference in sensitivity as compared with the non-treated plates.

The positions of fifty-two stars ranging in brightness[6] from $6^m.1$ down to $10^m.7$ were measured on the Gaertner machine. With few exceptions the faintest stars were well measurable on all plates. The measures were made in two co-ordinates, X and Y, which are approximately in the direction of right ascension and of declination, respectively. The plates were carefully set and oriented in the machine so as to have the corresponding readings for the same star in practically the same part of the screw for all plates, thus eliminating the systematic (progressive and periodic) errors of the machine.

For each plate the images were measured in the order of increasing screw-reading (right to left), two successive settings being made on each image. A magnifying power of 20 was used. All measurements were repeated immediately with the plate reversed 180°, so as to eliminate personal errors. Individual readings were made to 0.001 mm; in the final means 0.0001 mm were used. All the measurements were carried out by one of us. It should be noted that the non-treated and the normalized plates were subject to identical conditions both at the telescope and during the measurements. For each plate the mean of two exposures has been considered as the position for the plate.

In order to study the accuracy of the measured photographic position on each plate, four groups of five plates each were formed.

1. Emulsion A. Non-treated
2. Emulsion A. Normalized
3. Emulsion B. Non-treated
4. Emulsion B. Normalized

[6] *Bulletin of the Astronomical Institutes of the Netherlands*, 1, 79, 1922.

Within each group the mean position (mean of five) was formed for each star, X and Y being treated separately. Next, for each of the five plates the deviations (Δx, Δy) of each position from the mean of five were derived. These deviations were corrected for zero point (c), scale (a), orientation (b), and magnitude error (d). Scale and orientation were derived from sixteen stars, four in each plate quadrant, and the measured positions were corrected accordingly. Next, a zero-point correction was applied, which was derived by making the sum of the corrected deviations equal to zero. Afterward a magnitude correction was derived, assuming the latter to vary linearly with the visual magnitudes of the stars.

The probable value of this magnitude error per magnitude for a plate is $0.00044 \pm .00003$ mm, the extreme value being equal to 0.0018 mm. The deviations corrected for scale, orientation, zero point, and magnitude were called residuals (δ).

Thus for any one star, for the X co-ordinate:

$$x - \frac{\sum_{5} x}{5} = \Delta x$$

$$\delta = \Delta x - ax - by - c - d(m - \bar{m}) .$$

For each plate: $\sum_{52} \delta = 0 .$

The Y co-ordinates were treated similarly.

We have thus at our disposal 2080 residuals, equally distributed over two emulsions. These again were divided into two groups of

TABLE I

Star Group	No. of Stars	Characteristics
a	12	Bright, central
b	12	Faint, central
c	12	Bright, non-central
d	12	Faint, non-central
e	4	Edge

five non-treated and five normalized plates. Further division of the material was suggested by the following considerations: (1) stars

TABLE II

SUMMARY OF $\Sigma\delta^2$

Unit (0.0001 mm)^2

EMULSION A. NON-TREATED PLATES

STAR GROUP	PLATE	B 438		B 441		B 443		B 445		B 447		ALL		
	No	x	y	x	y	x	y	x	y	x	y	No.	x	y
a	12	9067	5221	4287	3584	5511	5028	8357	1803	5337	2494	60	32559	18130
b	12	8041	5334	4958	2400	8241	4735	4567	5582	4714	4261	60	30521	22312
c	12	4364	6054	14508	4433	9014	6266	10655	3720	7436	4815	60	45977	25288
d	12	10767	4103	8672	3530	10408	5415	15341	4323	21422	6280	60	66610	23651
e	4	5683	27503	3417	8484	838	5927	4658	6771	8741	2643	20	23337	51308
$a+b+c+d$	48	32239	20712	32425	13947	33174	21444	38920	15428	38909	17850	240	175667	89381

EMULSION A. NORMALIZED PLATES

STAR GROUP	PLATE	B 439		B 440		B 442		B 444		B 446		ALL		
	No.	x	y	x	y	x	y	x	y	x	y	No.	x	y
a	12	3560	3622	2988	2791	4329	4145	3327	2336	8510	2462	60	22714	15356
b	12	1983	3859	4186	3734	5182	2293	1902	2940	6852	5232	60	20105	18058
c	12	2823	4367	5840	2486	6132	2267	5245	1219	19297	1303	60	39337	11642
d	12	6433	6821	6321	1710	3994	2596	3518	3546	9152	3716	60	29418	18389
e	4	1235	1150	854	1305	1923	1742	1535	1489	3262	6187	20	8809	11873
$a+b+c+d$	48	14799	18669	19335	10721	19637	11301	13992	10041	43811	12713	240	111574	63455

EMULSION B. NON-TREATED PLATES

STAR GROUP	PLATE	B 449		B 451		B 453		B 455		B 457		ALL		
	No.	x	y	x	y	x	y	x	y	x	y	No.	x	y
a	12	4121	5567	3655	6586	2107	4279	3225	3234	2781	3843	60	15889	23509
b	12	3985	1234	1882	2207	1639	1279	2741	818	4024	1671	60	14271	7209
c	12	4030	1029	2597	7336	4443	2091	3810	2311	4251	4834	60	19131	17601
d	12	4902	3009	3052	5609	2776	3076	4121	2434	2975	2120	60	17826	16248
e	4	1119	2355	13314	12024	761	4131	4222	4185	3911	6649	20	23327	29344
$a+b+c+d$	48	17038	10839	11186	21738	10965	10725	13897	8797	14031	12468	240	67117	64567

EMULSION B. NORMALIZED PLATES

STAR GROUP	PLATE	B 448		B 450		B 452		B 454		B 456		ALL		
	No.	x	y	x	y	x	y	x	y	x	y	No.	x	y
a	12	2785	2350	5425	4405	4682	2743	2176	1905	2809	3676	60	17877	15079
b	12	4061	2186	3297	4341	2246	6656	4401	2115	1841	1466	60	15846	16764
c	12	5101	2554	5266	7084	3230	5923	2045	1366	3911	2584	60	19553	19511
d	12	5225	2830	3063	2460	1378	2055	2216	1610	4181	3455	60	16063	13010
e	4	2601	1092	1338	865	714	473	1458	2435	1702	1230	20	7813	6095
$a+b+c+d$	48	17172	9920	17051	18290	11536	17977	10838	6996	12742	11181	240	69339	64364

away from the center of the plate are more affected by errors in the plate constants; (2) a preliminary inspection of the residuals showed an excess of large values for stars near the edge of the plate, especially for the non-treated plates; (3) the great range in magnitude ($6^m.1 - 10^m.7$) may very well correspond to a difference in accuracy of the measured positions for the brighter and the fainter stars.

It was therefore decided to divide the fifty-two stars into five groups, according to their brightness and location, as is shown in Table I.

The limit between bright and faint is at about magnitude 9; the central part of the plate is the area approximately within 4 cm of the center. Group *e* contains stars within 1 cm from the edge.

Table II gives the sum of the squares of the residuals for the five subgroups *a*, *b*, *c*, *d*, *e*, for each of the twenty plates. At the extreme right of the table, sums of $\Sigma\delta^2$ for each set of five plates have been given. Summations over all groups of stars, omitting the edge group *e*, are also given.

An inspection of Table II will show that certain features of this material, discussed below, are not only apparent in the summations of the $\Sigma\delta^2$ over five plates, but persist almost without exception in the $\Sigma\delta^2$ of the individual plates.

From Table II we derive Table III, which shows the behavior of $\Sigma\delta^2$ for the four groups of stars: central, non-central, bright, and faint.

Taking all plates together, there appears to be no appreciable systematic dependence of the accuracy on the brightness of the star. As the error of measurement of the bright stars is slightly larger than that of the faint stars, it appears that the photographically recorded position of the bright stars is certainly not inferior to that of the faint stars, at least for the present investigation. The diameters of the brightest stars in the present work are seldom over 0.3 mm. There is some indication of higher accuracy for the central stars. This may be partly explained by the negligible effect of the plate constants for these stars.

For a comparison of the non-treated and the normalized plates it seems of no further advantage to keep the groups *a*, *b*, *c*, *d*, separated. Table IV gives a summary of $\Sigma\delta^2$ for all four groups combined.

For the purpose of drawing final conclusions it is desirable to convert the $\Sigma\delta^2$ into probable errors. Let R be the probable error of a measured photographic position. This error is made up of two component errors: (*a*) the error inherent in the photographic position on

TABLE III

SUMMARY OF $\Sigma\delta^2$ FOR CENTRAL, NON-CENTRAL, BRIGHT, AND FAINT STARS

Unit (0.0001 mm)²

STAR GROUP	No.	EMULSION A				EMULSION B			
		Non-treated		Normalized		Non-treated		Normalized	
		x	*y*	*x*	*y*	*x*	*y*	*x*	*y*
Central (*a*+*b*)	120	63080	40442	42819	33414	30160	30718	33723	31843
Non-central (*c*+*d*)	120	112587	48939	68755	30031	36957	33849	35616	32521
Bright (*a*+*c*)	120	78536	43418	62051	26998	35020	41110	37430	34590
Faint (*b*+*d*)	120	97131	45963	49523	36447	32097	23457	31909	29774

TABLE IV

SUMMARY OF $\Sigma\delta^2$ FOR ALL EXCEPT FOUR EDGE STARS

Unit (0.0001 mm)²

No.	EMULSION A				EMULSION B			
	Non-treated		Normalized		Non-treated		Normalized	
	x	*y*	*x*	*y*	*x*	*y*	*x*	*y*
240	175667	89381	111574	63455	67117	64567	69339	64364

the plate—probable error, r_p; (*b*) the error due to the measurement (machine and personal)—probable error, r_m.

The first error may be considered as the resultant of two errors: (1) film error or distortion, due to a change or (partial) relief of a stress in the photographic film during development[7]—probable error,

[7] A direct comparison of non-treated plates with normalized plates showed no definite systematic behavior of the film error; it was therefore considered to have an accidental character.

r_f; (2) image error in the representation by the photographic image of the geometric location of the star—probable error, r_i.

The accidental errors of measurement are those which remain in the measurements after the systematic errors due to machine and person have been eliminated. Thus:

$$R^2 = r_p^2 + r_m^2 ,$$
$$r_p^2 = r_f^2 + r_i^2 .$$

In order to convert $\Sigma\delta^2$ into probable errors we must keep in mind that for each plate the δ's depend on adjusting the observed Δx (or Δy) for four unknowns—c, a, b, and d. For each plate the residuals furnish the probable error R' of one star through the formula

$$R' = 0.6745\sqrt{\frac{\Sigma\delta^2}{5^2-4}} = 0.6745\sqrt{\frac{5^2}{48}}\cdot\sqrt{\frac{\Sigma\delta^2}{5^2}} .$$

In order to convert the probable error R' into the probable error R of a measured photographic position we have allowed for the error of the mean of five plates by using the relation

$$R = R'\sqrt{\tfrac{5}{4}} .$$

Thus, for any set of five plates, the following formula has been used for the derivation of the probable error R of all stars or of any subgroup of n stars:

$$R = 0.6745\sqrt{\frac{5^2}{48}}\cdot\sqrt{\frac{5}{4}}\cdot\sqrt{\frac{\Sigma\delta^2}{n}}$$

or

$$R = 0.785\sqrt{\frac{\Sigma\delta^2}{n}} .$$

Applying this formula to Table IV, we obtain Table V for all stars except the edge stars, and Table VI for the edge stars.

The probable errors of the probable error have been computed from the formula

$$\frac{0.477}{\sqrt{n}}\cdot R ,$$

where n is the number of residuals on which R is based.

From Table V and VI we may draw the following conclusions: (*a*) For both emulsions the normalizing process has greatly improved the accuracy of the photographic position of the four edge stars. (It should be mentioned that three of the four edge stars are near the *X*

TABLE V

PROBABLE ERRORS OF MEASURED POSITIONS, WITH THEIR PROBABLE ERRORS, FOR ALL EXCEPT FOUR EDGE STARS

(Unit = 1 mm)

EMULSION A				EMULSION B			
Non-treated		Normalized		Non-treated		Normalized	
x	*y*	*x*	*y*	*x*	*y*	*x*	*y*
0.00212 ± .00007	0.00152 ± .00005	0.00170 ± .00005	0.00128 ± .00004	0.00131 ± .00004	0.00129 ± .00004	0.00133 ± .00004	0.00129 ± .00004

TABLE VI

PROBABLE ERRORS OF MEASURED POSITIONS, WITH THEIR PROBABLE ERRORS, FOR EDGE STARS

(Unit = 1 mm)

EMULSION A				EMULSION B			
Non-treated		Normalized		Non-treated		Normalized	
x	*y*	*x*	*y*	*x*	*y*	*x*	*y*
0.00268 ± .00029	0.00398 ± .00043	0.00165 ± .00018	0.00191 ± .00020	0.00268 ± .00029	0.00301 ± .00032	0.00155 ± .00017	0.00137 ± .00015

edge of the plate and one is near the *Y* edge. It looks as if the unrelieved stresses for these stars are largest in a direction perpendicular to the edge.) However, merely drying by alcohol has sometimes shown a similar effect; it is therefore not possible to judge from the present investigation whether this improvement is due to the relieving of stresses before exposing or to the prevention of stresses during the drying process, which have been known to occur when the

plates are allowed to dry after washing in water. (*b*) For emulsion A there is a decided indication of greater accuracy in the Y co-ordinate than in the X co-ordinate. An inspection of the plates for guiding error and a consideration of the computed magnitude errors show that both sets of plates, A and B, are similar in this respect. The only apparent difference between the plates of the two emulsions seems to be that the plates of emulsion B were taken in somewhat better seeing. The cause of this difference in accuracy of the co-ordinates X and Y for emulsion A cannot be explained at present. (*c*) The normalizing process leads to an appreciably greater accuracy in both co-ordinates for the plates of emulsion A. In this case, taking into account all stars except the four near the edge, the probable error R is reduced by an amount $0.00042 \pm .00009$ mm in X and $0.00024 \pm .00006$ mm in Y. This increase in accuracy should be considered as real. In the case of emulsion B there has been no improvement whatever. The accuracy of the normalized plates of emulsion A is not very different from that of emulsion B.

We are thus led to conclude that different emulsions of the same brand of plates react in a different way to the normalizing process. (Perhaps different groups of plates of the same emulsion may show this different behavior, but evidently that fact cannot be derived from the present material.)

A probable explanation of the effects of the normalizing process is that in the process of coating the glass with the emulsion, non-uniformity may enter into any of three items: process, glass, or emulsion. It might happen that some plates would come through with very small film stresses, which cannot be appreciably reduced by the normalizing process. The present emulsion B would be an example. Other plates would leave the factory possessing appreciable film errors which could be relieved by the normalizing process; emulsion A is an example.

The improvement may be expressed by the value of the film error eliminated by the normalizing process. A comparison of the probable error R (non-treated) and R_n (normalized) gives

$$r_f = \sqrt{R^2 - R_n^2} .$$

This quantity is shown in Table VII for the various sets of data.

It appears that for both emulsions a probable film error of about 0.0025 mm is eliminated near the edge. As far as the rest of the plate is concerned, emulsion B shows no film error, emulsion A, non-treated, shows a film error of about 0.0011 mm.

For emulsion B the error of the measured position with the mean value 0.0013 mm may be considered as due to image error and to errors of measurement only. The latter is 0.0008 mm,[8] leaving 0.0010 mm for the image error. Assuming that the normalized plates

TABLE VII

PROBABLE FILM ERROR, ELIMINATED BY NORMALIZING PROCESS

(Unit = 1 mm)

EMULSION A				EMULSION B			
All except Edge Stars		Edge Stars		All except Edge Stars		Edge Stars	
x	y	x	y	x	y	x	y
0.0013	0.0009	0.0021	0.0035	0.0000	0.0000	0.0022	0.0027

of emulsion A are free from the film error, we find values of 0.0015 and 0.0010 mm for the image error in X and Y, respectively. We come, then, to the conclusion that as far as the present results go, the probable error of a measured photographic position (two exposures) is made up of the following sources of error:

Error of measurement ..... $r_m = 0.0008$ mm
Image error (average of emulsions A and B, mean of 2 images) ..... $r_i = 0.0012$ mm
Film error ..... $r_f = 0.0000$ mm for emulsion B
$= 0.0011$ mm for emulsion A

Of these three sources of error, the image error cannot be reduced appreciably, the error of measurement can be cut down somewhat; the normalizing process is effective in removing a considerable film error whenever film stresses are inherent in the plate. In case of

[8] This error was obtained from remeasurements, on different days, of four of the present plates.

emulsion A, for example, the process effects a decrease in total error from 0.00182 to 0.00149 mm (average of X and Y), or an increase in weight of 50 per cent! The normalizing process may therefore be considered as a powerful tool for obtaining more accurate photographic positions.

In view of the fact that emulsions A and B react so differently to the normalizing process, it is obviously of great importance to examine the relative frequency of stress-free emulsions among plates of a certain brand. For this purpose the investigations are being continued here, using as many different emulsions of the same brand as seem to be practicable. For special astronomical problems where no chance should be taken, for example in eclipse observations for the Einstein effect, the normalizing process should undoubtedly always be used in order to be on the safe side.

We take pleasure in expressing our appreciation to Messrs. D. Cooksey and C. D. Cooksey for valuable discussions of the problem during their respective visits here. We are indebted to Dr. Reuyl of this Observatory for having taken eight plates of the present material, and to Mrs. Emmy van de Kamp-Basenau for carrying out the reductions.

Leander McCormick Observatory
University of Virginia